Dissertation

Submitted to the

Combined Faculties for the Natural Sciences and for Mathematics

of the Ruperto-Carola University of Heidelberg, Germany

for the degree of

Doctor of Natural Sciences

Presented by

Master of Science (Biophysics) Kartik Bane

Born in: Mumbai, India

Oral-examination: 22nd Feb 2016

Coronin regulates motility in malaria parasites

Referees: Prof. Dr. Michael Lanzer

Prof. Dr. Friedrich Frischknecht

Dedicated to my Family

Mother (Supriya Bane)
Father (Subhash Bane)
Brother (Sidhesh Bane)
Sister in law (Shravani Bane)
Niece (Snezka Bane)
Niece (Slaariya Bane)
Fiancee/Wife (Titiksha Raul/Bane)

Danksagung / Acknowledgements

The list for acknowledgement is in the chronological order.

Priyanka: Hi! The first time I saw you, I was at Frankfurt airport and you were holding the same sheet of paper that I had in my hands. It was my first time in Europe and you were my first friend here. Thank you so much for nurturing that friendship with little understanding, more care and nourishing it with awesome food that you cooked together with Vihang on almost every weekend. You and Vihang have taught me how to cook, the most important thing to survive away from home. Thanks also for sharing a place with me and treating me like a younger brother. It really made me feel being in a family.

Harshal and Mitasha: The coolest buddies I ever had! Even though, you did not spend too much of time in my life, you have taught me a number of things. The most important being, how to be OK in the most stressful circumstances? Thanks Mitasha for hosting Priyanka and I in Switzerland.

Freddy: The first time, I saw him, he was with my CV in his hands asking Oliver Bilker, where is this Indian guy? And I turned my ear to their conversation still showing my back. A moment later, Oliver called me and introduced me to Freddy. Few days later, I was in HD. I have a lot to say about you Freddy, but just like a corresponding author, I reserve my thanks giving till the end of acknowledgements.

EVIMalaR friends: Sonia - I think, I was her 1st friend in HD and shared her first lunch at Menza on Friday. This Friday lunch date continued and is still going well under all circumstances. Thanks Sonia for understanding me scientifically, personally, emotionally and in all aspects! You are still the one who knows every secret of mine!

All the EVIMalaR friends – I will never forget the time I spent with you guys at Steffi's hostel. Since, this was my first hostel experience and still the best hostel experience than any of my friends in India ever had. We were from Asia, Middle-east, Africa, Europe to Mexico, a blend of diverse cultures. I still wonder even though we were so different, we are so similar. A year later, you celebrated my Birthday on the streets of Berlin, I still have that T-shirt and in fact I am wearing it now, with Fast food and EVIMalarians. Superb gift! I still remember the jokes of Jenny, specially the pretzel one and still laugh thinking about them. The trip to Italy was memorable. Many thanks to Gabriella and Pablo! One-day on the spot organized tour by Sonia

and Mariana to the biggest waterfall in Germany was also nice! Bigger thanks to Mariana for putting in great efforts in giving me the feeling of floating on water. I would never have that feeling without you. I still can't imagine how you managed to hold me just above water while you yourself were floating. You are a true Baywatch!

Simone: Amongst all the teachers who have taught me, Simone, you are the best. Thanks for making me independent in the lab. I wish, you could have stayed in the lab till summer of 2012 and I would have learned swimming as well. But no worries! I did learn floating on my back.

Mirko: You were always there in the absence of Simone and after she left. You have always helped everyone in the lab including me, that's what comes naturally to you. I am sure, one day I shall hear your name in the crowd and tell my children, hey that's my friend. Thanks for a beautiful album you and Iris have made for me. My parents show it to our relatives and friends proudly.

Jessica: Thank you and Hirdesh so much for dinners in Rajarani! Apart from that you were an amazing mate in the lab. Together with Simone and Mirko, you as well had a helping hand in the lab in making me an indepdent planner and executer of the experiments.

Leandro: (or Leander as Jessica gave him a name). They used to say Leander was the meanest person in the lab but actually you were not. I still remember Simone's farewell party at your place and if I remember correctly; Mirko, Simone and I were the last to leave you house.

Marek: Chronologically, you should be the first as we both worked on the same electron microscope in Mumbai. But we didn't meet due to different working timings. I have to thank you for rescuing my life not once but twice while water-skiing. I have to admit that I am able to finish my PhD only because I am alive today. Marek, you are a true water-gun.

Jagadeesh: Amongst all my outside friends, I wish to include only your name in this acknowledgement. Thank you very much for being the best buddy throughout my thesis.

Catherine: Thank you very much for teaching me how to behave! I shall try to imbibe in me all the etiquettes required for a well-behaved gentleman.

Gunnar: Constant pushing from you has catalyzed the finishing up of my thesis and finding a postdoctoral position. The process would have been very slow otherwise. Additionally, thanks a lot for helping me with all the stupid questions related to cloning, writing, etc.

Dennis: Thanks you for providing me with a marker free parasite line with a fluorescent background. Working with this parasite line would certainly raise the level and quality of my paper. Additionally, I also thank Konrad for characterizing that parasite line with me.

Andrea (special thanks): You are the best student I ever had. I still wonder how you managed to clone *Pf*-coronin in one week, which I could not manage in 4 months. You truly have magical hands, Andrea. And then in few days, you became a good friend of mine and we watched so many bollywood movies together. Thanks a lot for organizing my 28th Birthday, taking me for ice-skating followed by a delicious Mexican food! Everything was so properly and timely organized.

Hirdesh: Bhai tu bhai hai bhai! Tere liye toh apun hindi mech likhega! Yaar tu solid hai bhai! Tunech apun ko sikhaya life ko kaise jite hai. Bhai tu nahi hota toh main toh, tere ko toh sab pata hai na bhai! Thanks a lot for late night dinners and back to working in lab times. It would have been difficult otherwise.

Miriam: Thanks a lot for carrying out some of the experiments which were a part of my project and assisting me in the lab with mice smearing, going to animal facility, mouse hotel, etc. in fact, there is a lot that you help with for everyone. Your helping hands are highly appreciated. Thank you very much!

Ross: Thanks a lot! You are the one who made me laugh with his jokes after Freddy, of course! Apart from actin', you have taught me how to create a double meaning humor. If you have not realized it in previous sentence then I am still not yet good at it. Also thank you for correcting my TAC reports, SOPs, CVs, abstracts, cover letters etc. It really helped me progress and get the next job.

Konrad and Frea: Thank you for teaching me how important it is to be a yes man types! Apparently, I realized it helps overcome supreme circumstances. Thanks a lot for being very understanding!

Mendi: You are my first African-Fijian friend! The delicious food you have brought in the lab will always be remembered. Thanks a lot for having great conversations in the lab on various topics. Similar to Jagadeesh, you and Ross also have taught me how to converse with people.

Inari Kursula and Dominique Soldati: You two have taught me one of the most important lessons in science. i.e. with whom one should communicate his or her research. Specially, you two will always be remembered whenever I will discuss my scientific ideas with someone.

Ben and Leena: The most amazing couple! Thanks Ben very much for the great fun time in the lab. Thanks also for repairing my hard-disk. You together with Konrad have rocked my time in the lab.

Julia: In line with Priyanka, you are yet another elder sister of mine! Thank you very much for helping in the coronin project! The efforts you have put in are highly appreciable. You enabled us to accomplish a plethora of experiments in time. Hats off to your organization! Thanks also for assisting in formalities with job contract and VISA when I was injured. Many thanks for translating the abstract of this thesis in German!

Saskia: Thanks for above translation of the abstract. Although you were in the lab only during my final year, the discussion on some of the interesting papers (e.g. aldolase paper) will always be remembered. You were also an important actin binding person along with Ross, Julia and Catherine.

Key players during and after my knee operation:

Bishal: The first time, I heard your name was on Plasmodium ADF structure paper. Then you together with Jagadeesh started our Sunday afternoon Science clubs. Later, you proved to be my best mate from the day of my operation. I still remember you made the Holi happen in HD and you yourself did not celebrate it because it was organized on the same day of my knee surgery. That food from Mensa and ice packs that brought down the knee swelling! Thanks man! Half of the credit that I am able to walk now is yours.

Jubin: Of course, you share other half of the credit. Thanks for lunch and dinner at appropriate times. Thanks for taking me and bringing me back to and from the hospital 3 times a week for 6 weeks continuously. I also want to thank you for restarting my calcium-signaling project. I had almost stopped thinking about it. The continuous discussions with you about your previous cancer signaling project has given me anchors to hold onto my signaling project. And, see how it evolved!

Special Thanks to Jake and Freddy……

Jake along with Maya: Thanks Jake for hosting me in your lab at WEHI, Melbourne. One of the most important thing, I learnt in your lab was bac-to-bac system. The credit is all yours

Maya. The discussions Freddy and I had with you on the coronin front were simply great. Thanks a lot! And we will keep in touch!

Freddy: Thanks a lot for making me a part of your lab and great scientific atmosphere you created around me. You have made me amazed by science and let me enjoy my PhD. This initially freaked me a bit but in the long run boosted my confidence to follow my ideas. It feels so good when our own ideas are getting tested. You have provided me a platform to experience this feeling. You have provided me with excellent teachers, Simone-Mirko-Jessica and an intelligent student, Andrea. Both the learning and teaching experiences were great! Apart from science, you have opted multiple ways to train me. Consequently I got multiple opportunities to hone my skills in writing, presenting, communicating and scientific session chairing. Thank you very much for everything!

Zusammenfassung

Coronine sind Aktin-bindende Proteine und regulieren eine Vielzahl an zellulären Prozessen einschließlich der Zellmigration diverser Zellen von *Dictyostelium* bis hin zu Neuronen. Malaria-Parasiten müssen sich bewegen, um in Gewebe eindringen und Wirtszellen infizieren zu können. In der vorliegenden Arbeit zeige ich, dass *Plasmodium berghei* Coronin ein wichtiger Regulator der gleitenden Bewegung von Sporozoiten ist. Sporozoiten stellen die motilen Lebensformen des Erregers dar und werden von Moskitos an den Nagetierwirt übertragen. Mit Hilfe von *in situ* Fluoreszenzmarkierung konnte Coronin an der Peripherie der Sporozoiten lokalisiert werden. Dort liegt zwischen der Plasmamembran und dem inneren Membrankomplex der Aktin-Myosin Motor verankert, welcher die Parasiten vorwärts treibt. Sporozoiten können mittels externer Liganden aktiviert werden. Diese lösen eine intrazelluläre Freisetzung von Kalzium und eine Bindung von Coronin an Aktin aus. Interessanterweise, re-lokalisiert Coronin nach Aktivierung der Sporozoiten von der kompletten Peripherie an das hintere Ende des Parasiten. Hier findet der cAMP-Protein Kinase A-Signalweg statt, welcher eine essentielle Funktion in der Depolymerisation von F-Aktin besitzt. Dies lässt darauf schließen, dass Kalzium- und cAMP-gesteuerte Signalwege miteinander verbunden sind, wobei die Kalzium-abhängigen Signalwege hauptsächlich während der Parasitenbewegung agieren, während cAMP-Signalwege bei der Hepatozyteninvasion eine größere Rolle spielen. Die Mutation der Aktin-Bindestellen im endogenen Coronin führt zu ähnlichen Defekten bei der Sporozoitenbewegung wie bei der kompletten Deletion von Coronin. Im Gegensatz zu *coronin (-)* Sporozoiten, welche kleinere Leberstadien entwickeln, zeigen Sprozozoiten mit Mutationen in der Aktinbindestelle von Coronin keinen Defekt in der Leberstadienentwicklung. Dies deutet auf eine Aktin-unabhängige Funktion von Coronin für diese Entwicklungsphase hin. Die Bewegungs- und Entwicklungsdefekte, welche durch eine Deletion von Coronin auftreten, können mit *Plasmodium falciparum* Coronin komplementiert werden. Dieses weist eine 57 prozentige Ähnlichkeit mit *Pb*Coronin auf und es konnte experimentell gezeigt werden, dass *Pf*-Coronin Aktinfilamente bündelt. Abschließend ist zu sagen, dass eine Überexpression von Coronin weder das Wachstum noch die Entwicklung von *P. berghei* nachteilig beeinflussen, was im Kontrast zu Überexpressionsdefekten von Coronin in Hefe steht. Dies ist hilfreich, da die

Überexpression von fluoreszent-gelabeltem Coronin in Ookineten verwendet werden kann um die Anwesenheit von Aktinfilamenten zu erforschen.

Abstract

Coronins are actin-binding proteins that regulate many cellular processes including cell migration in a diverse range of cells from *Dictyostelium* to neurons. Malaria parasites need to migrate in order to penetrate tissue barriers and enter host cells. Here I show that *Plasmodium berghei* coronin is an important regulator of gliding motility in sporozoites, the highly motile life cycle forms of the parasite that are transmitted by mosquitoes to the rodent host. Using *in situ* tagging coronin was found to localize to the periphery of sporozoites, where an actin-myosin motor propels the parasite. During sporozoite activation through external ligands, which triggers intracellular calcium release and coronin binding to actin, coronin relocalizes to the rear end of the parasite; there cAMP-protein kinase A pathway is essential for depolymerization of F-actin. I suggest that calcium and cAMP mediated signaling are linked such that calcium dominated signaling operates during motility, while cAMP dominated signaling operates during the hepatocyte invasion. Ablation of the actin binding sites of endogenous coronin leads to defects in sporozoite motility similar to *coronin(-)*. However, unlike *coronin(-),* which develops smaller liver stages, the actin-binding mutants do not exhibit this liver stage developmental defect suggesting an actin-independent function of coronin. Motility and developmental defects exhibited by *coronin(-)* are partially complemented by *Pf*-coronin which displays 57% identity with the *P. berghei* protein and has experimentally been shown to bundle actin filaments. Finally, the overexpression of coronin is not deleterious to growth and development of *P. berghei,* unlike the overexpression defect exhibited by yeast coronin. This benefits the study of ookinete motility as the overexpression of fluorescent coronin aids in probing the presence of actin filaments.

Abbreviations

µg	Microgram
µL	Microliter
µM	Micromolar
PBS	Phosphate buffered saline
AMP	Adenosine monophosphate
cAMP	cyclic Adenosine monophosphate
ATP	Adenosine triphosphate
BSA	Bovine serum albumin
DNA	Deoxyribonucleic acid
Jas	jasplakinolide
Cyto D	Cytochalasin D
FBS	Fetal bovine serum
F-actin	Filamentous actin
G-actin	Globular actin
IFA	Immunofluorescence assay
HSP 70	Heat shock protein 70 kD
eGFP	Enhanced green fluorescent protein
IMC	Inner membrane complex
ORF	Open reading frame
PCR	Polymerase chain reaction
PKA	Protein kinase A
AC	Adenyl cyclase
NMRI	Navel medical research center
SAS	Supra-alveolar space
Spp	Species
TRAP	Thrombospondin related anonymous protein
UTR	Untranslated region
v/v	Volume / volume
w/v	Weight / volume
WT	Wild type
RPMI	Roswell Park Memorial Institute medium
N-terminal	Amino terminal
C-terminal	Carboxy terminal
Taq	Thermus aquaticus
ECM	Experimental cerebral malaria
PKC	Protein kinase C
PLC	Phospholipase C
CK 2	Casein kinase II
PI(4,5)P2	Phosphotidylinositol (4,5)-bisphosphate
DIC	Differential Interference Contrast
EMAA	Erythrocte Membrane Associated Antigen
UF	Unfolded

Pi	Inorganic phosphate
ADF	Actin depolymerizing factor
Aip	Actin interacting protein
NMJ	Neuromuscular junction
AChR	Acetylcholine receptor
GTPase	Guanosine nucleotide triphosphatase
GDP	Guanosine diphosphate
GTP	Guanosine triphosphate
PDGF	Plate derived growth factor
VSMC	Vascular smooth muscle cell
HL	Haemolymph
MGS	Midgut sporozoites
SGS	Salivary gland sporozoites
RT	Room temperature
HCl	Hydrochloric acid
PAGE	Polyacrylamide gel electrophoresis
SDS	Sodium dodecyl sulfate
BME	β-mercaptoethanol
HepG2	Liver hepatocellular carcinoma
BAPTA-AM	1,2-bis(o-aminophenoxy)ethane-N,N,N',N'-tetraacetic acid)-Acetoxymethyle ester
DAG	Diacyl glycerol
IP3	Inositol (1,4,5)-trisphosphate
GFP	Green fluorescent protein
FRAP	Fluorescence recovery after photobleaching
MLC	Myosin light chain
MTIP	Myosin tail interacting protein
GAP	Glideosome associated protein
bb	Bite back
i.v.	intravenous
i.p.	intraperitoneal
RBC	Red blood cell
NA	Numerical aperture
F/R	Front to rear
ROI	Region of interest
DMEM	Dulbecco modified eagle’s medium

Table of contents

List of figures

List of tables

List of graphs

1. Introduction

Cells exhibit a plethora of biological phenomena. In order to survive, cells need to migrate, divide, traffic metabolites or proteins from one compartment to another, secrete or internalize substances and degrade toxic products. To accomplish this, cells are equipped with a panoply of proteins. For example, cytoskeletal proteins like actin and tubulin form dynamic filaments that assist in migration and cytokinesis. These long filaments also serve as a structural scaffold over which vesicles can be transported. However, the dynamicity of these filaments needs regulation with respect to their stabilization, polymerization or depolymerization. This regulation is generally brought about by several actin or microtubule binding proteins working in concert with each other. Amongst them, coronin appears to be *'The jack of all trades'*. This is evident from previous work, as coronin from amoeba to human is shown to be involved in; (i) actin dynamics (migration), (ii) microtubule reorganization (cytokinesis), (iii) vesicular trafficking and (iv) anterio-posterior polarity. In addition coronin is shown to play a role in the retrograde transport (of secretory membrane for further endocytosis) and ubiquitination of proteins (protein degradation) (refer section 1.4).

1.1 Coronin family of proteins and the WD40 repeats

Corona stands for crown. The protein was originally identified in the crown-like projections of the amoeboid cell, *Dictyostellium discoidium* (*Dd*) (de Hostos et al, 1991) and was thus named coronin (crown-like). Coronin was found in the extract of proteins that form the cytoskeleton in *Dd* and was therefore associated with motility and chemotaxis of these cells (de Hostos et al, 1993; Gerisch et al, 1993). Later, while studying phospholipase C, Suzuki et al identified a protein in calf spleen and human leukemia cell line (HL60). It had a molecular weight of 57 kDa and was hence named p57. It had phosphoinositide hydrolytic activity. P57 showed 40% similarity to *Dd*-coronin. However unlike *Dd*-coronin, which consists exclusively of 7 WD repeats, p57 has 2 domains; the WD repeats and a leucine zipper (Suzuki et al, 1995). WD repeats interact with other proteins while leucine zipper motifs help in the formation of homo or hetero-oligomers.

A leucine zipper is a stretch of basic amino acids at the C-terminus of a protein that helps to form an oligomer with a protein having a similar stretch of basic amino acids. Proteins, like transcription factors possess such leucine zipper motifs that assist in the formation of heterodimer with other transcription factors having similar domains. However, p57, identified in calf spleen or HL60 has a non-conserved leucine zipper domain. Thus, it could only form homo-oligomer and not hetero-oligomer (Oku et al, 2005; Vinson et al, 1993).

Unlike the leucine zipper domains, which are found at the C-terminus, WD repeats begin at amino acid 6-94 from the N-terminus. The repeats begin with glycine and histidine (GH) and are usually about 40 amino acids long. Typically containing the dipeptide motif WD these domain are also referred to as WD40 repeats. These fold into a propeller-like structure, called a β-propeller. Each of the individual WD40 repeats is also called a blade. It has been proposed that less than four and more than 8 WD40 repeats are thermodynamically not capable to form a stable β-propeller. Less than 4 WD40 repeats will not form a complete β-propeller, 9 or more WD40 repeats would result in the center being exposed to the solvent. Since, the amino acids that form the WD40 repeats are hydrophobic, a β-propeller with more than nine WD40 repeats will be thermodynamically unstable. An exception to this is a WD40 repeat protein of cyanobacteria. It is predicted to have 11 blades/WD 40 repeats (PCC6803). Thus, it is most likely to form two β-propellers instead of one; the function of that is however still unknown (Hisbergues et al, 2001). All the structures of WD40 repeat proteins deposited in PDB (www.pdb.org) to date have 7 blades. They include e.g. guanine nucleotide binding protein beta subunit 5 and coronin 1A (Appleton et al, 2006; de Hostos et al, 1991; Watson et al, 1994).

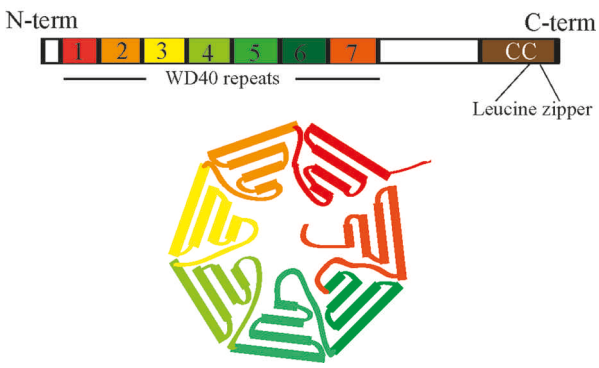

Fig 1.1: Molecular architecture of coronin. Linear architecture of coronin showing positions of WD40 repeats at the N-terminus and leucine zipper in the coiled-coiled (CC) domain at the C-terminus (top). The WD40 repeats fold in a propeller like structure, where each of 7 WD40 repeats forms a ß-sheet with 4 antiparallel strands (bottom).

However, Cdc4 (PDB:1NEX) and Sif2p (PDB: 1R5M) have eight WD40 domains (Cerna & Wilson, 2005; Orlicky et al, 2003). The general PROSITE motif (amino acid architecture) of WD40 repeats family of protein is $[X_{6\text{-}94} – (GH – X_{23\text{-}41} – WD)] N^{4\text{-}8}$ (Smith, 2008).

To probe the functional homology of WD repeat proteins, one must consider the number of WD repeats, the equivalent positions of WD repeats and a statistically significant similarity in the amino acids at the carboxy terminus (Neer et al, 1994). Interesting to note here is that similar to WD40 type, there are 20 other types that form a propeller with 4-8 blades. It is a common fold since three billion years, with each blade consisting of 4 antiparallel beta strands radiating outwards having conserved aromatic and hydrophobic amino acids (Neer & Smith, 2000). Thus, it is important to be able to distinguish between WD repeats and non-WD repeat proteins, which are summarized in the following table:

Parameters	**WD repeat proteins**	**Non-WD repeat proteins**
Shape of propeller	β-propeller	disc shaped
Organisms	eukaryotes	prokaryotes
Function	protein-protein interaction	enzymatic

Adapted from Vilmos Fulop and David Jone (1999)

The diameter of the β-propeller is 40 Å with a thickness of about 25 Å. There are about 160 WD repeat proteins identified of which more than 50 are from the yeast *Saccharomyces cerevisiae* (Smith et al, 1999). A plethora of WD40 repeats containing proteins belong to the coronin family of proteins. Coronins have been classified without a mutually agreed upon classification scheme. Thus, I recapitulate the previously proposed scheme of nomenclature:

Proposed name	**Proposed symbol**	**Current name**	**Current symbol**	**Spp. distribution**
Coronin 1	CRN1	Coronin 1B	CORO1B	Vertebrates
Coronin 2	CRN2	Coronin 1C	CORO1C	Vertebrates
Coronin 3	CRN3	Coronin 6	CORO6	Vertebrates
Coronin 4	CRN4	Coronin 1A	CORO1A	Vertebrates
Coronin 5	CRN5	Coronin 2A	CORO2A	Vertebrates
Coronin 6	CRN6	Coronin 2B	CORO2B	Vertebrates
Coronin 7	CRN7	--	CORO7	Mycetozoa, Fungi, Metazoa
Coronin 8	CRN8	--	--	Invertebrates
Coronin 9	CRN9	--	--	Invertebrates
Coronin 10	CRN10	--	--	Alveolata
Coronin 11	CRN11	--	--	Fungi
Coronin 12	CRN12	--	--	Amoeba

Adapted from Morgan RO and Fernandez MP, 2008 (Morgan & Fernandez, 2008)

1.2 Coronin in the molecular context

Coronin was originally found in actomyosin extracts of slime mold and its homologue in mammals, p57 was later found as a contaminant while purifying phospholipase C (Suzuki et al, 1995). These initial studies suggested that coronin binds to both the actin cytoskeleton and phosphoinositides such as PI(4,5)P2.

1.2.1 Coronin binds to filamentous actin (F-actin)

Dd-coronin was found to bind actin in an *in vitro* system (de Hostos et al, 1991; Gerisch et al, 1995). To identify the regions of p57 that assist in its binding to actin, *Teruki et al,* fused the short constructs of the gene encoding either the N-terminus or C-terminus or WD repeats to glutathione S-transferase. By cosedimentation of these with filamentous actin *in vitro* and colocalization with actin *in vivo,* they suggested two regions of p57 responsible for binding to actin filaments (Oku et al, 2003). A third actin-binding site was later detected in p57; it lies in the leucine zipper motif at the C-terminus of the protein (Liu et al, 2006).

The structure of mouse coronin 1A was solved in 2006. It suggested that the WD40 repeats of coronin stabilizes its structure. Therefore, the short constructs of coronin that lack individual blades or the C-terminal extension may not fold properly. Thus, the experiments with such short coronin constructs may lead to false ideas about how coronin acts in the cellular context (Appleton et al, 2006).

In order to understand the mechanism through which coronin 1A binds to F-actin, one must first examine the structure of actin itself. The actin protomer (G-actin) is composed of 4 subunits: subdomains 1, 2, 3 and 4. In an actin filament (F-actin), these protomers are arranged such that subdomains 2 and 4 of one molecule interact with subdomains 1 and 3 of a neighboring protomer. The exposed surfaces of subdomains 1 and 3 form the barbed end of actin filament, where actin is usually polymerized, whereas the exposed surfaces of subdomains 2 and 4 form pointed ends where actin is usually depolymerized (Fujii et al, 2010; Reisler & Egelman, 2007). Coronin 1A simultaneously binds to 3 protomers of actin. It interacts with the subdomain-1 and subdomain-2 of two actin protomers on the same strand of F-actin with subdomain 4 of the third protomer on the parallel strand. This way, coronin 1A staples the opposite strands of the actin filaments, consequently stabilizing them (Galkin et al, 2008). Coronin 1B displays nucleotide dependent affinity for F-actin. It has a strong affinity for ATP/ADP-Pi-F-actin (170nM) when compared to ADP-F-actin (8 μM). The amino acid residue (Arg^{30}) of coronin 1B is crucial for its

binding to F-actin *in vitro* (Cai et al, 2007). The recent evidence in mammalian coronin 1C (synonym: CRN2) suggests that there is a second actin-binding site present other than the conventional Arg^{30}. Unlike coronin 1A and 1B, it confers cooperative binding of coronin1C to actin filaments (Cai et al, 2007; Chan et al, 2012).

Systematic mutagenesis of the functional surfaces of yeast coronin (*Sc*-coronin) has shed light on the actin-binding residues of coronin. Alignment of 180 coronin proteins resulted in the identification of 21 conserved sites. Each of these consists of 2-4 amino acid residues. Furthermore, mutations of *Sc*-coronin by a 'charge to alanine' strategy were probed for actin-binding, colocalization with actin and overexpression defect in *S. cerevisiae*. This study implicates that there are 5 actin-binding sites in coronin (Gandhi et al, 2010). These actin-binding sites were labeled according to the mutation profile: they are (i) 1,2 (for K10A, R12A); (ii) 1,6 (for R141A, K142A); (iii) 1,13 (for K295A, D297A); (iv) 1,17 (for E320A, R323A) and (v) 1,19 (for R361A, R362A, E364A and E365A). Apart from these 5 sites, they also identified a conserved site present on coronin surface. It showed moderate phenotypes when mutated, labeled as 1,16 (for E312A, E315A). This was predicted to be a cofilin binding site, but experimental data to probe this interaction is still missing.

When these sites were mapped onto the mouse coronin crystal structure, all actin-binding sites were found to be present on the surface of the β-propeller region of coronin. An alternative coronin structure available in PDB is from the apicomplexan parasite *Toxoplasma gondii (Tg)*. It is structurally very similar to mouse coronin 1 (Salamun et al, 2014). As expected, actin-binding sites are conserved on the surface of *Tg*-coronin. However, biochemical assays found that *Tg*-coronin only weakly binds to rabbit actin, the protein used in classic actin-binding studies. These findings are congruent with studies in *Plasmodium falciparum (Pf)*, a species also belonging to the phylum Apicomplexa. In *P. falciparum,* only a fraction of coronin binds to rabbit actin (*Plasmodium* actin has hitherto not been able to be produced in sufficient quantities in order to perform such binding studies with endogenous *Plasmodium* protein components). Alternatively, this could hint towards another function of coronin. Interestingly, the absence of a leucine zipper motif at the C-terminus of *Tg*-coronin and *Pf*-coronin (like in *Dd*-coronin) suggested that, apicomplexan coronin cannot form homo-oligomers (Tardieux et al, 1998). Nevertheless, size exclusion chromatography and static light scattering experiments showed that *Tg*-coronin indeed does form a dimer ((Salamun et al, 2014), also refer section 1.7).

The C-terminal coiled coil domain of coronin binds to the Arp2/3 complex (a complex of the actin related protein (Arp) 2, Arp3 and 5 other proteins that nucleates actin filaments) thereby inhibiting its nucleation activity (Humphries et al, 2002). The inhibitory effect of coronin on actin filament formation via binding to Arp2/3 is dependent on the concentration of coronin. At higher concentrations of coronin, F-actin is decorated with coronin and thus Arp2/3 cannot bind to F-actin resulting in no nucleation of actin filaments. At lower concentrations coronin recruits Arp2/3 on actin filaments for the nucleation and elongation (Liu et al, 2011).

While coronin recruits Arp2/3 for nucleating the branches of ATP-F-actin, it is also known to recruit cofilin for severing of ADP-F-actin at the pointed end. Therefore, coronin is known to switch roles depending on the nucleotide state of actin. Although, the coiled coil domain present in C-terminal region of coronin antagonizes cofilin activity, coronin without the coiled coil domain enhanced the cofilin mediated disassembly of actin filaments (Gandhi et al, 2009).

Interestingly, *Plasmodium* has only a minimal set of actin-binding proteins, however I focus on Arp2/3, ADFs and coronin in this section. The organisms of the genus *Plasmodium* lack Arp2 and Arp3 subunits that form a complex for actin filament branching, but has two actin depolymerizing factors ADF1 and ADF2, along with one homologue of coronin. In *P. falciparum*, ADF1 lacks conventional F-actin-binding sites, but it switches the nucleotide state of monomeric actin (G-actin) from ADP-G-actin to ATP-G-actin, unlike other ADF proteins (Schuler & Matuschewski, 2006). Recently chemical crosslinking and mass spectrometry (XL-MS) experiments described the previously unidentified actin-binding interface of Pf-ADF1 (Wong et al, 2014). In contrast, *Plasmodium* ADF2 is sequentially similar to canonical actin depolymerizing factors. Pb-ADF2 expressed and purified from *E. coli* binds to both G-actin and F-actin (Singh et al, 2011). Lastly, *Plasmodium* coronin binds weakly to actin filaments but the mechanistic details ((Tardieux et al, 1998); also refer section 1.7) and regulation of actin by actin-binding sites on coronin are still unexplored.

```
Mm_coronin1A 23 QCYEDVRVSQTTWD 36 ----- 284 LCGKGDSSIRY 294 ----- 322
Sc_coronin   22 LQYEKLKVTNNAWD 35 ----- 292 LVGKGDGNIRY 302 ----- 329
Pf_coronin   17 NLYGDLRICSRATE 30 ----- 279 LIGKGDGNCRY 289 ----- 316
Pb_coronin   18 SGFDDLRICTRITE 31 ----- 280 IIGKGDGNCRY 290 ----- 317


Mm_coronin1A PKRGLEVNKCEIAR-FYKLHERKCEPIAMTVPRK-SDLFQEDLYPPTAGPDP 372
Sc_coronin   PKRMVNVKENEVLKGFKTVVDQRIEPVSFFVPRR-SEEFQEDIYPDAPSNKP 382
Pf_coronin   PKRMCDVYKCEIGRVYKNENNTDIRPISFYVPRKNSSIFQEDLYPPIIMRDP 367
Pb_coronin   PKQVCNIYKCEIGRIYKNENDKSIKPISFYVPRKNPNIFQEDLYPPIIMHDP 368
```

Fig 1.2: Actin binding sites are conserved in coronins. Multiple sequence alignment of different coronins showing amino acids important for actin binding are conserved across mammals, yeast and apicomplexans (marked in red).

After comparison of *P.berghei (Pb)* coronin with the above studies and multiple sequence alignments with mammalian, yeast and apicomplexan coronin, I identified the conserved putative actin-binding sites on *Pb*-coronin: (i) R24, R28 ($Arg^{29 \text{ or } 30}$ in mammalian coronin, this site has not yet been studied in yeast.); (ii) K283, D285 (1,13 from *Sc*-coronin); (iii) E327, R330 (1,17 from *Sc*-coronin) and (iv) R349, K350 (partially of 1.19 from *Sc*-coronin).

1.2.2 Coronin-interaction sites on actin

The previous section discussed the coronin's side in coronin-actin interaction. Here, I focus more on actin's side of it. A seminal study in this regard is the cryo-EM structure of *Sc*-coronin bound to *Sc*-actin filaments. It shows 5 distinct coronin-binding sites on actin; R37, R39; K50, D51; D80, D81; E83, D84 and D363, E364. Mutational studies with these residues resulted in a clear 2-fold decrease in affinity to coronin (Ge et al, 2014).

In addition to the cryo-EM structure of *Sc*-coronin bound to F-actin together with *Galkin et al*'s atomic model of doubly cofilin decorated F-actin implies that there exists a competition between the coronin and cofilin in binding to actin. Specifically, one monomer of cofilin binds on the actin surface at aa 112-126 and another binds at aa 359-364 (Galkin et al, 2008); that latter can also be bound by coronin. The presence of coronin on this site of actin filaments ablates the binding of the second monomer of cofilin. Consequently, depolymerization of F-actin mediated by cofilin is inhibited leading to more stable and long-lived filaments. These studies provide a clear mechanistic insight how coronin protects actin filaments from the cofilin-mediated severing of the newly formed actin filaments. Similar to the coronin induced inhibition of cofilin's action on F-actin, structural basis of Arp2/3 binding to F-actin also suggests that Arp2/3 mediated actin nucleation is inhibited, when F-actin is decorated with coronin (Liu et al, 2011; Rouiller et al, 2008).

After comparing with *P. berghei* actins, it appears that in actin I, there exists R36, K38; K49, D50; D81, D82; E84, K85 and D364, E365. Similarly, in actin II, they are I35, K37; K48, E49; D80, D81; E83, K84 and D364, E365.

1.2.3 Phosphoinositides regulate the function of coronin.

The membrane phospholipid phosphatidylinositol (4,5)-bisphosphate [PI(4,5)P2] interacts with various actin-binding proteins. For example, gelsolin, cofilin and profilin are known to be regulated by PI(4,5)P2 (Gorbatyuk et al, 2006; Janmey & Lindberg, 2004; Yin & Janmey, 2003; Yonezawa et al, 1990). Coronin serves no exception to this rule as the proteomic data of acid phospholipid binding proteins suggested that phosphoinositides regulate coronin 1A by inhibiting its activity of actin filament disassembly (Tsujita et al, 2010). This could be because the actin-binding sites present on the surface of coronin overlap with the PI(4,5)P2 binding sites. In *P. falciparum*, coronin localizes close to the plasma membrane. The experiments with surface plasma resonance suggested that *Pf*-coronin has affinity for PI(4,5)P2 in a micromolar range with dissociation constant (K_d) being 0.64 μM as compared to K_d of 27 nM for PH domain of phospholipase C (Olshina et al, 2015).

The prediction that PI(4,5)P2 binding sites overlap with actin-binding sites and the evidence from *P. falciparum*, the close relative of *P. berghei* suggest that systematic mutagenesis of actin-binding sites could give mechanistic insights about membrane binding and PI(4,5)P2 mediated regulation of coronin.

1.2.4 The post-translational modification by phosphorylation regulates coronin function.

The function of coronin is also regulated by phosphorylaiton. For example, coronin 1B is phosphorylated by protein kinase C (PKC) at position ser-2. This, in turn, inhibits binding of coronin to Arp2/3 complex without affecting the localization and homo-oligomerization of coronin (Cai et al, 2005). In contrast, coronin 1C (synonyms: coronin 3, CRN2) is phosphorylated at another residue; ser-463 by another protein kinase; CK2 (synonyms: casein kinase II or CK II). Moreover, the phosphomimetic mutants of coronin 1C indicated that phosphorylation only inhibits the disassembly of coronin trimer, however it does not influence actin polymerization (Xavier et al, 2012). This suggests that the phosphorylation of coronin accomplishes different modes of F-actin regulation in two different coronins. This could be expected as the phosphorylation site of coronin 1B is far from the coiled coil domain that causes

the homo-oligomerization, while the phosphorylation site of coronin 1C is within the coiled coil domain.

In sum, coronin regulates actin dynamics by interacting with actin, Arp2/3 and cofilin/ADFs, while the function of coronin is regulated by phosphoinositide PI(4,5)P2 and kinases that phosphorylate coronin.

1.3 Coronin in a cellular context

Interactions of coronin with proteins (described in section 1.2) have major effects on migration and cytokinesis. Both of these are associated with the actin and microtubule regulatory functions of coronin. Some members of the coronin family are known to perform diverse functions including protein degradation, retrograde transport and signaling. This section summarizes these functions of coronin in various cell types from *Dictyostelium* to humans.

1.3.1 Actin and microtubule associated functions of coronin

Dictyostelium discodium Dd-coronin fused to a fluorescent tag (GFP-CorA) localizes to sites where actin is disassembled (Bretschneider et al, 2009; Heinrich et al, 2008). Perhaps, this is why *coronin* null *D. discoidium* cells have numerous surface protrusions that are enriched in F-actin and cofilin. The deletion of *coronin* together with *Aip* (actin interacting protein) often fails to form fruiting bodies. Thus, cells are retarded in growth. This double mutant fails to form proper cleavage furrow and therefore are defective in cytokinesis. These defects were attributed to the hyper-polymerization of actin filaments (Ishikawa-Ankerhold et al, 2010).

In budding yeast *S. cerevisiae*, the Crn1p (synonym: *Sc*-coronin) forms complex networks of F-actin by crosslinking them. This property of Crn1p resides in the coiled coil domain indicating that dimerization of coronin is a prerequisite for this crosslinking. Crn1p has sequences similar to MT binding protein MAP1B; not conserved in other members of coronin family. The fact, that coronin cosediments microtubules in the presence of F-actin may provide a link between these two cytoskeletons. In addition, the overexpression of Crn1p also alters actin and microtubule organization, consequently causing a growth arrest (Goode et al, 1999). This implicates that the expression levels of coronin are equally important for the function. In *Drosophila,* the coronin-like protein dpod1 localizes to the ends of growing axons, where actin filaments may interact with MT. Dpod1 also has a microtubule-binding domain, like MAP1B. Similar to *Sc*-coronin-F-actin bundles, dpod1-F-actin also cosediments with tubulin. It is

speculated that dpod1 crosslinks F-actin and MT for a proper axonal guidance in the growth cones, which in turn leads to normal development of the nervous system in *Drosophila* (Rothenberg et al, 2003; Rybakin & Clemen, 2005). In *C. elegans*, POD-1 (coronin like protein, synonym: CABP11) colocalizes with cortical actin and attaches vesicles to actin microfilaments and consequently assists in vesicular trafficking. Furthermore, POD1-deficient early embryos exhibit the loss of molecular and physical defects in the anterior-posteriro polarity and therefore form abnormal cellular structures (Rappleye et al, 1999). In vertebrates, coronin is generally localized to the leading edge of migrating cells (Mishima & Nishida, 1999); specifically it enhances chemotaxis in human lung endothelial cells (Usatyuk et al, 2013). In vascular smooth muscle cells (VSMC), upon stimulation with platelet-derived growth factor (PDGF), coronin 1B induces migration. Phosphorylation of coronin 1B negatively regulates this migration, as the phospho-deficient S2A mutant of coronin 1B decreased migration of VSMC. The overexpression of WT coronin also decreases cell migration via a mechanism that is not yet properly investigated (Williams et al, 2012). In *Leishmania*, coronin regulates the subpellicular corset microtubule re-organization during cytokinesis and is thus essential for survival of *Leishmania*. Interestingly, it is present in the posterior portion of dividing *Leishmania* cells colocalizing with tubulin and kinesin (Sahasrabuddhe et al, 2009).

1.3.2 Other cellular functions of coronin

Protein degradation: Coronin 7 (CRN7) causes the degradation of the protein tob by increasing its ubiquitination. Coronin 7 also interacts with the components of ubiquitin ligase complex like elongin B and elongin C. Although tob is a negative regulator of cell cycle progression, enforced overexpression of coronin 7 has no effect on the cell cycle. Thus, the significance of coronin 7 in the degradation of tob is still unexplored (Watanabe et al, 2011).

Retrograde transport: In the pancreatic β cells that secrete insulin by exocytosis, internalization of the secretary membrane is needed. A small GTPase, GDP-Rab27a binds to coronin3 after the activation by glucose and the membrane is internalized so it could be transported back for following endocytosis (Kimura et al, 2010).

Linking plasma membrane receptor to actin cytoskeleton: The seminal study in this area investigated the neuromuscular junction (NMJ) that links motor neurons to skeletal muscles. At the NMJ the extracellular ligands like agrin or laminin induce clustering of the acetylcholine receptors (AChRs) for the efficient transmission of signals to the synapse. This clustering at the

cytoplasmic side is mediated by coronin 6, which forms a complex with AChRs and actin cytoskeleton. As could be expected, deletion of *coronin 6* leads to destabilization of these clusters (Chen et al, 2014). Therefore, it is clear that coronin 6 provides a structural scaffold linking receptor in the plasma membrane to actin cytoskeleton.

1.3.3 Coronin in signaling

Coronin is a genuine multifunctional protein that plays diverse roles in many biological processes. Given the sequence similarity of coronin with the beta subunit of the multimeric G-protein complex (de Hostos et al, 1991), it is unsurprising that coronin plays a role in signaling. In addition, coronin has been shown to interact with well-known signaling proteins like Gαs, phospholipase C (PLC, a protein involved in calcium signaling) and Rac (a small GTPases of the Rho family that relay outside-in signaling leading to actin polymerization).

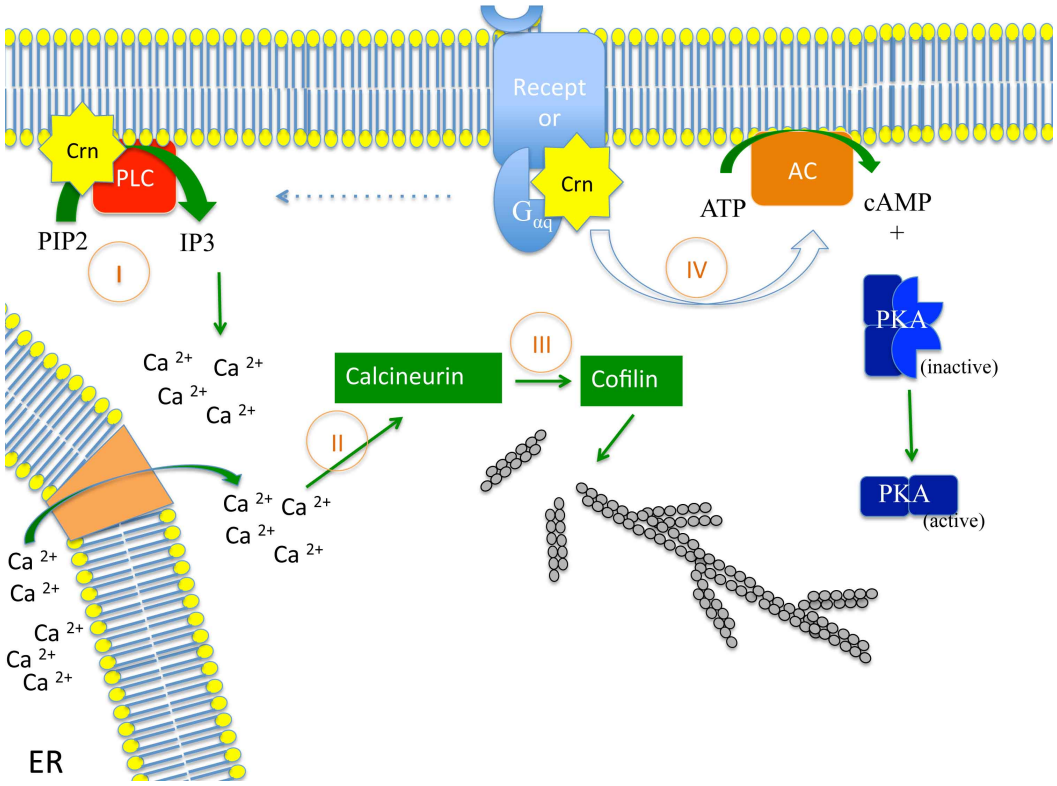

Fig 1.3: Coronin in signaling. Coronin is involved in numerous signaling events in diverse cell types (I-IV). In T-cells, coronin (Crn) orients phospholipase C (PLC) at the membrane to convert PIP2 to IP3, which in turn causes release of intracellular calcium (I). In mycobacterium tuberculosis infected macrophages, coronin activates calcium-calcineurine signaling that prevents fusion of phagosome to lysozomes by yet unknown mechanism, thereby preventing mycobacterial killing (II). In *Aplysia californica*, calcium induced activation of calcineurin increases the cofilin activity and consequently increases retrograde actin flow (III) (Zhang et al, 2012), not mentioned in the text. In MelJuSo cells, coronin is essential for activation of cAMP-PKA signaling (IV).

1.3.3.1 Coronin initiates Ca^{2+} signaling in immune cells.

The role of coronin in signaling is poorly understood in general, however in immune cells, the coronin-mediated signaling is well characterized, for example in macrophages and T-cells. Upon mycobacterial infection of macrophages, coronin localizes to the membrane of phagosomes and further activates Ca^{2+}-calcineurin signaling. Activated calcineurin further prevents the fusion of the lysosome with phagosome consequently allowing the mycobacterial survival. In *coronin* deficient cells calcium signaling is not activated, moreover calcineurin phosphatase activity is comparable to non-infected macrophages, leading to mycobacterial clearance (Jayachandran et al, 2007). Interestingly Kupffer cells, which are liver resident macrophages do not express coronin and therefore serve as mycobacterial clearing sites (Pieters et al, 2013). In T cells, coronin 1 was shown to interact with phospholipase C-γ1 (PLC- γ1). This interaction is essential for the generation of inositol (1,4,5)-triphosphate from phosphatidylinositol(4,5)-bisphosphate, which results in the mobilization of Ca^{+2} from intracellular stores. T-cells lacking *coronin* develop normally, but manifest defects in cytokine production, proliferation and survival (Mueller et al, 2008). Coronin 1 with its WD repeats interacts with integral membrane proteins as well as lipids providing an association with the plasma membrane and a connection with the actin cytoskeleton underneath it (Gatfield et al, 2005).

1.3.3.2 Coronin relays signals from surface receptors to cAMP-PKA pathway.

In Mel JuSo cells (a type of neuronal cells), Coronin 1 was shown to associate with Gαs, which in turn activates the cAMP/protein kinase A (PKA) pathway. The inhibition of interaction between coronin and Gαs by site directed mutagenesis resulted in decreased cAMP signaling, which affected the synaptic plasticity. Further, the *in vivo* infusion of 8-Br-cAMP, the membrane permeable structural analogue of cAMP could retain the synaptic plasticity suggesting coronin relays signal from Gαs to the cAMP/PKA pathway. Since, coronin colocalizes with F-actin, cAMP signaling was later tested in the presence of the actin depolymerizing compound latrunculin. No alteration in cAMP signaling suggested that coronin mediates the production of cAMP independent of F-actin (Jayachandran et al, 2014)

The above described functions of coronin from higher eukaryotes prompted me to probe some of these functions in *Plasmodium.* Should *Plasmodium* coronin play these roles, a plethora of unresolved questions could be answered. Firstly, gliding motility in *Plasmodium* is mediated

through an actomyosin motor linked to the surface through different adhesins. It was long thought that aldolase was the adapter linking actin filaments to surface adhesins. Yet, recent data suggests this is not the case and hence we don't know what protein provides the link (section 1.6). Perhaps coronin could play this role? Given the motility defects observed in *coronin*-deficient *P. berghei* sporozoites (unpublished results, section 1.7) along with the peripheral localization of coronin in *P. falciparum* schizonts (Olshina et al, 2015), this possibility cannot be ruled out. Secondly, does coronin play a role in calcium signaling in *Plasmodium*? And if yes, how? The treatment of *P. berghei* sporozoites with PLC, adenyl cyclase and protein kinase A inhibitors causes reduced motility suggesting that calcium signaling plays a role in their motility (Carey et al, 2014; Kebaier & Vanderberg, 2010). Therefore, the role of coronin in calcium signaling could be investigated.

1.3.3.3 CRIB motif of coronin regulates migration in dictyostellium.

Coronin proteins harbor besides actin and cofilin binding sites also a CRIB (cdc42 and rac-interactive binding) motif. This motif is present on the surface of the second and the third WD repeats, where it interacts with Rac, a member of Rho family of GTPase that is known to regulate the actin dynamics. Interaction of coronin with Rac inhibits binding of Rac to P21 activated kinase (PAK). This in turn activates the myosin heavy chain kinase (MHCK) leading to disassembly of myosin (Lee et al, 1996). The lack of *coronin* in *D. discoidium* leads to defects in cytokinesis and phagocytosis. Interestingly, CRIB mutated coronin failed to complement coronin in *D. discoidium*, although the localization and oligomerization of CRIB mutated coronin were unaffected (Swaminathan et al, 2014). In stark contrast, coronin 1C of zebra fish translocates rac1 from non-protrusive membranes to the active protrusive membranes implicating coronin assists in migrational guidance (Williamson et al, 2014).

In *P. berghei*, coronin has a conserved CRIB motif between the 2nd and 3rd WD repeat domain, however the protein rac is not annotated. Investigation of the CRIB motif of *Pb*-coronin could give new insights about the presence and role of rac in *P. berghei*. It may also shed light on the signaling mechanisms regulating myosin disassembly and its effects on sporozoite motility.

1.4 Migration of cells

Migration of cells is a universal phenomenon. Cells migrate in the quest for food, for mating, during tissue organization or to keep homeostasis. Migration is achieved by beating of

extracellular appendages like flagella, cilia or by formation of specialized dynamic structures such as protrusions of the cell body like pseudopodia, filopodia or lamellipodia. The extracellular appendages usually have a microtubule and dynein motor, whereas the protrusions of cell membrane rely on an actin-myosin motor or actin polymerization. This chapter majorly focuses on the actin-myosin basis of cell migration. Interestingly though, malaria parasites exhibit microtubule-dynein based flagella as well as actin-myosin motor in different stages of its life cycle.

1.4.1 Actin-based migration: amoeboid and mesenchymal migration

Eukaryotic cells show a crawling type of movement also referred to as amoeboid movement. Their movement is associated with a change in the cell shape that is caused by formation of cell membrane protrusions. The shape changes either to form a variety of structures, e.g. pseudopodia, filopodia, lammelipodia. Filopodia are microspikes whereas lammelipodia are sheet like projections. The typical crawling movement emerged from the studies of amoebae, *Chaos chaos* and a much larger organism, *Amoeba proteus*. The cytoplasmic extracts isolated from these amoebae contain actin and myosin in filamentous form. These showed contraction and relaxation in experimental conditions similar to those of skeletal muscle's contraction and relaxation (Stebbings, 2001).

Mammalian leukocytes also exhibit the crawling type of movement with the formation of lammelipodia. This crawling locomotion enables them to extravasate from blood and lymph vessels to the extracellular matrix in response to chemokines (Yadav et al, 2003). Fibroblasts, neuronal growth cones and cancer cells also display the crawling type of movement. When these cells are isolated from their respective tissues and placed in culture on a substrate, they spread and start to migrate. The migrating fibroblasts use lammelipodia in conjugation with filopodia, which leads to ruffling of membranes at the leading edge of a cell. Additionally, fibroblast cells are known to influence the migration of neighboring fibroblast cells by contact inhibition (Sixt, 2012). Similarly, neuronal growth cones in axons also have both lammelipodia and filopodia, which can be extended or retraced based on the external stimuli (Dent et al, 2003). In line with this motility, the caner cells disseminate from primary tissue to a distant tissue, an important mechanism for metastasis. Invasion of cancer cells is also in response to the chemical and physical cues from the environment (Wolf & Friedl, 2006).

Mechanism of migration (Cytoskeletal model): Crawling cell migration of eukaryotic cells involves cooperative function of multiple proteins. (i) Actin-myosin motor: Actin, myosin and actin-binding proteins provide the structural integrity inside the migrating cells. (ii) Adhesive proteins: They belong to the integrin family that spans the plasma membrane having domains both on the extracellular and cytoplasmic side. (iii) Signaling proteins: These involve among others proteins of the class small GTPase i.e. Rac, Cdc42 and Rho family of proteins. (iv) Microtubules: Migrating cells are usually polar with defined leading and trailing edges. This polarity with respect to the position of the nucleus is maintained via microtubules (Vicente-Manzanares et al, 2005).

Filamentous actin (F-actin) plays a key role in the actin-myosin motor. Actin-binding proteins control actin polymerization. Arp2/3 binds actin filaments on the side and hence form branched network. This leads to dendritic structures. (Rouiller et al, 2008). Three proteins majorly regulate Arp2/3 dependent nucleation; (i) Wiskott-Aldrich syndrome protein (WASP), (ii) Neural Wiskott-Aldrich syndrome protein (N-WASP) and (iii) WASP family verprolin homologous protein (WAVE) (Suetsugu et al, 1999). The activity of WAVE/Scar is positively regulated by a small GTPase Rac and that of WASP and N-WASP is by Cdc42 (Raftopoulou & Hall, 2004). Formins linearly polymerize the barbed ends of actin filaments whereas profilin serves as a reservoir of monomeric G-actin that promotes the polymerization of actin (Kovar et al, 2006). Altogether, it appears that actin polymerization and actin-myosin contraction occur in response to the signaling via small GTPase. For instance, RacGTP stimulates p21-associated kinase (PAK) leading to its higher kinase activity that inhibits myosin heavy chain kinase. This results in the myosin assembly (Raftopoulou & Hall, 2004). In the complex series of events, coronin displays a multifunctional nature. It not only plays a structural role by bundling actin filaments, but with its CRIB domain, it also negatively feedbacks the actin polymerization through the small GTPase. As it is known that coronin with its affinity for Rac and Cdc42 inhibits the activation of PAK, leading to myosin disassembly (Swaminathan et al, 2014). However, a third small GTPase, RhoA is not influenced by coronin. RhoA stimulates formin (mDia) directly to induce actin polymerization or activates a Rho kinase (ROCK), which could lead to two outcomes. One possibility is that ROCK phosphorylates and activates LIM kinase, which in turn inactivates cofilin by phosphorylation. This leads to inhibition of the cofilin-mediated depolymerization of actin and stabilization of actin. The other possibility is that ROCK

inhibits a phosphatase of myosin light chain (MLC), leading to phosphorylation of MLC and actin-myosin crosslinking (Raftopoulou & Hall, 2004). Myosin anchors itself in a cavity of MLC with its tail domain, while its head domain potentiates the retrograde flow of the polymerized actin filaments (Douse et al, 2012). The traction force generated by dynamic actin-myosin motor is linked to surface adhesins. The molecules implicated in this linkage are talin, vinculin and α-actinin. Talin directly links the actin cytoskeleton to integrins while it could also bind to vinculin, which in turn binds to α-actinin (Calderwood et al, 2000). The complex of talin, vinculin and α-actinin transmits the force generated by actin cytoskeleton to integrins (Ciobanasu et al, 2014). However, integrins do not transmit all the force to the substratum and thus, this mechanism is referred to as molecular slippage (Huttenlocher & Horwitz, 2011). This is because, α-actinin moves with the same velocity as the retrograde flow of actin filaments, whereas integrins are stable and other proteins move with an intermediate pace (Brown et al, 2006). Binding of integrins to the ligands on ECM activates downstream signaling. It causes clustering of integrins in the plasma membrane. Further the adapter proteins link integrins to actin filaments. This leads to an assembly of focal adhesions at the leading edge. There are over a hundred molecules known to be involved in focal adhesion dynamics. However, the molecular mechanisms that couple adhesion dynamics to actin dynamics are poorly understood. The small GTPases of Rho family are predicted to be the effectors of this coupling. RhoGTPases in turn are regulated by outside in signaling via integrin molecules. As the cell migrates, the focal adhesions mature and they need to be disassembled at the trailing edge. However, signals that lead to disassembly of focal adhesions are still elusive. The disassembly appears to be associated with the trailing edge retraction and detachment of the cell body from the substrate (Huttenlocher & Horwitz, 2011).

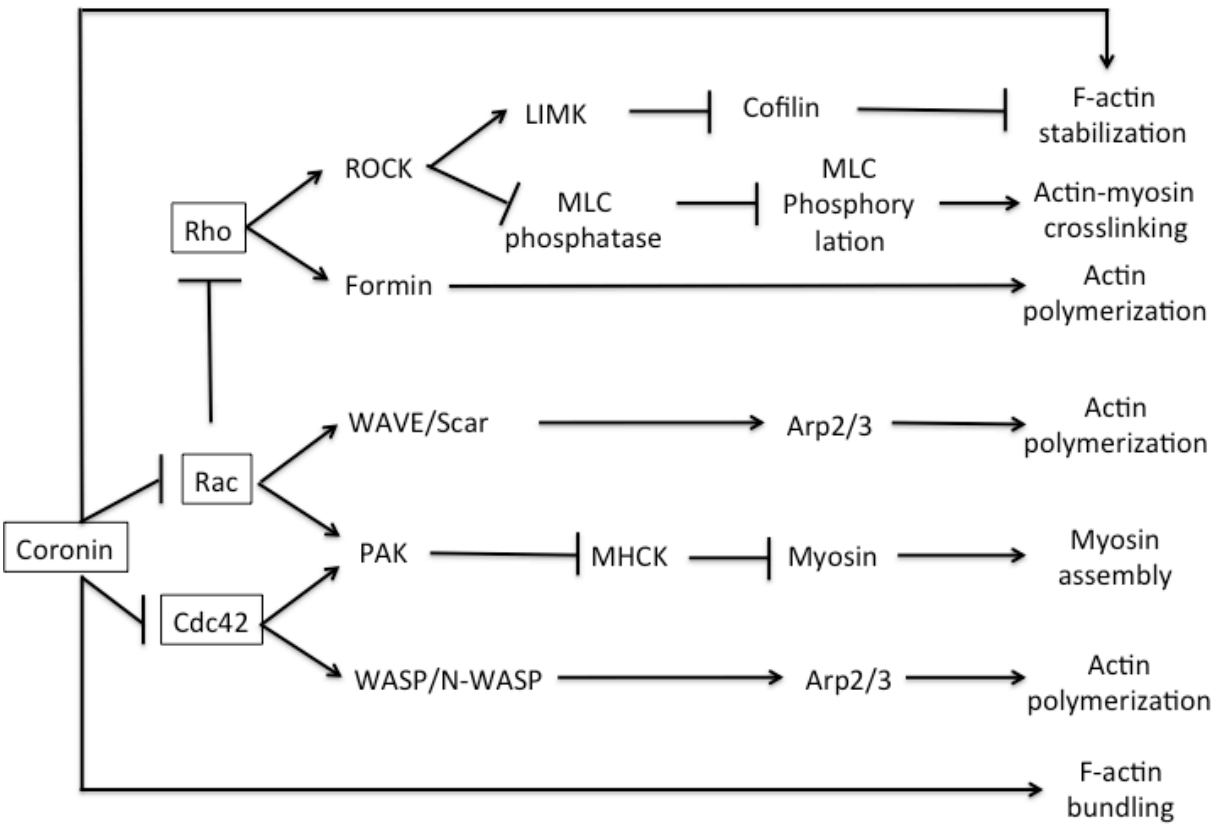

Fig 1.4: Role of coronin in cell migration (Cytoskeletal model: modified from Raftopoulou M; 2004)

Lastly, the polarity of a migrating cell is crucial for its directional migration. It is distinguished not only by leading-trailing edges of the cell but also the positioning of the nucleus, the Golgi complex and the microtubule organizing center (MTOC) towards the leading edge. The classic role of cell polarity is governed by microtubules. The small GTPase, Cdc42 is known to positively regulate these processes through the activation of protein kinase C and par proteins. These in turn regulate the dynein-dynactin complex that orients microtubules and gives polarity to the migrating cell (Etienne-Manneville, 2008).

In summary, coupling of adhesion dynamics to the actin-myosin motor through signaling by small GTPase together with microtubule dynamics are essential for the efficient cell migration.

Mesenchymal v/s amoeboid migration patterns: Although a general mechanism for actin-based migration exists, there are slight differences between mesenchymal and amoeboid migration. Mesenchymal migration is a property of cells that secrete proteases in order to degrade the extracellular matrix prior to migration within tissues. This generates a path and cells display focalized integrins (Pankova et al, 2010). In contrast, amoeboid migration proceeds with

the formation of a constriction ring. It is a path finding migration i.e. protease independent and have non-clustered integrins. After ablation of extracellular proteolysis, HT1080 fibrosarcoma and MDA-MB231 mammary carcinoma cells show mesenchymal to amoeboid transition (MAT) in migration (Wolf et al, 2003).

1.4.2 Integrin-independent migration

Although adhesion mediated or integrin mediated cell migration is a common mode of migration, cells also exhibit non-adhesive migration. Non-adhesive migration is usually integrin independent and interestingly consumes less energy. The first evidence for non-adhesive migration comes from dendritic cells migrating in 3 dimensions, when talin or integrins were deleted. Talin null and integrin null dendritic cells still underwent normal migration in 3D. However, these null mutants were unable to extravasate the blood vessel suggesting that the adherence is important for their migration in 2D (Lammermann et al, 2008).

The mechanism of integrin independent migration differs from the integrin dependent migration. Cells migrate with a protrusion formed by actin polymerization at the leading edge. The trailing edge follows the leading edge passively and the nucleus is simply dragged with the rear end of the migrating cell. In narrow environments, cell squeeze through and this is where myosin (II) dependent contraction functions. The nucleus gets deformed while squeezing through the narrow environment and is propelled forward. Cells lacking myosin II do not deform their nuclei while squeezing through a 3D environment and thereby slow down. This suggests that the contraction by myosin only plays a role in 'squeeze and propel' motion of the integrin independent migration (Bergert et al, 2015; Lammermann et al, 2008).

1.4.3 Single cell migration v/s collective migration

Life cycle stages of *D. discoidium* serve as a model for both single cell and collective migration. It migrates as a single cell as well as collectively. As opposed to mammalian counterparts, *D. discoidium* cells do not possess integrins and surface proteases. Although the actin cytoskeleton is still conserved, they have a different chemotactic mechanism for migration. In starvation conditions about 10.000 cells aggregate to form a slug-like multicellular organism and start to migrate towards light or heat. This multicellular mode of migration can last for days. In favorable conditions, the multicellular organism differentiates into fruiting bodies. Upon germination of the fruiting bodies, the life cycle completes by forming a new generation of single cell amoebae (Friedl & Gilmour, 2009).

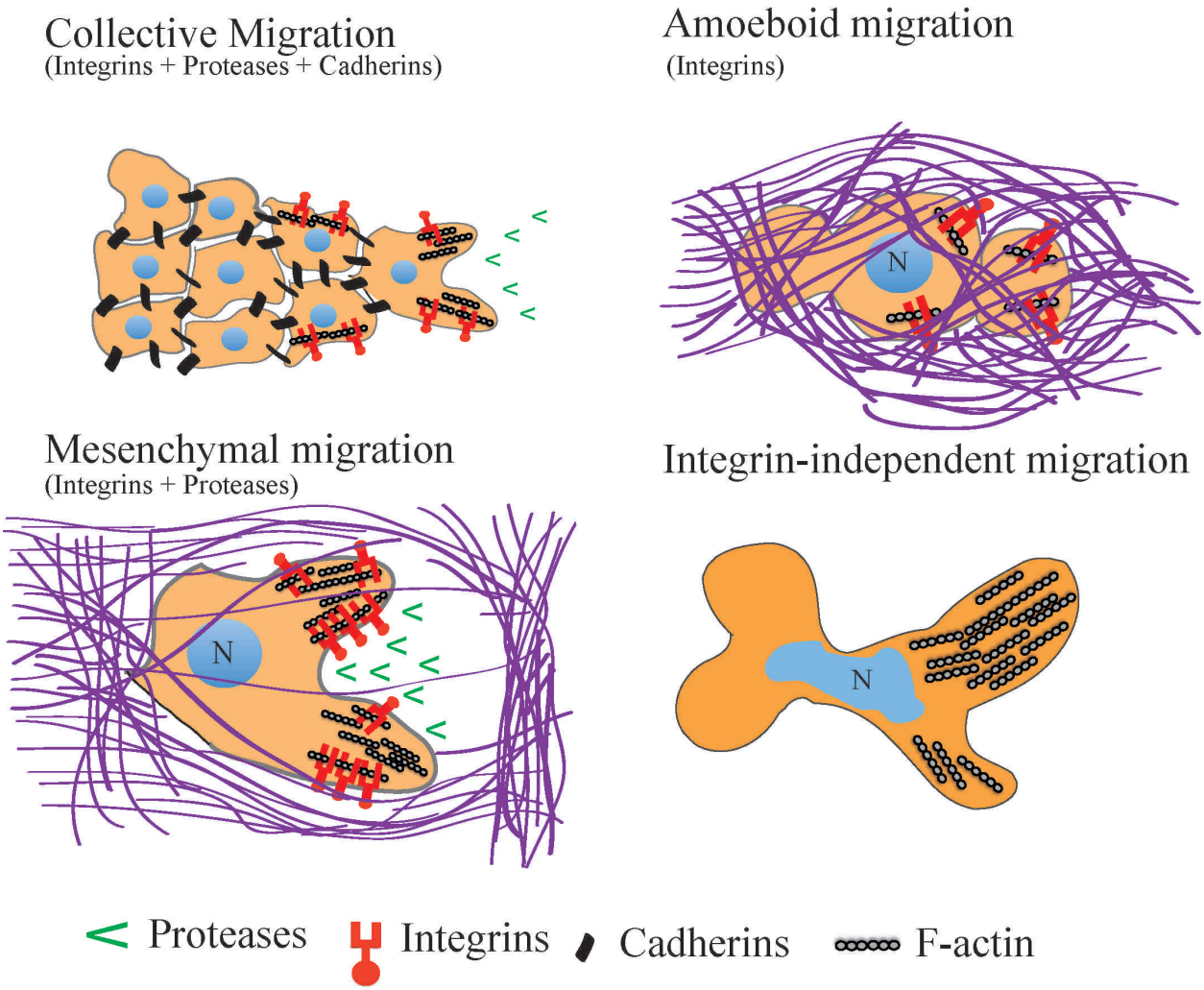

Fig 1.5: Cell migration. Different types of migrations are mediated by either the presence or absence of protease, cadherins, integrins and F-actin.

Collective cell migration is also a characteristic of highly differentiated tumors. In response to the resistive environment of the primary tumors, a mass of cells detaches and migrates to the less resistive environment. Along with the cortical actin network and integrins, cell-cell adhesion is prerequisite for collective cell migration. It is not surprising that epithelial melanoma cancers exhibiting collective migration also express cadherines, connexins with the help of which they communicate through gap junctions (Friedl et al, 2004). Similarly during an embryonic development in drosophila, the border cells and keratinocytes also display collective cell migration (Montell et al, 2012). Since the cells of heterogenous origin are migrating together, it could be expected that their different biological abilities function together.

1.4.4 Actin-myosin based gliding motility

The organisms of phylum Apicomplexa migrate in a unique way. They lack extracellular appendages and migrate without altering their shape. However, they still move with an average speed of 1-3 μm lack extracellular appendages and migrate eukaryotic gliding motility. In the next section (1.6), I introduce the gliding motility of the genus *Plasmodium*.

1.5 Motility in the life cycle of *Apicomplexa*

Malaria is a major health burden caused by five human infecting species of *Plasmodium*. Organisms of the genus *Plasmodium* are parasites of both vertebrates and invertebrates. In order to successfully invade a new host and establish an infection, the parasite has to be motile at multiple stages to cross different barriers among tissues and species; (i) Merozoites - the blood stage parasites released from the ruptured red blood cells (RBC) need to actively invade new RBCs. (ii) Ookinetes – zygotes formed by the fusion of male and female gametocytes in the midgut of the mosquitoes have to migrate and invade the midgut wall of the mosquitoes. Here, they transform into oocysts where sporogenesis (i.e. formation of sporozoites) occurs. (iii) Sporozoites – Depending on the location where sporozoites are present, they are referred to as the midgut sporozoites or salivary gland sporozoites. Midgut-sporzoites need to egress from oocysts and invade salivary glands. Salivary gland sporozoites have to migrate in the skin of the vertebrates in order to reach the nearest blood vessel. They further have to cross the cells lining the liver and invade the liver. Sporozoites show interesting motility pattern. These organisms do not have any extracellular appendages, but still move without changing shape at the speed of 1-3 μm/s (Vanderberg, 1974).

These three motile stages of the malaria parasites are separated by the intracellular growth and development of the parasite in the respective host. The motility of apicomplexan parasites is hampered in the presence of actin modulating compounds, e.g. jasplakinolide and cytochalasin D. Jasplakinolide is a cyclic depsipeptide that stabilizes actin filaments (Scott et al, 1988). This leads to polymerization of actin into long filaments. On the other hand, cytochalasin D is an alkaloid that inhibits the actin polymerization leading to a disruption of actin microfilaments (Poupel & Tardieux, 1999). Deletion of one of the parasite myosins from the related parasite *T. gondii* shows diminished migration suggesting that the motility of malaria parasites is actin-myosin based.

Apart from actin and myosin, there are other components that regulate apicomplexan motility. Amongst them are a minimal set of actin-binding proteins (Sattler et al, 2011), myosin interacting proteins and surface adhesins (Hegge et al, 2010). Concerted action of these molecules empowers the parasite to navigate through the tissues of vertebrates and invertebrates. This molecular motor machinery is located between the space subtended by the parasite's plasma membrane and inner membrane, with the domains of surface adhesins exposed to the extracellular matrices (ECM). This space is called the supraalveolar space (SAS) (Baum et al, 2006).

Myosin is present in all motile parasite stages. It localizes to the periphery of merozoites in schizonts and to the anterior half of the periphery in merozoites liberated from schizonts (Pinder et al, 1998). Conditional removal of myosin results in severe defects in host cell invasion (Meissner et al, 2002). Myosin with its tail domain is held at the inner membrane complex in association with another protein, the myosin tail interacting protein (MTIP). As expected, MTIP is also expressed in the invasive stages and localizes to the periphery (Bergman et al, 2003). A short peptide similar to the C-terminal tail of myosin binds to MTIP in the parasite lysate and may inhibit parasite motility and invasion (Green et al, 2006). The interaction between myoA tail and MTIP is regulated by phosphorylation of ser-107 and ser-108 residues on MTIP, which loosens its grip on myosin (Douse et al, 2012). Therefore, the interaction between MTIP and myosin could be a new therapeutic target.

Myosin and MTIP form a ternary complex with the glideosome-associated protein, GAP45 and then associate with the glideosome associated protein, GAP50 (Ridzuan et al, 2012). GAP45 is regulated by phosphorylation by a calcium dependent protein kinase 1 (CDPK1). However, phosphorylation of GAP45 does not affect its subcellular localization or binding with myosin and MTIP, but prevents the binding of the ternary complex (Myosin-MTIP-GAP45) with GAP50 (Gilk et al, 2009). GAP50 is transported from the endoplasmic reticulum to the Golgi apparatus and later to the inner membrane complex (IMC). This transport of GAP50 is regulated by N-glycosylation.

According to the current understanding of the molecular motor, the myosin-MTIP-GAP45-GAP50 complex anchored to the inner membrane complex (IMC) pulls the actin filaments located in the supra alveolar space (SAS) (Bosch et al, 2006; Green et al, 2006). A minimal set of actin-binding proteins present in the SAS, regulates dynamics of actin (Schuler &

Matuschewski, 2006). Interestingly though, most of the cellular actin exist in its monomeric G-actin state and only less than 5% exist in polymerized filamentous form (F-actin) (Poupel & Tardieux, 1999). These actin filaments are very short and unstable (Schmitz et al, 2005). Low levels of steady-state *Plasmodium* actin filaments make them undetectable under physiological conditions with conventional fluorescent derivatives and electron microscopy (EM) (Kudryashev et al, 2010). Visualization of F-actin is important in understanding actin dynamics, as the understanding of the parasites' actin and its actin regulatory proteins may provide us with targets for specific intervention. After treatment with jasplakinolide, *P. berghei* parasites expressing a GFP tagged actin showed concentration of F-actin dynamics at the parasite pellicle and at polar apices (Angrisano et al, 2012a). Electron microscopy studies with jasplakinolide treated *Toxoplasma* tachyzoites revealed that F-actin is abundant in the membrane protrusions formed by jasplakinolide treatment (Shaw & Tilney, 1999). Apicomplexan specific actin antibodies have been used to visualize parasite actin filaments in presence of jasplakinolide (Angrisano et al, 2012b; Siden-Kiamos et al, 2012; Yasuda et al, 1988). Compounds like jasplakinolide or cytochalasin D alter actin dynamics and therefore affect the mobility of parasites *in vitro*, making the visualization of native actin dynamics difficult. Alternatively, filamentous actin-binding proteins can be used to visualize F-actin. These include e.g. GFPmtalin, a recombinant protein containing C-terminal portion of mouse talin (amino acids 2345-2541) fused to the fluorescent protein GFP. It has successfully been used to visualize actin filaments in plants (Kost et al, 1999). Another alternative is to fluorescently label the endogenous homologue of genuine, F-actin-binding protein. Localizing such a protein could give a hint on the presence and localization of otherwise invisible actin filaments. One way to tackle this might be the expression of a fluorescently tagged coronin under a motile stage specific promoter. Moreover, the retrograde flow of the actin filaments in the SAS is transmitted to the surface adhesins that span the plasma membrane. This results in the motion of the parasite. Surface adhesins have integrin like A-domain (head domain that interacts with ECM), a TSR domain (transmembrane domains that spans a plasma membrane) and a C-terminal tail. In *Plasmodium,* Thrombospondin-related anonymous protein (TRAP) and TREP (S6) are surface adhesins expressed at the oocysts - sporozoite stages and their deletion causes a severe defect in salivary gland invasion (Combe et al, 2009; Morahan et al, 2009). TRAP and S6 are important for initial adhesion, while a protein structurally similar to TRAP, referred to as TRAP-like protein (TLP) is also expressed at

sporozoite stage. The sporozoites lacking TLP move less efficiently than WT sporozoites (Hegge et al, 2010).

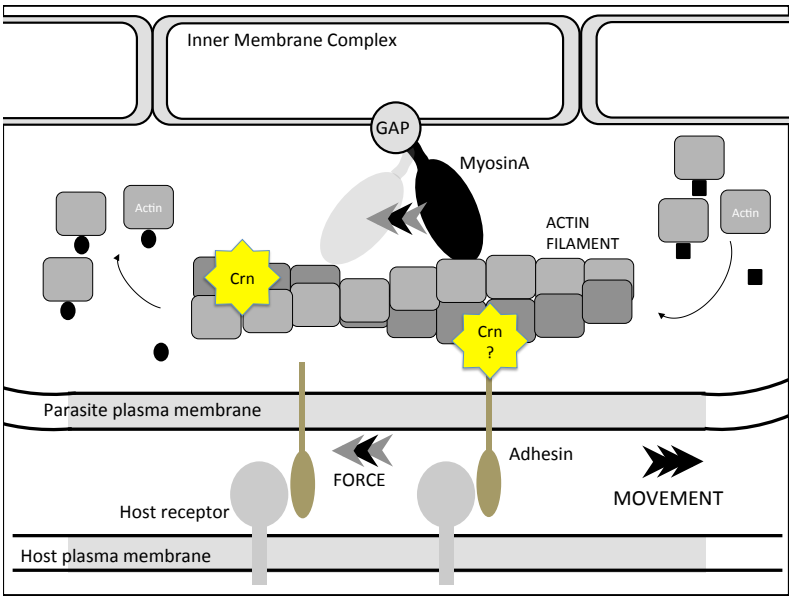

Fig 1.6: Hypothetical model of gliding motor. The protein machinery for gliding motor is present in the supra-alveolar space (SAS) between the plasma membrane (PM) and inner membrane complex (IMC). The dynamic actin filaments are pulled back with myosin anchored to the IMC together with glideosome-associated proteins (GAPs). How this force generated by retrograde flow of actin filaments is transferred to the surface adhesins is unclear. Considering the previously known interaction of coronin with PM and actin cytoskeleton in eukaryotes, we hypothesize *Plasmodium* coronin bridges actin filaments to surface adhesins. (modified from Douglas et al, unpublished)

Until now, the connection between the actin-myosin based motor and the surface adhesins is not clear. Previously, aldolase was believed to link the actin filaments to surface adhesins. Aldolase being a glycolytic enzyme is notorious for binding to proteins without specificity. It is hence known as a common contaminant in the biochemical assays. Recently, it was discovered that only the growth of the aldolse null mutant is inhibited in the presence of glucose in *T. gondii*. The motility, invasion and replication of *T. gondii* are dependent on its growth in glucose. Curiously aldolase null mutants were able to invade when grown in glucose free medium and had no defect in migration of *T. gondii* parasites (Shen & Sibley, 2014). Considering that coronin associates with the plasma membrane as well as the actin cytoskeleton and the recent findings of coronin-mediated receptor clustering as well as the linkage to the actin filament coronin could play a role in connecting surface proteins with actin filaments in the SAS. The next section (1.7) describes the role of coronin in Apicomplexa.

1.6 Role of coronin in the motility of *Apicomplexa*

In Apicomplexa, coronin was first found in the human malaria parasite, *Plasmodium falciparum*. It shows 32% amino acid sequence homology to *Dd*-coronin and was detected in an insoluble fraction of triton extract with an antibody against *Dd*-coronin. *Pf*-coronin binds to the filaments of rabbit skeletal muscle actin *in vitro*. However, only a fraction of *Pf*-coronin binds to

filametous actin (Tardieux et al, 1998). *Pf*-coronin was later purified using a baculovirus protein expression system and its binding to actin was tested. *Pf*-coronin bundles actin filaments and was shown to bind to phosphoinositol (4,5)-bisphosphate (PI(4,5)P) (Olshina et al, 2015). Fluorescent tagging of *Pf*-coronin under endogenous 5'UTR suggested that it is expressed in the blood stages as well as ookinetes, where it is localized to the periphery of schizonts and ookinetes (Olshina et al, 2015). Another apicomplexan parasite, Babesia bovis (*Bb*, a causative agent of Babesiosis, a tick transmitted disease of mammalian hosts) also has one copy of a *coronin* like protein. It has 30% amino acid sequence identity to that of *Pf*-coronin. As expected, *Bb*-coronin was shown to associate with filaments rabbit liver actin *in vitro* (Figueroa et al, 2004). Toxoplasma gondii, an apicomplexan parasite as well has one copy of the *coronin* gene. The treatment with actin modulating compounds could not alter the localization of *Tg*-coronin suggesting that the localization is independent of actin. As expected, *Tg*-coronin only minimally cosediments with actin filaments, *in vitro*. However, *Tg*-coronin might play a role in microneme secretion. This is unsurprising, as another member of the coronin family was previously known to regulate vesicular trafficking. Phenotypically, inducible knock down of *coronin* had a slight defect during invasion of and egress from the host. The structure of *Tg*-coronin is similar to already available coronin structure from mouse (*Mus musculus)* (*Mm*-coronin 1A*)*. It has 7 bladed β-propeller formed of WD40 repeat domains and a C-terminal coiled coil extension (Salamun et al, 2014). Although the C-terminal part of *Tg*-coronin is longer than that of *Dd*-coronin, it does not seem to have a leucine zipper motif that is known to homo-oligomerize coronin.

1.7 Specific aims and objectives of the thesis

In line with coronin from other apicomplexan parasites, *Pb*-coronin also belongs to the WD40 repeat family of proteins (Logan-Klumpler et al, 2012). Although no complete knock out was possible in *P. falciparum*, the *Pb*-coronin gene could easily be deleted by double homologous recombination. The *coronin*-deficient *P. berghei* parasites exhibited defects during the invasion of salivary glands of the mosquitoes along with the defects in gliding motility and liver stage development *in vitro.* Furthermore, the overexpression of fluorescently tagged coronin under a sporozoite specific promoter showed that coronin is localized to the periphery of midgut sporozoites (MGS) and non-activated salivary gland sporozoites (SGS). Upon activation of (SGS) with serum albumin, coronin localized to the rear of now-motile sporozoites. This provides a hint that coronin is important for motility and liver stage development. However, its

expression in the entire life cycle and the molecular mechanism of coronin's action are still to be elucidated. Therefore, the specific aims of my thesis are to fluorescently tag endogenous coronin and probe its expression in the entire life cycle of *P. berghei.* Given that coronin plays a role in the actin-based gliding motility of sporozoite, it is possible that coronin is expressed in sporozoites. Thus, it is important to test if actin-modulating compounds affect the localization of coronin. Since the actin-binding sites of coronin are well known and conserved in apicomplexan parasites, I further planned to test the effect of these mutations on the localization of coronin as well as on the life cycle of *P. berghei.* Besides probing the actin-binding, I planned to test if *Pb*-coronin interacts with PI(4,5)P2. Depending on the observation, I aimed to find out how coronin would be involved in calcium signaling. To this end, fluorescent coronin overexpressed under sporozoite specific promoter can serve as an excellent tool, as posterior v/s peripheral localization of coronin serves as a natural molecular indicator. The role of coronin in calcium signaling could be tested by the use of chelators of calcium ions and inhibitors of proteins involved in calcium signaling pathway. Lastly, I planned to overexpress coronin in the *P. berghei* stages, where coronin is not expressed. This way, it might be possible to test if the overexpression of coronin is deleterious to *P. berghei.*

2. Material and Methods

2.1 Tagging of endogenous coronin with mCherry

To monitor spatial and temporal expression of coronin through the whole life cycle the protein was C-terminally tagged with mCherry. To address this, the vector p262 containing the *human dihydrofolate reductase* (*hDHFR*) and the mCherry gene was used. The vector p262 is derived from p236 (Deligianni et al, 2011). Furthermore, the 3'UTR of *coronin* and the *coronin* ORF was amplified from genomic DNA with the primers P434 and P435 as well as P436 and P433, respectively. For primer sequences see S6 fig. The PCR products were digested with BamHI and EcoRV (3'UTR) as well as EcoRI and NdeI (*coronin*) and subsequently ligated into the vector p262. The resulting vector, termed p262-eCRN (for endogenous *coronin*) was linearized with BstZ17I within the ORF of *coronin* for transfection according to standard protocols (Janse et al, 2006). Correct integration of the transfected DNA sequence was investigated by PCR analysis at the 5' end (primers P132 and P6) and at the 3' end (primers P394 and P133).

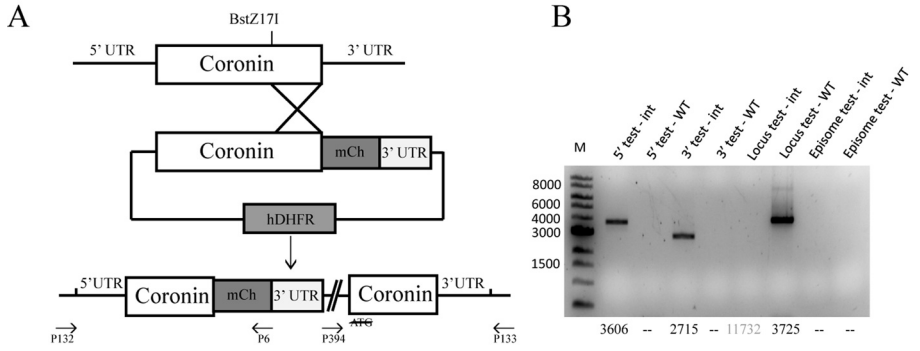

Fig 2.1: Endogenous tagging of *Pb*-coronin (A-B); transfection strategy (A) and genotyping PCR confirming proper integration of plasmid with primers indicated in A(B).

2.2 Overexpression of Pb-coronin-mCherry, Pf-coronin-mCherry and mutants with 5'UTR of uis3 gene

The gene for the fluorescent protein mCherry was amplified (primers P57 and P58) and cloned (SpeI, PacI) in the B3D+ vector (Silvie et al, 2008); the promoter region of *uis3* (amplified with primers L1 and L2) was cloned in front of *mCherry* (SacII, NotI) and the ORF of *Pb-coronin* (amplified with primers P71 and P72) was cloned between the two previous

fragments (NotI, XbaI). Similarly, the ORF of *Pf-coronin* (amplified with primers P457 and P458) was cloned (NotI, XbaI). Mutations in actin binding sites were introduced by site directed mutagenesis using complementary primers. In this way the following seven mutants were generated: (i) R24A, R28A, K283A, D285A, E327A, R330A, R349A, K350A; (ii) R24A, R28A; (iii) R24E, R28E; (iv) K283A, D285A; (v) K283E, D285R; (vi) R349A, K350A and (vii) R349E, K350E. The final vectors are referred to as B3D+oCRN. For genome integration, vectors containing all seven mutations as well as the non-mutated vector were linearized with NdeI and transfected according to standard protocols (Janse et al, 2006). Correct integration in the *uis3* locus was verified by PCR analysis amplifying the 5' (primers P976 and P480) and 3' (primers T7 and P977) overlap between chromosomal and introduced DNA.

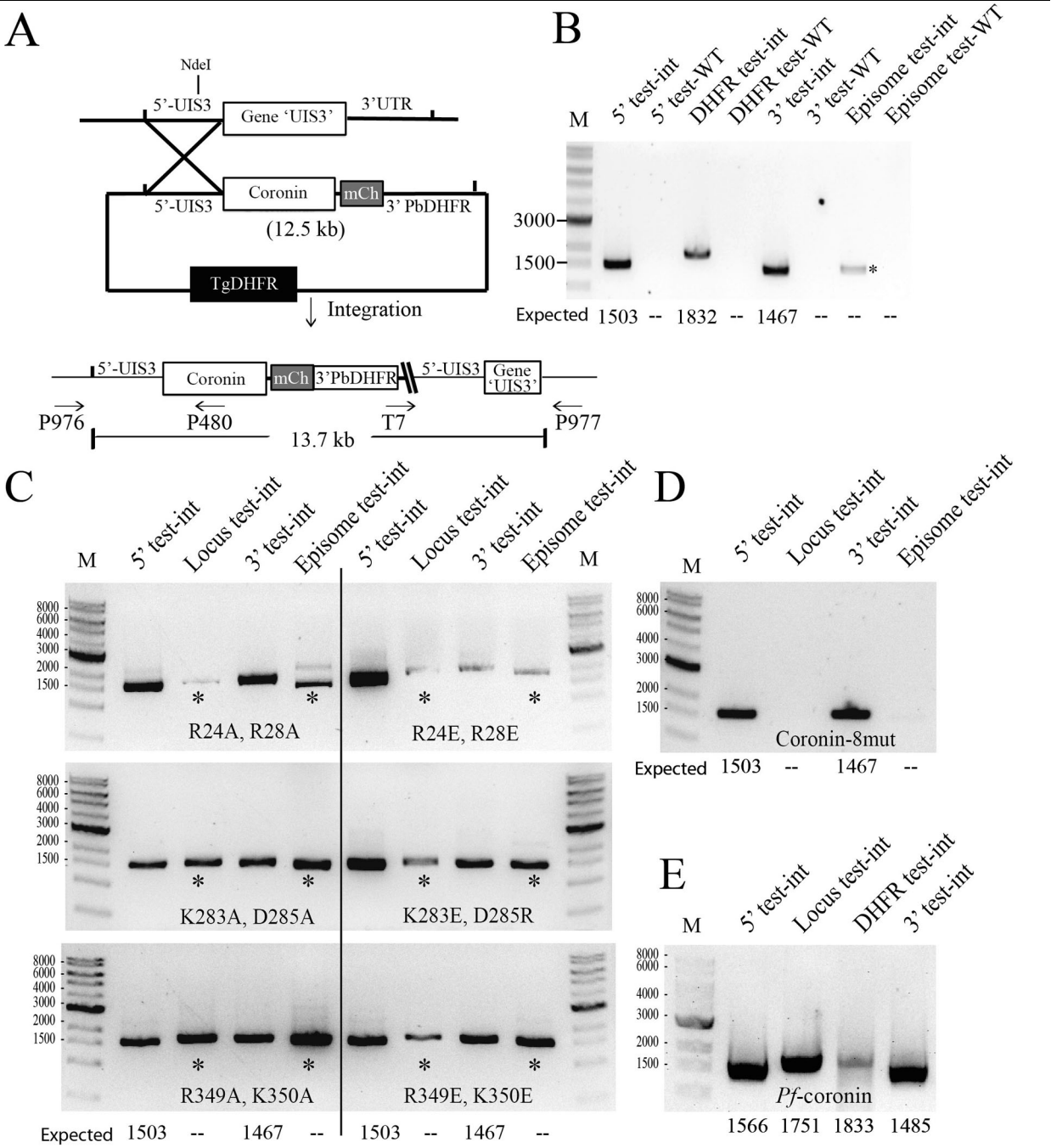

Fig 2.2: Overexpression of WT-coronin and mutants. (A) Schematic of the strategy used to generate P. berghei lines expressing coronin-mCherry from the *uis3* promoter. A single crossover-strategy integrated a plasmid containing the resistance cassette (hDHFR) and *coronin* fused to the coding sequence for mCherry after digestion of the plasmid with NdeI within the 5'UTR of *uis3*. Locations of the primers for PCR in B are indicated. **(B)** Genotyping PCR indicating desired integration of wild-type coronin-mCherry in the uis3 locus (5'int, 3'int and selection marker). Expected amplicon sizes are below the gel. (C-E) Genotyping PCRs indicating desired integration of R24A, R28A; R24E, R28E; K283A, D285A; K283E, D285R; R349A, K350A and R349E, K350E (C), Coronin-8mut (D), *Pf*-coronin (E). Note that the PCR to test for the whole locus integration failed to amplify 14 kb sequence, however the band appearing corresponds to the WT locus. This could be expected, as the parasite lines overexpressing coronin are non-clonal. On the other hand the bands appearing in episomal test are non-specific bands.

2.3 Replacement of WT *coronin* with mCherry tagged mutants of coronin and *Pf*-coronin

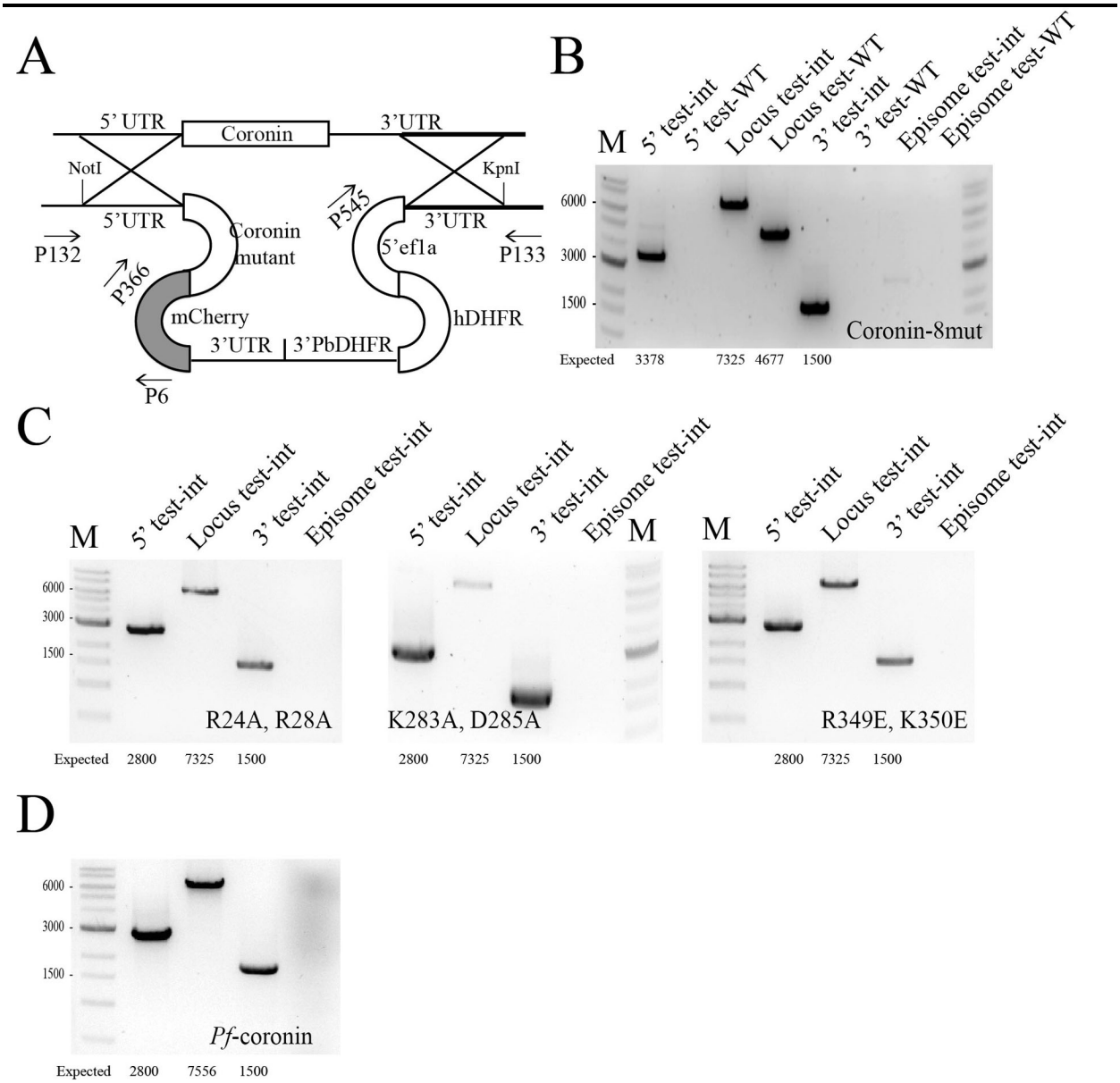

Fig 2.3: Replacement of *Pb*-coronin with mutants and *Pf*-coronin fused to mCherry: Transfection strategy for replacement of *Pb*-coronin (A) and genotyping PCR showing proper integration (B-D); Coronin-8mut (B); R24A, R28A; K283A, D285A; R349E, K350E (C); *Pf*-coronin (D). Note that all the replacements are done with mCherry fused at the C-terminus.

To generate replacements of the endogenous *coronin* with mCherry tagged *coronin* mutants the previously generated p262-eCRN was used. Replacement vectors were generated in 3 steps of cloning. In the first step the extended 3'UTR was amplified (P735 and P736) and the PCR product digested (HindIII and KpnI) and cloned into p262-eCRN. In a next step the mutated ORFs of *coronin* (R24A, R28A; K283A, D285A and R349E, K350E), the mutant having all

putative actin-binding sites mutated (R24A, R28A, K283A, D285A, E327A, R330A, R349A, K350A) and *Pf*-coronin were cloned from the B3D+oCRN vectors (EcoRI and PstI) into the replacement vectors (p262-eCRN). In a last step the 5'UTR of the *coronin* gene was amplified with the primers P563 and P564 and cloned (NotI, EcoRI) in front of the mutated *coronin* ORFs. The final vector (P262-rCRN for *coronin*-replacement) was linearized with NotI and KpnI and transfected according to standard protocols (Janse et al, 2006). Correct replacements were verified via PCR analysis by 5' integration (primers P132 and P366 or P132 and P6), the complete locus (primers P132 and P133) as well as 3' integration (primers P545 and P133). All mutant lines were sequence across the *coronin* gene and inserted point mutations were verified.

2.4 Expression of coronin in blood and ookinete stages

The B3D+ vector obtained from Silvie (Silvie et al, 2008) was modified by Mirko Singer University of Heidelberg such that it contains two regions of Chromosome 12 of *P. berghei*. This assists in the integration of vector in chromosome-12 region by double homologous recombination. The vector also contains a human dihydrofolate reductase (hDHFR) gene as a resistance cassette. The vector for the overexpression of coronin from the promoter of erythrocyte membrane associated antigen (EMAA) was generated in three steps. In the first step, eGFP (amplified by primers P743 and P744) was cloned (NdeI, BamHI). In the second step, *Pb-coronin* (amplified with primers P71 and P433) was cloned (NotI, NdeI). In the last step, the 5'UTR of erythrocyte membrane associated antigen (EMAA) (amplified with primers P741 and P742) was cloned (SacII, NotI). Similarly, the vectors for overexpression of coronin from a promoter of actin I was also generated in three steps. In the first step, eGFP (amplified with primers P899 and P744) was cloned (NdeI, BamHI). In the second step, *Pb-coronin* and *coronin-8mut* (amplified with primers P71 and P433 from B3D+oCRN vector) were cloned (NotI, NdeI). In the final step, the 5' UTR of actin (amplified with primers P737 and P738) were cloned (SacII, NotI). These vectors were double digested with SalI and HaeII and transfected as described (Janse et al, 2006).

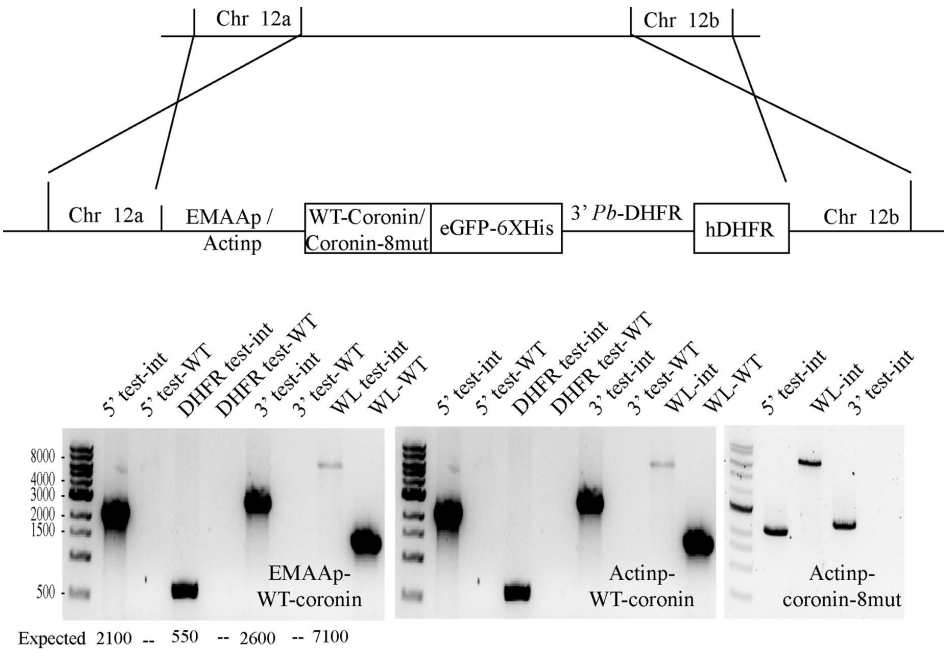

Fig 2.4: Overexpression of Coronin in blood and ookienete stages: Strategy for overexpression of WT-*Pb*-coronin and coronin-8mut under EMAA (Erythrocyte membrane associated antigen) and actin promoters (A). Genotyping PCR to test the correct integration of plasmid in the chromosome 12 region

2.5 Mosquito infections

Anopheles stephensi mosquitoes (Sda500 strain) were raised at 28°C, 75% humidity, under a 13/11 h light/dark cycle and maintained on 10% sucrose solution containing 0.05% para-aminobenzoic acid. NMRI mice (Charles River) were infected by intraperitoneal injection of 200 µL frozen parasite stocks. After 3 to five days post infection the number of exflagellation events were determined with a Zeiss light microscope and a counting grid. If >3 exflagellation events were observed, mice were anaesthetized with a mixture of 10% ketamine and 2% xylazin in PBS (100 µL per 20 g mouse body weight i.p.) and fed to *Anopheles stephensi* mosquitoes (3–5 d after hatching). Post infection mosquitoes were maintained at 20°C and 80% humidity. Mosquitoes were used 10–23 days post infection for further experiments.

2.6 Analysis of sporozoite motility *in vitro*

Salivary glands of 20-25 mosquitos were dissected in 100 µL RPMI medium (GIBCO) in a plastic reaction tube (Eppendorff). Isolated salivary glands were grounded with a pestle and released sporozoites were purified with an Accudenz density gradient (Kennedy et al, 2012). Purified sporozoites were resuspended in 100 µL RPMI containing 3% BSA, transferred to a 96

well plate and centrifuged for 3 min at 1000 rpm. Sporozoites were imaged with differential interference contrast (DIC) and fluorescence using a 25x (NA: 0.8) objective on an inverted light microscope (Axiovert 200M, Zeiss). Video microscopy was performed with taking an image every 3 seconds unless otherwise stated for 5 min (Kebaier & Vanderberg, 2010).

2.7 Analysis of sporozoite motility *in vivo*

Ears of naïve mice were waxed with the hair removal gel cream Veet 24 hours prior to intravital imaging to avoid autofluorescence by hair. Mosquitos were separated in cups to 10-12 each and starved overnight to increase their biting rate. On the day of imaging, mice were anaesthetized as described above and the ears were placed on the cups containing the infected mosquitoes. Ears were exposed to mosquitoes for 10-15 minutes and formed hematomas were slightly marked with a permanent marker. Bitten mice were placed on the microscope table in such a way that ears could be scanned for hematomas (Amino et al, 2006). Upon finding a bite site, sporozoite migration was imaged for 10 – 15 minutes with an image every three second using the Zeiss Axiovert 200M widefield fluorescence microscope.

2.8 Infection of liver cells

HepG2 cells were seeded into 24 well plates with a density of $5x10^4$ and cultivated in DMEM under standard conditions for three days. Salivary glands were isolated 17 days post infection; homogenized with a pestle in 100 µL DMEM and released sporozoites were counted using a Neubauer haemocytometer. 50000 sporozoites were seeded to each well of a 24 well plate with confluent HepG2 cells. After infection wells were filled up with DMEM to a total volume of 200 µL and incubated for 30 minutes at room temperature. After incubation cells were cultured for further 2 hours under standard cell culture conditions. The medium was removed and wells were washed twice with PBS to remove non-invaded sporozoites. Afterwards cells were treated with 200 µL (0.05% trypsin) for 10 minutes. To each well 800 µL of DMEM supplemented with Antibiotic-Antimycotic (GIBCO, Life technologies) was added and cells were split in fresh 24 well plates containing cover slips ($12x12mm^2$, thickness 1mm) for 2 time points. Medium was refreshed every 24 hours. The coverslips were transferred to another 24 well plate after the fixed timepoint. The liver cells were fixed with 4% PFA at RT for 15 min and stored at 4^o C till immunofluorescence assay was performed. After fixation of all the timepoints (2 days post infection), cells were washed twice with PBS. Washing is followed by

permeabilization with 0.5% TritonX and 2% BSA for 30 min at RT. Further, the blocking of liver cells were performed with 0.2% of Triton and 2% BSA for 30 min at RT. The antibody against HSP70 (heat shock protein 70kD) from mouse was used as a primer antibody to stain the parasitophorous vacuole of parasites in infected HepG2 cells. The alexa fluor goat 488 anti-mouse antibody (Invitrogen) was used as a secondary antibody and 1 µg/ml Hoechst was used to stain the nuclei.

2.9 Infections of mice

Naive mice were infected by salivary gland sporozoites isolated 17 days post infection either by mosquito bite or by intravenous (i.v.) injection into the tail vein. To infect mice by bite, C57BL/6 mice (n = 4 per group per experiment) were anesthetized as previously above and individually exposed to cups containing 10 - 12 infected mosquitoes. Mosquitoes were starved 24 hours prior to the experiment to increase their biting rate. Mice were exposed to mosquitoes for 10-15 minutes, turning them every 4 minutes. After the experiment blood fed mosquitoes were put on ice and salivary glands isolated to quantify the number of sporozoites. The time between the infection and the first emergence of parasites in the blood, in the following referred to as prepatency, was monitored microscopically by Giemsa stained blood smears. Smears were performed daily from day 3 to day 20 (unless otherwise stated). For intravenous infections, salivary glands of infected mosquitos (17 days post infection) were dissected in 100 µL PBS and homogenized. The number of sporozoites was counted in a Neubauer haemocytometer. Sporozoite solutions were diluted with PBS to 10.000 sporozoites per 100 µL and injected i.v. into the tail vein. The prepatency was determined as above. A mouse was considered to be positive if >1 parasite was observed during 5-10 minutes of observations. The survival of infected mice and the appearance of experimental cerebral malaria were monitored for 20 days.

2.10 Fluorescence imaging

Imaging was performed on an inverted Zeiss Axiovert 200M microscope using a GFP or rhodamine filter set at room temperature. Images were collected with a CoolSnap HQ2 camera at 1 or 0.5 Hz using Axiovision 4.8 software and 10X (NA: 0.5), 25X (NA: 0.8) or 63X (NA: 1.4) objectives depending on the experimental setting. Image processing was generally done using ImageJ.

2.11 Expression and purification of *Pb*-coronin using baculovirus-mediated insect cells

The codon optimized *Pb*-coronin gene was ordered from geneart and cloned in pFastBacHTB vector with BamHI and XhoI. The recombinant bacmid DNA was generated and recombinant baculovirus was produced according to the protocol given in the Bac-to-Bac Baculovirus expression system (Invitrogen manual).

2.11.1 Purification of *Pb*-coronin from insect cells.

1) Harvest 500 ml expression (5000 g, 10 min, 40 C), freeze pellet at -800 C
2) Thaw pellet at room temperature, resuspend in 40 ml lysis buffer.
3) Add 1 tablet protease inhibitor tablet, dissolved in 1 ml lysis buffer.
4) Freeze-thaw in liquid N2 twice.
5) Add DNAseI and incubate 30 mins on a rocking shaker at 40 C.
6) Recover supernatant and add 5 ml Ni-NTA resin that has been equilibriated in lysis buffer. Add 10 mM imidazole to prevent non-specific binding.
7) Incubate on a rocking shaker for minimum of 2 hrs.
8) Pour into glass column and collect flow through (keep). Take 20 µL smaple for gel.
9) Wash with 50 ml wash buffer 1. Take 20 µL sample for SDS-PAGE.
10) Wash with 50 ml wash buffer 2. Take 20 µL sample for SDS-PAGE.
11) Wash with 50 ml wash buffer 3. Take 20 µL sample for SDS-PAGE.
12) Elute 1 ml fractions with elution buffer – incuate1 min for each fraction, test with Bradford reagent to assess color change. Stop eluting when there is no more color change. Take 20 µL samples of each fraction for SDS-PAGE.
13) Run SDS-PAGE (reducing gel).

2.11.2 Extraction of insoluble recombinant *Pb*-coronin from insect cells

1) Obtain freshly harvested or frozen insect cells.
2) Resuspend the cell pellet in PBS containing 1 mM EDTA (1.8 ml PBS-EDTA per 10^8 cells). Add protease inhibitors. Centrifuge at 500-600Xg for 15 min. Discard the supernatant.

3) Resuspend the cell pellet in the same volume of lysis buffer (1.8 ml per 10^8 cells) and add protease inhibitors. Homogenize the suspension by pipetting upwards and downwards. Remove 10 µL of aliquote for SDS-PAGE.
4) Add 180 µL of 10% (w/v) nonident P-40 per 1.8 ml of lysis buffer to the remaining cell suspension. –mix by inverting to lyse cells. Lysis is effectively instantaneous. Centrifuge at 5000-10000 g for 30 min.
5) Remove 10 µL of supernatant for SDS-PAGE and discard the remaining. Wash the pellet by resuspending in 1.8 ml of PBS-EDTA per 108 cells. Add protease inhibitors and centrifuge at 5000-10000 g for 10 min.
6) Discard the supernatant and resuspend the pellet in 1.8 ml distilled water per 10^8 cells and immediately add protease inhibitors. Add 100 µL of 5% (w/v) sodium deoxycholate per 1.8 ml. Mix by inverting and incubate for 10 min. Note the appearance of particulates and increase in viscosity (DNA release) of the lysate. Retain 10 µL of aliquote for SDS-PAGE.
7) Following reagent must be then sequentially added to the lysate (per 10^8 cells).

    3.1 ml of 50 mM HEPES, pH 7.5
    40 µL of 1 M $MgSO_4$
    770 µL of 5 M NaCl
    Protease inhibitor tablet
    3.1 ml of 50 mM HEPES, pH 7.5
    DNAseI (RNAase free) – 10 µg/ml

8) Incubate for 18 hrs. at 4° C followed by 2 hrs. at RT. Centrifuge at 5000-10000 g for 15 min.
9) Discard the supernatant and resuspend the pellet in 8 ml preliminary solubilization buffer per 108 cells. Centrifuge at 10000 g for 10 min.
10) Resuspend the pellet in 2 ml solubilization buffer per 10^8 cells. If the protein solubilizes at this point then proceed to prechromatic sample preparation. Since Pb-coronin does not solubilize, centrifuge at 10000 g for 15 min.
11) Discard the supernatant and resuspend the pellet in 2 ml guanidine-HCl solubilization buffer per 10^8 cells and incubate at RT for 1 hr. Protein solubilization is indicated by disappearance of a gelatinous pellet.

12) Perform sequential dialysis against 50 volumes of 6 M and 3 M urea (buffered with 50 mM Tris-Cl, pH 8.0) to remove guanidine-HCl. The extracted protein should be stored at -20° C to -70° C or ideally used immediately.

2.11.3 Purification of *Pb*-coronin under denaturing conditions

1) Prepare insect cell lysate under denaturing conditions as described above.
2) Centrifuge the lysate at 3000 g for 15 min to pellet cellular debris. Transfer supernatant to fresh tube.
3) Add 8 ml lysate to the prepared purification column.
4) Allow the binding of protein to the beads at RT for 15-20 min.
5) Settle the beads by gravity or centrifugation (800 g). Remove the supernatant if centrifuged or let the flow through.
6) Wash column with 4 ml of denaturing binding buffer by resuspending the resin by gravity/ low speed centrifugation.
7) Wash the column with 4 ml denaturing wash buffer pH 6.0 by resuspending the resin by gravity / low speed centrifugation (800 g).
8) Clamp the column and elute the protein with denaturing elution buffer.
9) Pool the fractions and try refolding.

2.12 Coronin-mCherry localization assays for calcium signaling

The parasite line uis3-coronin-mCherry was used to for localization experiments conducted to investigate calcium signaling. The salivary glands of mosquitoes were dissected in 100 µL of RPMI medium and smashed with pestle in an eppendorff tube. Furthermore, 900 µL of RPMI medium was added to obtain a total volume of 1 ml RPMI medium containing sporozoites. Simultaneously, 17% of accudenz solution was prepared in PBS and 3 ml of it was poured in 15 ml falcon tube. Then 1 ml of sporozoite containing RPMI medium was gently overlaid on top of 17% accudenz solution. This falcon tube was then centrifuged at 2500 g for 25 minutes with minimum acceleration and deceleration. The sporozoites layer was obtained at the interface. This layer was aspirated with a pasteure pipette and taken into a new eppendorff tube. The sporozoites were centrifuged in a tabletop centrifuge at 10000 rpm for 2 min. The pellet contained sporozoites, which was then washed once with RPMI solution. The sporozoite pellet obtained after washing is suspended in 30 µL of RPMI solution (before testing activation by

forskolin) or in RPMI containing 3% BSA (before testing inhibition by SQ22536 or H89). This 30 μL of suspension was next transferred to a well of 384 well plate and centrifuged at 1000 rpm for 3 min. The 2 fold higher concentration of stimulant or inhibitors is prepared in RPMI or RPMI containing 3% BSA respectively. This 30 μL of stimulant or inhibitors is added from the top and mixed by pipetting. The 384 well plate was centrifuged again for 1000 rpm for 3 min and imaged under 63x objective (NA: 1.4). To test the localization of coronin in midgut sporozoites, RPMI and RPMI containing 50 μM BAPTA-AM were prepared.20 μL of these solutions (a drop) is taken in mattek dish. The midguts of 3 mosquitoes were dissected and suspended in a drop of either RPMI or RPMI + 50 μM BAPTA-AM. The round coverslip was placed gently from the top and sporozoites released from the midguts were imaged under 63x objective (NA: 1.4). The video microscopy was done one frame per 3 seconds for 90 frames. The sporozoites that moved with a speed higher than 0.25 μm/s were classified as motile and other as non-motile. The localization was classified by visually examining every sporozoite for a complete duration of a movie. The localization was classified as (i) rear (if F/R intensity ratio appeared less than 0.5), (ii) peripheral (if signal was pronounced in the periphery and F/R intensity ratio appeared more than 0.5) and (iii) cytoplasmic (if signal was not pronounced in the periphery). The localization of coronin-mCherry and motility were examined for every sporozoite in a movie.

2.13 Fluorescent Recovery After Photobleaching (FRAP)

For FRAP experiments 2-3 infected salivary glands 17-23 days post mosquito infection were isolated in 100 μL RPMI or RPMI + 3% BSA and grounded with a pestle. Sporozoites expressing mCherry tagged *coronin* were transferred to a glass-bottom culture dish, (35 mm petridish; 14 mm microwell with No. 1.0 coverglass (MatTek) and mixed with small molecule inhibitors or activators. Imaging was performed with a spinning disc Nikon TE2000 inverted microscope and a 100X (NA: 1.4) objective. The region of interest (ROI) (10x10 pixel size or 1.76 μm^2) was bleached on each sporozoite followed by imaging for 300 frames with 5 frames per second. The fluorescence intensity of the bleached sporozoite surface was measured using a fixed-size ROI moved by hand to ensure that it is always centered over the moving sporozoites. The fluorescence intensity in a fixed ROI immediately adjacent to the sporozoite was measured and a value for every frame was subtracted from the frapped signal to correct for background fluorescence. As the area imaged was small and sporozoites were moving, it was not possible to correct for photo-damage or sporozoites loosing focus. The resulting background-subtracted data

was then normalized to the highest intensity of the pre-bleached image. The maximum recovery intensity was determined by averaging the intensities from frame 90 to 140 after bleaching, when recovery was complete for all experiments. The half recovery was calculated as $T_{1/2}$ = (Intensity of Max recovery + Intensity of 1st frame after frap)/ 2 and the time required to reach this intensity determined as half time recovery.

2.14 Reagents

2.14.1 Chemicals and compounds

Product	Company
PCR tubes	G kisker, Germany
1 kb DNA ladder	Invitrogen, Germany
10x Taq buffer with	NH42SO4
MgCl2 reaction buffer	Fermentas, USA
dNTPs Mix 2mM each	Fermentas, USA
Agarose gel	SERVA, Germany
Taq polymerase	Fermentas, USA
Platinum Taq, High Fidelity DNA Polymerase	Invitrogen, Germany
Restriction enzymes and buffers	New England Biolabs, USA
Restriction enzymes and buffers	Fermentas, USA
CIP alkaline phosphatase	New England Biolabs, USA
T4 DNA ligase and buffer	Fermentas, USA
Ampicillin sodium salt	Carl Ruth, Germany
Diethyl ether	Sigma Aldrich, Germany
Fetal Bovine Serum	GIBCO, USA
Ketamine hydrochloride	Sigma Aldrich, Germany
Xylazine hydrochlorine solution	Sigma Aldrich, Germany
Nycodenz	Axis-sheild, Germany
Giemsa stain	Sigma Aldrich, Germany
Pyrimethamin	Sigma Aldrich, Germany
Saponin	SigmaAldrich, Germany
Heparin 25000 U	Ratiopharm, Germany
Alsever's solution or Freezing solution	Sigma Aldrich, Germany
Gentamycin	10 mg/ml
Penicillin/ Streptamycin 100x	PAA, Austria
RPMI 1640 + HEPES + L-glutamine	PAA Austria
Phosphate Buffered Saline, PBS without Ca^{2+} Mg^{2+}	PAA, Austria
Sea salt	Alnatura, Germany
Prolong Gold antifade reagent	Invitrogen, Germany
Accudenz –	Accurate Chemical and Scientific corporation
Xanthurenic acid –	Sigma Aldrich, Germany

Hypoxanthin –	Sigma Aldrich, Germany
Trypsin/EDTA 10x	c.c.pro, Germany
Para formaldehyde, PFA	Riedel-de Haen, Germany
TritonX-100	Merck, Germany
Tween 20	Carl Roth, Germany
Jasplakinolide	CalBiochem, USA
Cytochalasin D	Sigma Aldrich, Germany
BAPTA-AM	Company
Ionomycin	Sigma Aldrich, Germany
Ethanol	Sigma Aldrich, Germany
Forskolin	Sigma Aldrich, Germany
SQ22536	Santa Cruz Biotechnology
H89	Sigma Aldrich, Germany
BSA	Carl Roth, Germany
Hoechst	Sanofi

2.14.2 Kits

Kits	Company
High Pure PCR product purification kit	Roche, Germany
QIAprep Spin Miniprep Kit	Qiagen, Germany
QIAamp gDNA Blood Mini Kit	Qiagen, Germany
Amaxa human Tcell nucleofector kit	Lonza, Germany

2.14.3 General buffers and solutions

DNA loading buffer (6x):	6 % glycerol
	0.25 %(w/v) Bromophenol blue
	0.25 % (w/v) Xylenecynol
	1x TAE
TAE:	0.04 M Tris/acetate
	0.01 M Na_2EDTA
	pH = 8.0
LB medium:	10 g/l NaCl
	10 g/l Bacto-Tryptone (Peptone)
	5 g/l Bacto-Yeast extract
KX solution:	10% (v/v) Ketamine
	2% (v/v) Xylazine
	PBS
Freezing solution:	10 % (v/v) Glycerol in Alsever's solution

Pyrimethamin in water:	280 µM pyrimethamin
	pH (3.5-5.5) with HCl
	tap water
Nycodenz stock solution:	500 ml pH 7.5
	0.394 g Tris/HCl
	0.112 g KCl
	0.056 g Na_2EDTA
	138 g Nycodenz
	ddH_2O
PBS:	137 mM NaCl
	2.7 mM KCl
	8 mM Na_2HPO_4
	1.8 mM KH_2PO_4
	ddH2O
	pH = 7.4
Fixation solution:	4 % (v/v) PFA in PBS
Permeabilization solution:	0.5 % Triton X-100
	2 % BSA
	PBS
Blocking solution:	0.2 % Triton X-100
	2 % BSA
	PBS
Washing solution:	PBS
Antibody staining solution:	Antibody + blocking solution

Protein purification buffers (native conditions)

Lysis buffer:	50 mM Tris pH 8.0
	300 mM NaCl
	10 mM MgCl2
	5 mM β-mercaptoethanol
	0.5% Triton X-100

Wash buffer 1:	50 mM Tris pH 8.0
	300 mM NaCl
	5 mM β-mercaptoethanol
	20 mM Imidazol
Wash buffer 2:	50 mM Tris pH 8.0
	1 M NaCl
	5 mM β-mercaptoethanol
Wash buffer 3:	50 mM Tris pH 8.0
	300 mM NaCl
	5 mM β-mercaptoethanol
Elution buffer:	50 mM Tris pH 8.0
	300 mM NaCl
	5 mM β-mercaptoethanol
	250 mM Imidazol

Protein purification buffers (denaturing conditions)

Presolubilization buffer:	25 mM Tris-Cl
	2 M urea
	1 mM EDTA
	pH 8.0

Guanidine-HCl solubilization buffer):

	20 mM Tris-Cl
	6 M guanidine-HCl
	20 mM DTT
	pH 8.0
Binding buffer:	100 mM NaH_2PO_4
	10 mM Tris-Cl
	8 M urea
	pH 8.0
Wash buffer:	100 mM NaH_2PO_4
	10 mM Tris-Cl
	8 M urea

	pH 6.3
Elution buffer A:	100 mM NaH_2PO_4
	10 mM Tris-Cl
	8 M urea
	pH 4.2

2.15 Cell culture media and supplements

Bacterial culture medium:	10 g/l NaCl
	10 g/l Bacto-Tryptone
	5 g/l Bacto-Yeast extract
	ddH_2O
Schizont culture (T-medium):	RPMI 1640
	20 % (v/v) FBS(US)
	0.03% Gentamycin
Ookinete culture:	12.5 mg Hypoxanthine
	2.5 ml Penicillin-strepatamycin
	0.5 g NaHCO3
	100 µM Xanthurenic acid (5.12 mg)
	250 ml RPMI + HEPES + L-Glutamine
	pH = 7.8
	Add 20 % FBS (freshly added to the above solution)
Liver cell culture:	0.18 % (w/v) Gentamycin
	9 % (v/v) FBS
	0.9 % L-Glutamine
	DMEM

2.16 List of primers

#	Sequence
P124	TCCCCGCGGGGCAATTTATAAGTAGAAATGG
P125	ATTTGCGGCCGCGACAAACTTTAAATATTTTGTGACCC
P126	CCCAAGCTTTTATTAATAGTAATATTTACATTAATATGTAGG
P127	GGGGTACCCAAATCGAAAACACATATTCAC
P132	CAACAATATCGTTATACATCAAGTTCG
P133	CTTCAACTATGGTGTTATGTATTTCC

P177 ATGCATAAACCGGTGTGTCTGG

P176 CTAGACAGCCATCTCCATCTGG

P434 TATGGATCCTTATTAATAGTAATATTTACATTAATATGTAGGAAGAAG

P435 CGGGATATCGTTTCAAATCGAAAACACATATTCAC

P436 AACCGGAATTCGTGAATGATGTCCCTTGTATCAAAAAC

P433 TTCCATATGACCACCACCACCACCACCACCACCACCACCATTAGTTTTCGCAAATAATTTTTTACATG TTATAG

P6 CGGGATCCTTACTTGTACAGCTCGTCCATGCCGCCGGTGG

P394 TGTGCATTGAAGTACTTCG

P114 CCCGCACGGACGAATCCAGATGG

P115 CGCATTATATGAGTTCATTTTACACAATCC

P57 GCACTAGTGCAGCAGCAGCAGTGAGCAAGGGCGAGGAGGATAACATGG

P58 GCTTAATTAATTACTTGTACAGCTCGTCCATGCCGCC

L1 GCCCGCGGACAATTTCATTTCGTTAGGGATCG

L2 ATTTGCGGCCGCATACACTTTCATATATTTGTTATTTGTC

P71 ATTTGCGGCCGCAAAATGGTGAATGATGTCCCTTGTATC

P72 GCTCTAGAGCAGCAGCAGCAATTAGTTTTCGCAAATAATTTTTTACATG

P479 GATGACTTGGCCATCTGCACGGCAATTACCGAATC

P480 GATTCGGTAATTGCCGTGCAGATGGCCAAGTCATC

P481 TATATATAATTGGTGCAGGGGCAGGGAATTGTAGAT

P482 ATCTACAATTCCCTGCCCCTGCACCAATTATATATA

P483 GTAATATATATAAATGTGCAATAGGAGCCATATATAAAAATGAAAATG

P484 CATTTTCATTTTTATATATGGCTCCTATTGCACATTTATATATATTAC

P485 CTATATCATTTTATGTACCAGCAGCAAATCCAAATATATTTCAG

P486 CTGAAATATATTTGGATTTGCTGCTGGTACATAAAATGATATAG

P725 GATGACTTGGAGATCTGCACGGAGATTACCGAATC

P726 GATTCGGTAATCTCCGTGCAGATCTCCAAGTCATC

P727 TATATATAATTGGTGAGGGGCGAGGGAATTGTAGAT

P728 ATCTACAATTCCCTCGCCCCTCACCAATTATATATA

P729 CTATATCATTTTATGTACCAGAAGAAAATCCAAATATATTTCAG

P730 CTGAAATATATTTGGATTTTCTTCTGGTACATAAAATGATATAG

P976 GGATATATGTATACATATATAATGAAAGAAAGATATGTCATGG

T7 GAATACGACTCACTATAGGG

P977 GTCCTGATGATAACAAAGCAATTGCAAC

P735 CGAAGCTTAAATAATAATTATACTTTTGTATAAAGTAATGGAAATAATAATAATAAATTTGTCTTTTT AC

P736 ATGGTACCGGGCATTGGTATTATTAAATATCTTCATGCATATTGTATATATATATAC

P563 ATTTGCGGCCGCCCATATGATTTTTTTTAATTATATTATTTGTAATTTTTTATCTG

P564 AACCGGAATTCTTTGGGTCACAAAATATTTAAAGTTTGTC

P366 TCACCTTCAGCTTGGCG

P545 GAAATATAAATAATTACGCCTAGTTAATAAAGGGCAC

P743 GACATATGGTGAGCAAGGGCGAG

P744 CAGGATCCTTAGTGATGGTGATGGTGATGACCACCACCCTTGTACAGCTCGTCCATGC

P741 CTCCGCGGTTATCCCACATTATATTGTATATATACTATAACAACAAAGGG

P742	ATGCGGCCGCATCATATATAAATATATAATAAAAATCATAATATGCTAAAAATGTTTATAAGATGTG ATTTC
P899	ATTGACCGGTACCACCACCACCACCACCACCACCACCACCGGCGCCTTTGTATAGTTCATC
P737	CTCCGCGGATAAATAGGGATATGATAAAATAAGAATTTAGAAATTATGAAAATAC
P738	ATGCGGCCGCTTTAATTTTTTTTTTAAGTATATGAGTATATATATGTGTGTAAAAATTTATATTAAAT ATGC

2.17 Cell lines, insects and animals

P. berghei ANKA clone cl507	Kind gift from Prof. Kai Matuschewski
Anopheles stephensi (SDA500)	Nijmegen, Netherlands
C57Bl6 mice	Charles River Laboratory, Germany
NMRI mice	Janvier laboratories
HepG2 cells	Kind gift from R. Bartenschlager

2.18 Ethics statement

All animal experiments were performed concerning FELASA category B and GV-SOLAS standard guidelines. Animal experiments were approved by the German authorities (Regierungspräsidium Karlsruhe, Germany), § 8 Abs. 1 Tierschutzgesetz (TierSchG).

3. Results

3.1 Coronin is expressed in the sporozoites and liver stages of *P. berghei*.

To get insights in coronin function, I investigate the expression and the localization of coronin across life stages of *Plasmodium berghei*. To this end, I engineered a parasite line in which coronin is fused to mCherry at its C-terminus. Due to the addition of mCherry in the genomic context, the fusion protein is expressed from the endogenous promoter (Fig 3.1). As could be expected from the coronin knock out phenotype, coronin is not expressed in the asexual and sexual blood stages of the *P. berghei*. Coronin was also not detected in ookinetes. The first mCherry signal was found in oocysts and sporozoites developing in the midguts of the mosquitos. Coronin-mCherry was clearly localized to the periphery of midgut and salivary gland sporozoites isolated in RPMI buffer, not containing bovine serum albumin (BSA).

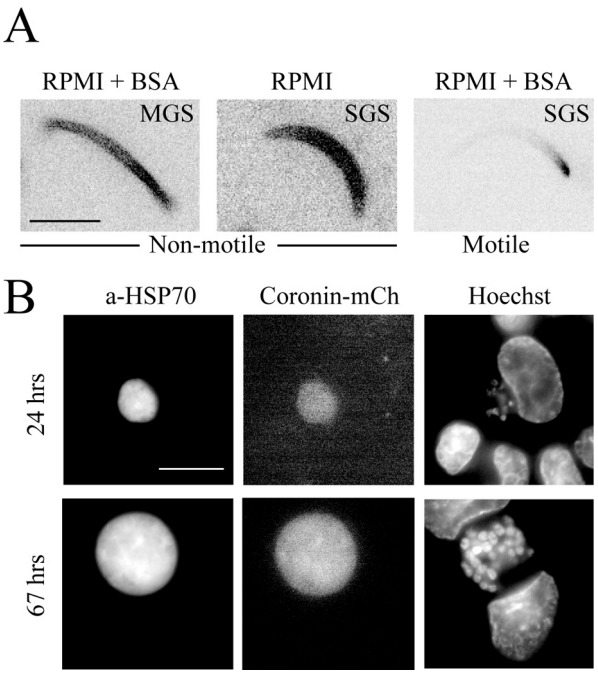

Fig 3.1: Coronin is expressed in sporozoite and liver stage of the *P. berghei* [A-B]. Coronin is distributed throughout the sporozoite, more pronounced in the periphery of the midgut sporozoite in the RPMI medium containing 3% BSA (left) and salivary gland sporozoite in PMI medium only (center). Coronin is localized to the rear of now motile salivary gland sporozoite in RPMI medium containing 3% BSA (right) (scale bar = 5 μm) [A]. Immuno fluorescence assay (IFA) performed using antibody against HSP70 shows expression of coronin-mCh. Nucleus is stained with hoechst (scale bar = 15 μm) [B].

BSA is known to activate motility of salivary gland sporozoites. Interestingly after addition of BSA in RPMI buffer, coronin localizes to the rear in the now motile sporozoites. The time difference between the localization of coronin and activation of motility in sporozoite is so miniscule that I could not distinguish one event from the other. Coronin continued to appear weakly in liver stages where the localization appears to be cytoplasmic.

3.2 Actin modulators alter the localization of coronin.

In order to probe the actin regulating function of coronin, I treated sporozoites with different nano-Molar concentrations of actin modulating compounds: cytochalasin D and jasplakinolide. Cytochalasin D depolymerizes actin filaments making them short, whereas jasplakinolide stabilizes actin filaments consequently elongating them (Brenner & Korn, 1979; Bubb et al, 2000).

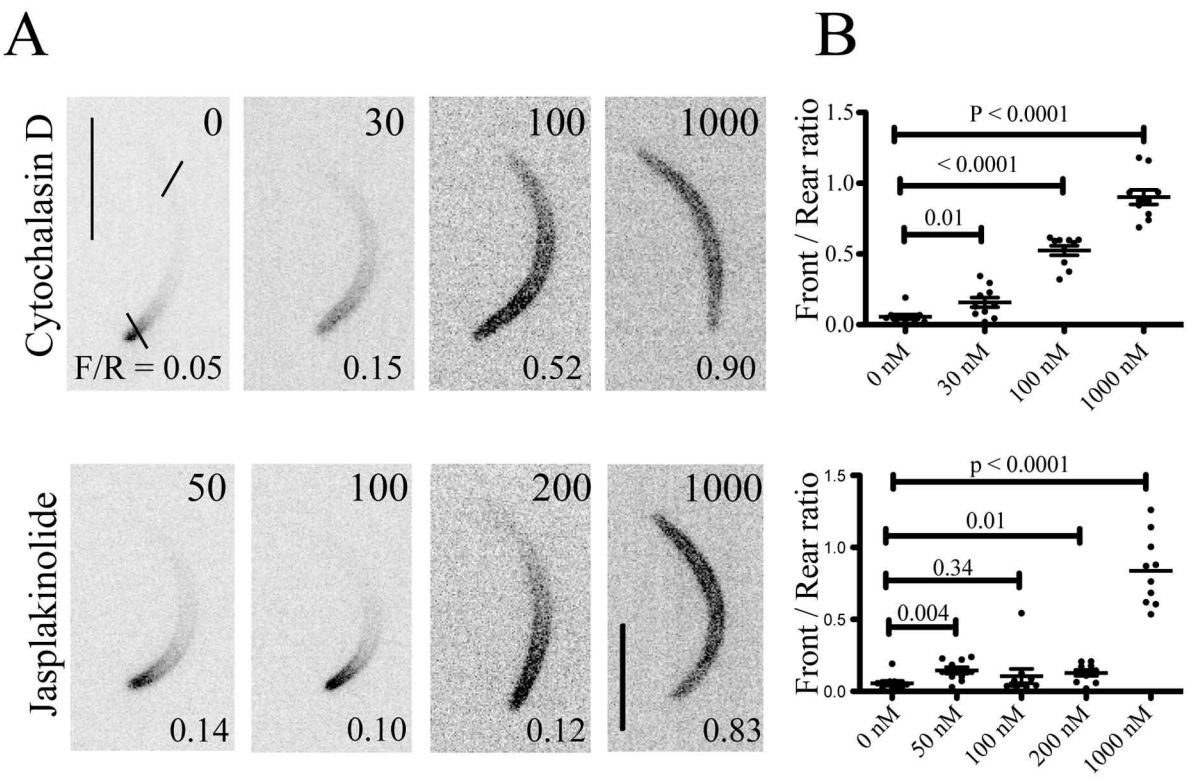

Fig 3.2: Actin modulating compounds alter localization of coronin [A-B]. Localization of coronin-mCherry in *P. berghei* sporozoites that were incubated in 3% BSA without cytochalasin D and jasplakinolide (top panel, left) or with 30 nM, 100 nM, 1000 nM cytochalasin D (top panel) and with 50 nM, 100 nM, 200 nM and 1000 nM jasplakinolide (lower panel). Ratio of the fluorescence intensities at the front (F) and at rear (R) of the sporozoites are measured by ploting the intensity profile along the lines as indicated in A (top panel left), n = 10, scale bar = 5 µm [A], Graph showing F/R ratio of 10 sporozoites for each concentration [B].

These two actin modulators were also known to affect motility of sporozoites (Hegge et al, 2009; Hellmann et al, 2013; Munter et al, 2009). At concentrations of above 200 nM of these compounds, coronin-mCherry is no longer localized to the rear end of the sporozoites. Instead, the fluorescent signal distributes along the whole periphery of the sporozoite. To quantify this, I calculated the ratio of the fluorescence intensities at the front to that at the rear of the sporozoites. The average of 10 sporozoites is shown for each concentration (Fig 3.2A). It showed

that the distribution of coronin along the periphery of sporozoites was apparent at 30 nM cytochalasin D and 200 nM jasplakinolide. These results suggest that coronin is present in the supra-alveolar space (SAS) at the periphery of the parasite. As soon as sporozoites are activated, coronin moves rearwards with actin filaments.

3.3 Mutant coronins reveal distinct binding to membranes and actin filaments.

In order to focus on the actin binding function of coronin, it was important to target actin-binding residues present on the surface of coronin. Systematic mutagenesis of yeast coronin had revealed its actin-binding residues (Gandhi et al, 2010). The determination of the structure of its homologue from *Mus musculus* showed that the actin-binding sites are present on the surface of coronin (Appleton et al, 2006). Based on these studies and multiple sequence alignments (MSA) (Fig 1.1), I shortlisted 4 sites for site directed mutagenesis. These are R24, R28; K283, D285; E327, R330 and R349, K350.

Taking into consideration the low expression of endogenous coronin-mCherry, I sought to use an extra copy of overexpressed coronin-mCherry. The parasite line expressing coronin-mCherry under 5' UTR of uis3 gene is available (Lepper, 2011). In fact, this was the preliminary experiment that showed coronin localizes to the rear in motile sporozoites and is used as a control in mutational studies (Fig 3.3A).

In the first mutational experiment, I applied a 'charge to alanine' strategy and mutated all these residues to alanine (Coronin-8mut). This resulted in the cytoplasmic localization of coronin (Fig 3.3B). Interestingly, this protein was found neither near membranes nor in the nucleus. This led me to look at the localization pattern of coronin, when each site is mutated individually. Thus, I decided to mutate 3 of these sites not just to alanine but also to the oppositely charged amino acids. This results in 6 more mutant forms of coronin. These are R24A, R28A; R24E, R28; K283A, D285A; K283E, D285R; R349A, K350A and R349E, K350E.

All these lines resulted in a remarkable difference in localization. R24A, R28A localized to the rear upon activation as has been found in WT-coronin. There was no significant difference between front/rear (F/R) ratios of WT-coronin and R24A, R28A. Reversing the charge at this site, R24E, R28E on the contrary resulted in peripheral localization of coronin in activated sporozoites. This is indicated in the F/R ratio (Figs 3.3B and 3.3C) and shows the importance of charges of the amino acid residues in coronin. A change in charge can clearly influence the interaction of a protein with its binding partners and therefore its localization (Cai et al, 2007).

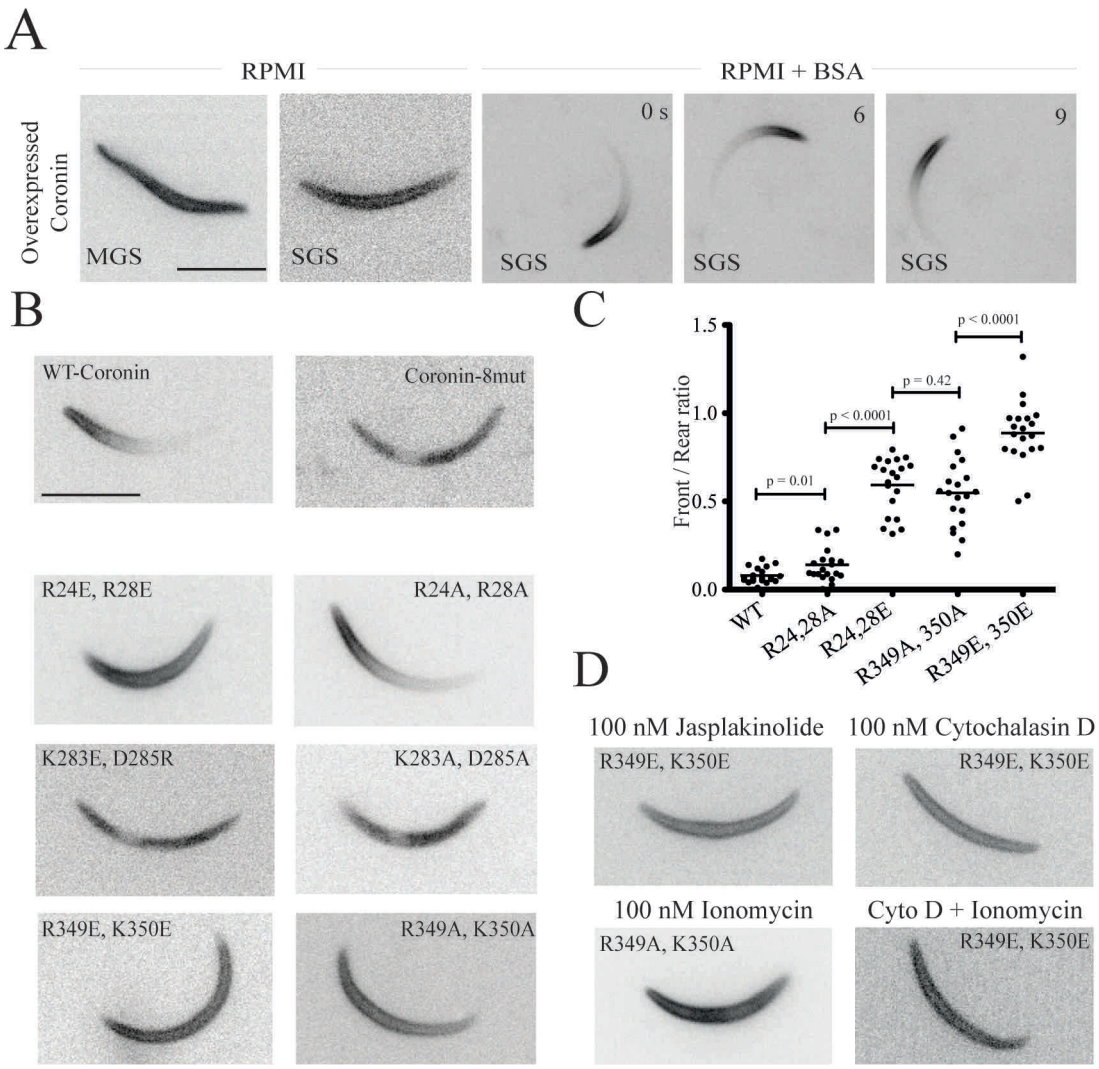

Fig 3.3: Mutations of coronin reveal binding to membrane and actin filaments [A-D]. Localization of over-expressed coroninunder *uis3* promoter in midgut sporoyoite (MGS), non-activated salivary gland sporozoite (SGS) and activated salivary gland sporzoite **[**A]. Localization of overexpressed WT and 7 mutant forms of P. berghei coronin fused to mCherry. Mutant residues are highlighted on the image of the sporozoite. Coronin-8mut is a mutant of coronin having all 8 residues mutated to alanine (scale bar = 5 µm) **[**B]. F/R of the fluorescence intensities of coronin mutants in P. berghei Sporozoites; no F/R ratios were calculated for mutants of coronin diffused in cytoplasm. **[**C]. Localization of R349A, K350A mutant of coronin in the presence of PIP2 hydrolysing compound ionomycin (1 µM) (top, left), localization of R349E, K350E mutant of coronin in the presence of 100 nM cytochalasin D (top, right); 100 nM jasplakinolide (bottom, left); 100 nM cytochalasin D + 500 nM ionomycin (bottom, right) **[**D].

The K283A, D285A mutant form of coronin localizes in the cytoplasm, similar to the coronin-8mut. K283E, D285R mutant form of coronin has its total charge conserved around the site, although each residue is mutated. It also localizes in the cytoplasm like its counterpart K283A, D285A (Fig 3.3B). Thus, this site seems to be important for associating coronin to the

membranes first. F/R ratios were not determined for these 2 mutant forms of coronin as they were cytoplasmic. Both R349A, K350A and R349E, K350E mutants of coronin localize to the periphery, like R24E, R28E mutant (Figs 3.3B and 3.3C). This suggests that the site R349, K350 mediates actin filament binding as has been suggested for coronin in yeast (Gandhi et al, 2010). If there was however, still actin mediated localization of these mutants, I argued that cytochalasin D should change in its localization with treatment with jasplakinolide being used as a positive control. This however was not the case suggesting that indeed coronin localizes to the periphery in actin filaments independent manner prior to sporozoite activation.

Coronin is known to bind to phosphatidylinositol (4,5)-bisphosphate [PI(4,5)P2] in the membrane (Tsujita et al, 2010). Ionomycin is a compound that hydrolyzes PI(4,5)P2 to ionositol (1,4,5)-trisphosphate [IP3] and diacyl glycerol [DAG] (Varnai & Balla, 1998). To probe the hypothesis that *Pb*-coronin is bound to the PI(4,5)P2 in the membrane, I treated R349E, K350E coronin mutant sporozoites with ionomycin. No change in the localization of this mutant in the presence of ionomycin (Fig 3.3D) generated another argument. As coronin is known to bind to both actin and PI(4,5)P2, coronin is perhaps binding to actin filaments in the presence of ionomycin and PI(4,5)P2 in the presence of cytochalasin D. Therefore, I subjected sporozoites to the treatment of both 100 nM cytochalasin D and 500 nM ionomycin. However, there was still no change in the peripheral localization of this mutant of coronin. Thus, how and to which part of the SAS coronin is targeted remains to be determined.

3.4 Effects of coronin mutations on the life cycle of *P. berghei.*

To probe the defects caused by the ablation of actin binding, I decided to replace WT-coronin with mutant forms of coronin. The localization screen of mutants (ref section 3.3) has indicated 3 distinct patterns of localization. Thus, I selected one representative mutant of each pattern for replacement. They were R24A, R28A (localization pattern: rear like WT), K283A, D285A (localization pattern: cytoplasmic), R349E, K350E (localization pattern: peripheral) and all sites mutated (localization pattern: cytoplasmic). After replacement, I tracked these parasite lines across the life cycle of *P. berghei* and compared them to (i) WT-*Pb*ANKA, (ii) coronin knock out and (iii) endogenous coronin-mCherry. This is because, (i) the transfections for all the parasite line were done on the background parasite line, WT-*Pb*ANKA, (ii) comparison to coronin knock out may support our hypothesis of actin binding function of coronin, (iii) all the

replacement lines have mCherry fused at the C-terminus of mutant coronin. This is depicted in the integration strategy (ref section 2.3).

3.4.1 Coronin is dispensible for the oocysts development in the midgut of mosquitoes.

Midguts of mosquitos were dissected between days 10 to 12 post infection. They were permeabilized and stained with mercurochrome. One way ANOVA analysis suggested that the oocysts counts were not significantly different between the knock out or any mutant parasite line and the WT or endogenous coronin-mCherry line (graph 3-1). This suggests that there is no effect of coronin mutations or absence in the initiation of oocysts formation. This could be expected as coronin was not detected in ookinetes.

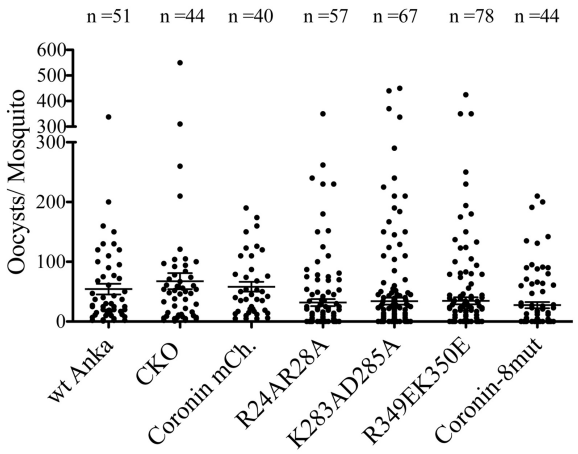

Graph 3-1: Comparison of oocysts - Number of oocysts per infected mosquito (y axis) and parasite line (X-axis); n=number of midguts counted.

3.4.2 The actin regulatory function of coronin contributes to the development of midgut sporozoites and invasion of salivary glands.

Although the coronin knock out and its mutations do not influence the number of oocysts formed, there seems to be a partial sporozoite developmental defect in oocysts as the coronin knock out parasite line has over 30% reduction in the number of midgut sporozoites as compared to the WT. K283A, D285A mutant also showed a similar reduction. Parasite lines R349E, K350E and coronin-8mut were less affected. R24A, R28A mutant and endogenous coronin-mCherry on the contrary showed an increased number of sporozoites, which remains unexplained (graph 3-2 and table 3.1). Possibly the natural variation of the range of infection is higher than can be determined with the few experiments performed here. Please note that each

point in the figure corresponds to the data obtained for one mosquito cage, whereas the table shows the compiled data of all cages for that parasite line.

In order to understand the role of coronin in salivary gland invasion, I plotted the ratio of salivary gland sporozoites to midgut sporozoites. I observed that the coronin knock out and some mutants of coronin affect salivary gland invasion. Amongst them are coronin-8mut and K283A, D285A, which showed half the invasion efficiency. Parasite lines R24A, R28A and R349E, K350E were moderately affected with about 30% reduction in invasion efficiency. This agrees well with the localization pattern to a certain extent. The K283A, D285A mutant and coronin-8mut localize both in the cytoplasm. But, the slight reduction observed for R24A, R28A could be attributed to a functional defect of sporozoites. It indicates that this mutant is unable to execute complete function of coronin, however it localized to the rear. One reason might be the added mCherry, as there was no reduction when compared to coronin-mCherry. Overall, these mutations suggest a role of the actin regulating function of coronin in salivary gland invasion.

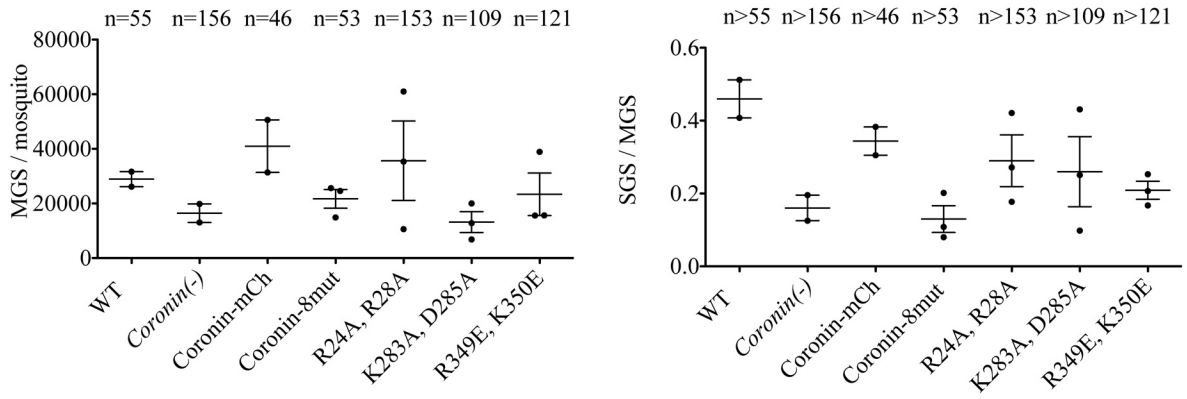

Graph 3-2. Invasion of salivary glands by sporozoites: Each data point corresponds to the average number of midgut sporozoites per mosquito dissected from one mosquito cage [left]. Average of ratio of the numbers of salivary gland sporozoites to the midgut sporozoites – Each data point corresponds to the mosquitos dissected from one mosquito cage [right]. The total number of mosquitos is denoted on top of each parasite line (n > 50).

Table 3.1: Comparison of the different parasite strains for the infectivity to mosquitoes and the *in vitro* speed of sporozoites. Note that sporozoites from the R24A, R28A mutant, despite lower numbers in the salivary gland moved with comparable speed to the coronin-mCherry parasites. * indicates significant differences from the WT for *coronin(-)* and from *coronin-mCherry* for the 4 parasite lines expressing mutated *coronin-mCherry*.

Parasites	Oocysts (infected midguts)	Ratio Infected vs total midguts	Midgut sporozoites (examined midguts)	Salivary gland sporozoites (examined midguts)	Ratio sal. Gland vs midgut sporozoites	Speed in µm/s (examined sporozoites)
WT	54 (51)	0.61	28000 (55)	13000 (75)	0.46	2.0 (62)
Coronin-mCherry	58 (40)	0.63	41000 (50)	14000 (79)	0.35	1.2 (77)
Coronin(-)	72 (44)	0.33	19000 (202)	2900 (247)*	0.15*	0.2 (85)*
Coronin-8mut	54 (44)	0.50	22000 (121)	2600 (265)*	0.12*	0.3 (144)*
R24A, R28A	63 (57)	0.49	38000 (53)	8200 (262)*	0.22*	1.2 (56)*
K283A, D285A	76 (78)	0.44	15000 (153)	2700 (322)*	0.18*	0.3 (61)*
R349E, K350E	71 (67)	0.48	20000 (109)	4300 (231)*	0.22*	0.2 (146)*

3.4.3 Actin binding nature of coronin is important for gliding motility of sporozoites.

To further address the importance of actin-binding sites of coronin, I performed a gliding motility assay for the mutant and WT salivary gland sporozoites. For this assay, salivary glands of mosquitoes were dissected and sporozoites were purified using the Accudenz purification technique. Gliding motility patterns of these sporozoites were studied and speeds measured (ref section 2.4). Imaging of these sporozoites suggests that the endogenous coronin-mCherry and R24A, R28A mutant sporozoites glide in counter-clockwise circles similar to the WT sporozoites. This was expected as the overexpressed R24A, R28A mutant had a similar localization pattern to WT. However, sporozoite migration speeds of both of these parasite lines were reduced as compared to WT sporozoites (graph 3-3). This again could possibly be attributed to the fusion of coronin with mCherry, which might interfere subtly with coronin function. This is in congruence with the previous finding that the effects of fusion tags for cytoskeletal proteins affect their dynamics (Deibler et al, 2011). Thus, it is conceivable that the fusion of coronin with mCherry may indirectly interfere with actin dynamics.

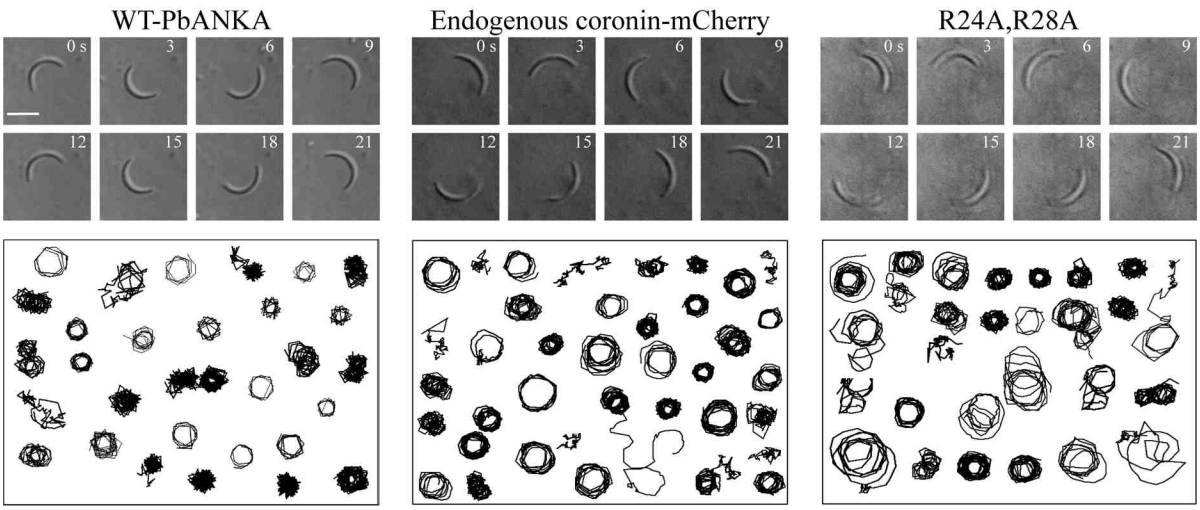

Fig 3.4: WT-*Pb*ANKA, endogenous coronin-mCherry and R24A, R28A sporozoite gliding assay: Stills from a gliding assay movie (top) and progressive lines of multiple manually tracked sporozoites (bottom) for WT-PbANKA (left), endogenous coronin-mCherry (middle) and R24A, R28A replaced mutant (right). The movies are taken with 25X objective under zeiss wide field microscope with differential interference contrast (DIC) settings. Each frame in the movie is separated by 3 seconds and duration of the movie is 5 min. (scale bar = 5 μm).

On the other hand, the K283A, D285A mutant and coronin-8mut glide aberrantly. The motility of these sporozoites is distinguished by continuous detachment of the sporozoites from the substrate, which could be the reason for or the effect of the non-directionality in the movement (Fig 3.5). A similar pattern of motility had also been previously observed for coronin knock out sporozoites (Fig 3.4). These 2 mutants forms showed cytoplasmic localization of the coronin (Fig 3.3B), which together with the abberant movement suggests that the peripheral localization of coronin is of primary importance to its function.

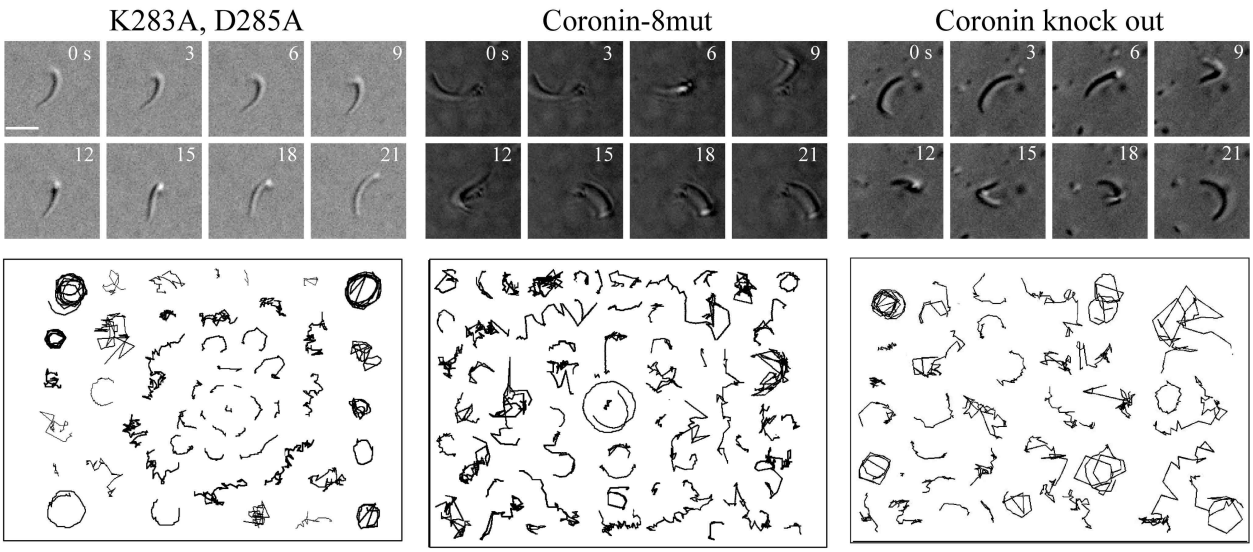

Fig 3.5: K283A, D285A, coronin-8mut and coronin knock out sporozoite gliding assays: Stills from a gliding assay movie (top) and progressive lines of multiple manually tracked sporozoites (bottom) for K283A, D285A replaced mutant (left), coronin-8mut (middle) and coronin knock out (right). The movies are taken with 25X objective under zeiss wide field microscope with differential interference contrast (DIC) settings. Each frame in the movie is separated by 3 seconds and duration of the movie is 5 min. (scale bar = 5μm).

To get deeper insight about the effect of peripheral localization on motility, I sought to study the gliding pattern of mutant R349E, K350E that localizes in the periphery with F/R ratio being nearly one. This mutant exhibits a very different pattern of motility as compared to above two distinct patterns. These sporozoites glide slowly (graph 3-3). Their motility is distinguished by the occasional presence of a kink in the rear one-third portion of the sporozoite (Fig 3.6). However, most sporozoites move aberrantly like coronin knock out sporozoites.

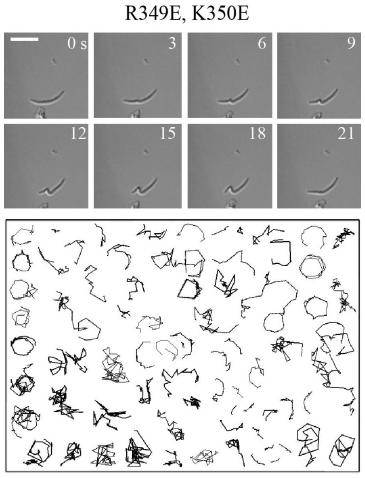

Fig 3.6: R349E, R350E sporozoite gliding assay: Stills of a sporozoite from a gliding assay movie (top) and progressive lines of multiple manually tracked sporozoites (bottom) for R349E, K350E. The movies are taken with 25X objective under zeiss wide field microscope with differential interference contrast (DIC) settings. Each frame in the movie is separated by 3 seconds and duration of the movie is 5 min (scale bar = 5 μm).

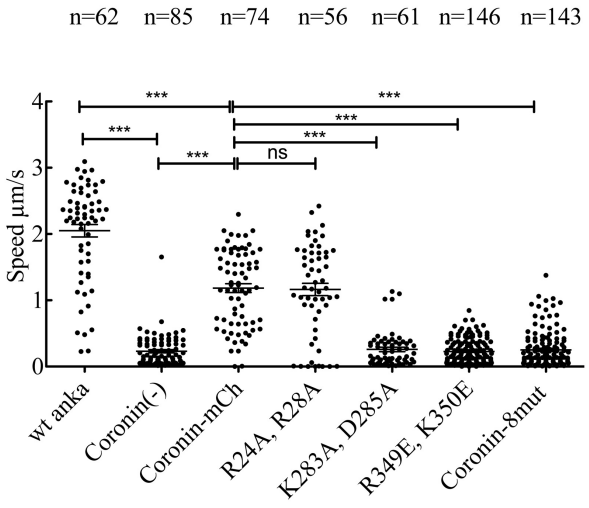

Graph 3-3. Speeds of sporozoites:

The speed of each sporozoite is calculated as an average of the speed per frame of that sporozoite for 101 frames taken every three seconds. Each dot represents the speed of individual sporozoite. The graph shows the comparison of the gliding speeds for all the parasite lines. (mean, SE), (bonferroni multiple comparison test, $p < 0.0001$).

To further investigate the differences in sporozoite motility, I classified the motility pattern in 5 different groups. They were (i) **moving** (this pattern classifies sporozoites that are moving in counter-clockwise circles for more than two and half minutes and completing at least 2 circles), (ii) **partially moving** (this pattern classifies active non-circular aberrant movement that is different from the other 4 patterns), (iii) **patch-gliding** (this pattern classifies sporozoites moving back and forth over a single adhesion site; this movement is exhibited by sporozoites present in the mosquito haemolymph but has not been observed in sporozoites isolated from the salivary gland prior to my study), (iv) **attached** (this pattern classifies sporozoites that are attached to the substrate but do not move) and (v) **drifting** (this pattern classifies sporozoites being rolled over with continuous attachment and detachment at the front and back portion of sporozoite). Sporozoites that are floating and moving around with the flow of the diffusion were not taken into account (graph 3-4).

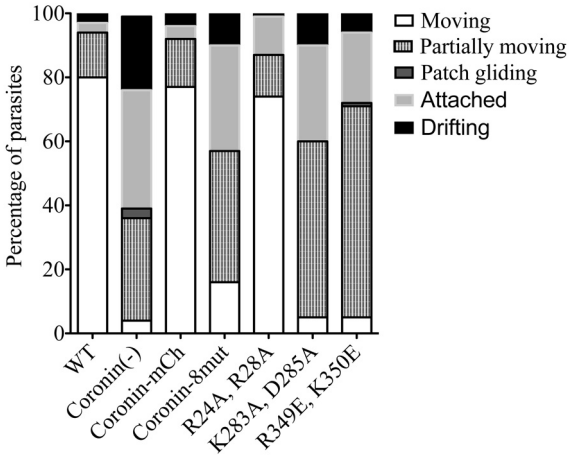

Graph 3-4: Motility patterns of sporozoites:

The percentages of sporozoites motility patterns (y-axis) exhibited by wild type (WT), coronin(-), endogenous coronin-mCherry and the 4 mutant parasite lines (x-axis).

3.4.4 Coronin plays a role in the development of preerythrocytic stages independent of actin.

Ex vivo liver cell assay was conducted with all the mutant transgenic parasite lines as described (ref section 2.7). HepG2 liver cells were fixed in a 24-well plate and immunofluorescence assay (IFA) was performed with antibody for HSP70 (ref section 2.7). The IFA slides were viewed under the microscope and images of the infected liver cells taken. Sizes of preerythrocytic forms were measured for all the transgenic lines and WT with ImageJ. The sizes of the liver stages for the parasites lines in this study were similar for the first 24 hrs. post infection. However, it was already known that at 48hrs, coronin knock out parasites form smaller liver stages than WT parasites (Lepper, 2011). Therefore, if the actin binding ablated mutants of coronin also form smaller liver stage sizes at 48 hrs then it would suggest the importance of actin regulatory functions of coronin in the liver stage as well. Interestingly, the sizes of the liver stages of the mutant parasite lines were not significantly different than WT parasites. The ideal control for these parasite lines was the endogenous coronin-mCherry line as the mutant parasite lines also had coronin fused to mCherry. This suggests that coronin plays a role in the liver stage growth of the parasite that is independent of actin regulatory function of the protein.

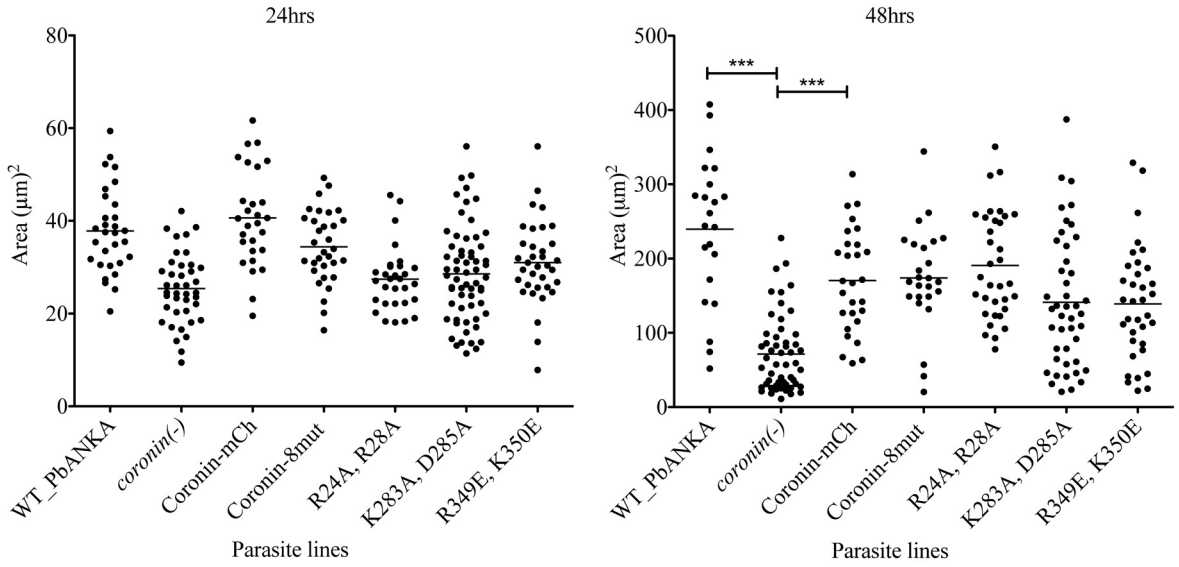

Graph 3-5. Liver stage development: The sizes of liver stage parasites at 24hrs time point (left) and 48hrs time point (right) in μm^2 (y-axis) and parasite lines (x-axis); One way ANOVA $p < 0.0001$).

3.4.5 Influence of coronin on the blood stage growth of *P. berghei* parasites

Blood stage infection was monitored in mice after infection with either intravenous (i.v.) injection of 10000 sporozoites or by bite of 10 mosquitoes. Upon i.v. injection, the comparison of coronin knock out, endogenous coronin-mCherry and replacement mutants of actin-binding ablated coronin yielded no major difference observed in the pre-patency (time to blood stage infection), number of infected mice. However, less number of mice succumbed to ECM in the case of coronin knock out and actin-binding ablated mutants. Interestingly, upon mosquito bite back, the similar comparison showed about half a day delay in the pre-patency of coronin-8mut and R349E, K350E mutants. The number of mice infected after the bite of mosquitoes with coronin knock out and mutant parasites were less than the mice infected with WT and endogenous coronin-mCherry parasites.

Table 3.2: Comparison of the different parasite strains for their growth within cultured liver cells and their infectivity for mice - Note that all parasites with a lowered number of sporozoites in their salivary glands (all but WT and coronin-mCherry) failed to infect all mice during 'natural transmission'. While 100% (24 out of 24) of the mice bitten by mosquitoes infected with either either wild type or coronin-mCherry expressing parasites were infected, only 78% (53 out of 68) of the mice bitten by mosquitoes infected with the various mutants developed a blood stage infection. As the motility was similar between WT, coronin-mCherry and R24A, R28A mutants on one hand and between all the other mutants on the other (Table 3.1), we further analyzed the time to infection of the mice successfully infected by mosquitoes. Hence, the first group showed an average time to blood stage infection of 3.4 (3.5) days and the second group of 3.8 (4.1) days for i.v. injected or 'naturally transmitted' parasites.

Parasites	**Liver stage size at 24 hpi in µm^2 (numbers of examined LS)**	**Liver stage size at 48 hpi in µm^2 (numbers of examined LS)**	**Infected mice by i.v. infecetion / total mice**	**ECM (time to blood stage infection)**	**Infected mice by 10 mosquito bites**	**ECM (time to blood stage infection)**
WT	39 (30)	240 (22)	27/27	25/27 (3.3)	16/16	11/16 (3.5)
Coronin-mCherry	41 (28)	170 (28)	8/8/	4/8 (3.4)	8/8	5/8 (3.9)
Coronin(-)	25 (40)	71 (53)	38/38	20/38 (3.8)	17/20	9/17 (4)
Coronin-8mut	34 (32)	174 (25)	12/12	7/12 (3.8)	10/12	6/10 (4.1)
R24A, R28A	27 (30)	191 (34)	12/12	8/12 (3.5)	10/12	9/10 (3.2)
K283A, D285A	29 (62)	141 (44)	12/12	5/12 (3.9)	5/12	3/5 (3.8)
R349E, K350E	31 (35)	139 (35)	12/12	3/12 (4)	11/12	5/11 (4.4)

3.5 Purification of *Pb*-coronin

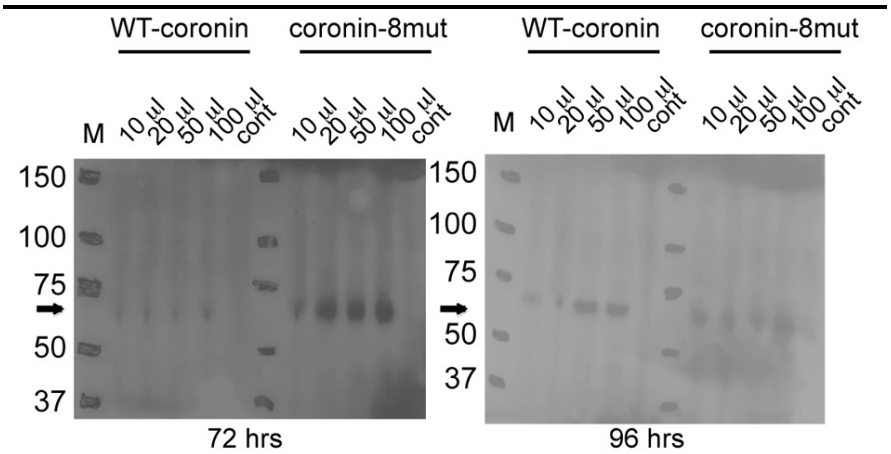

Fig 3.7: Purification of *Pb*-coronin: 10^6 SF21(Spodoptera frugiperda) cells were infected with 10-100 µL of viral stocks in 24 well plate. Upon incubation at 28^0C for 72 and 96 hrs. cells were extracted from wells and tested for expression of 6X-His-Pb-coronin by western blotting with anti-his antibody

Baculovirus-mediated expression of *Mm*-coronin and *Pf*-coronin resulted in soluble expression of respective coronin (Appleton et al, 2006; Olshina et al, 2015). Thus I sought to use

the same protein purification method for *Pb*-coronin. It was found that *Pb*-coronin is expressed at 72 hrs and 96 hrs post inoculation of baculovirus in SF21 insect cells as shown by the western blotting using anti his-antibody (Fig 3.7). After successful expression of WT-coronin and Coronin-8mut, I inoculated large-scale cultures of insect cells with baculovirus carrying his-tagged coronin. Various fractions of during purification were collected and loaded on SDS-PAGE. It appears that both WT-coronin and coronin-8mut are insoluble (Fig 3.8).

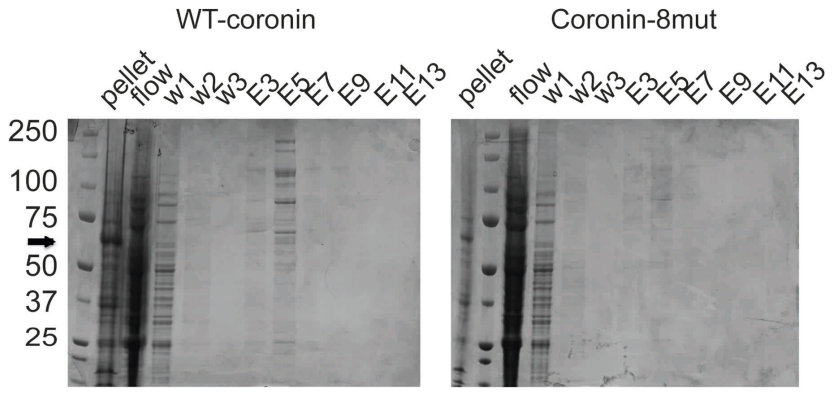

Fig 3.8: WT-coronin and coronin-8mut are insoluble - Various fractions collected during purification of *Pb*-coronin and coronin-8mut under native conditions show that both coronin and coronin-8mut are insoluble.

Therefore, it was important to first extract the insoluble fraction of coronin from inclusion bodies. This necessitated more stringent denaturing condition consisting of 6 M guanidine hydrochloride in the presence of the reducing agent β-mercaptoethanol (Fig 3.9).

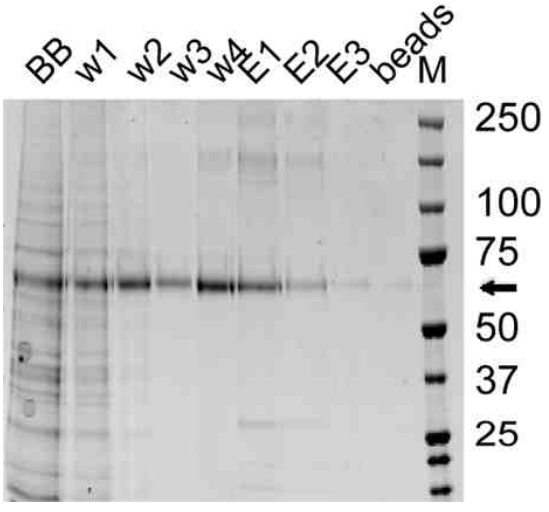

Fig 3.9: Extraction of insoluble coronin under denaturing conditions - Various fractions collected during purification of coronin-8mut suggesting that it is solubilized without aggregation under denaturing conditions.

Furthermore, to do the actin binding assays for probing the interaction of coronin with actin filaments, it was necessary to have coronin in refolded and soluble form. Hence, I decided

to use 27 different buffer conditions (tables 3.3 and 3.4) to refold the protein. To this end, 10 µL of extracted denatured protein was incubated with 100 µL of buffer at 4^0C for 24 hrs. Running the protein refolding reaction on semi-non-reducing gel (i.e. sample was prepared under non-reducing conditions and electrophoresed under reducing conditions) resulted in either the presence of smears in wells or sharp bands (Fig 3.10).

Table 3.3. Final concentration of constituents of refolding buffer

Buffer 50 mM	Ionic strength	Amphiphilic	Reducing agent	Additives
Na-Ac [pH 4]	NaCl (100 mM)	Glycerol (20%)	BME (20 mM)	Arg (800 mM)
Tris [pH 7]	NaCl (200 mM)	PEG (0.05%)		Glucose (500mM)
Tris [pH 8]	KCl (100 mM)			EDTA (1 mM)

Na-Ac: Sodium acetate, NaCl: Sodium chloride, KCl: Potassium chloride, BME: β-mercaptoethanol, Arg: Arginine, Tris: Tris base, PEG: Polyethelene glycol, EDTA: Ethelenediamine tetraacetic acid.

Table 3.4. Composition of refolding buffer

1 pH 4 BME Arg	2 pH 4 NaCl (1x) BME	3 pH 4 Glycerol	4 pH 4 PEG Glucose	5 pH 4 EDTA	6 pH 4 PEG Glucose	7 pH 4 KCl BME	8 pH 4 BME Glucose	9 pH7
10 pH 7 KCl	11 pH 7 Glycerol BME	12 pH 7 PEG Arg	13 pH 7 NaCl (1x)	14 pH 7 BME Arg	15 pH 7 BME	16 pH 7 PEG BME	17 pH 8 Arg	18 pH 8 EDAT Glucose
19 pH 8 Glycerol BME	20 pH 8 KCl BME Arg	21 pH 8 Glucose	22 pH 8	23 pH 8 PEG	24 pH 8 BME Glucose	25 pH 8 NaCl (1x)	26 pH 8 NaCl (2x) BME Glucose	27 pH 8 BME

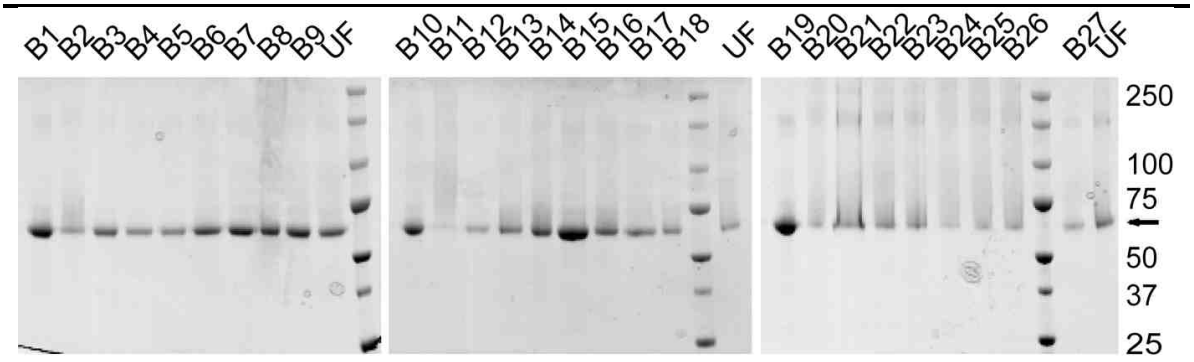

Fig 3.10: Screening of refolding buffers on semi-non-reducing gel - Semi-non-reducing gels for proteins incubated with screened refolding buffers 1-27 at 4^0C for 24 hrs. Protein not incubated with any of the above buffers is loaded as a control (UF or unfolded).

Amongst them, the protein incubated with buffers 2, 3, 4, 5, 8, 11, 13 and 16 did not form smears and thus were selected to run on a native gel. Absence of any band on the native gel indicates that coronin could not be refolded (Fig 3.11).

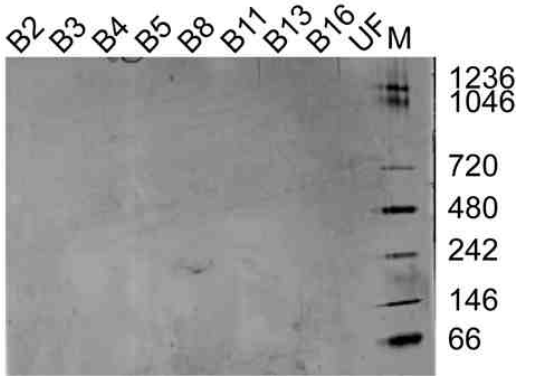

Fig 3.11: Screening of refolding buffers on native gel - Native gel for protein incubated with refolding buffers 2, 3, 4, 5, 8, 11, 13, 16. Protein not incubated with any of the above buffers was used as a control (UF or unfolded).

3.6 Overexpression of *Pf*-coronin and replacement of *Pb*-coronin with *Pf*-coronin

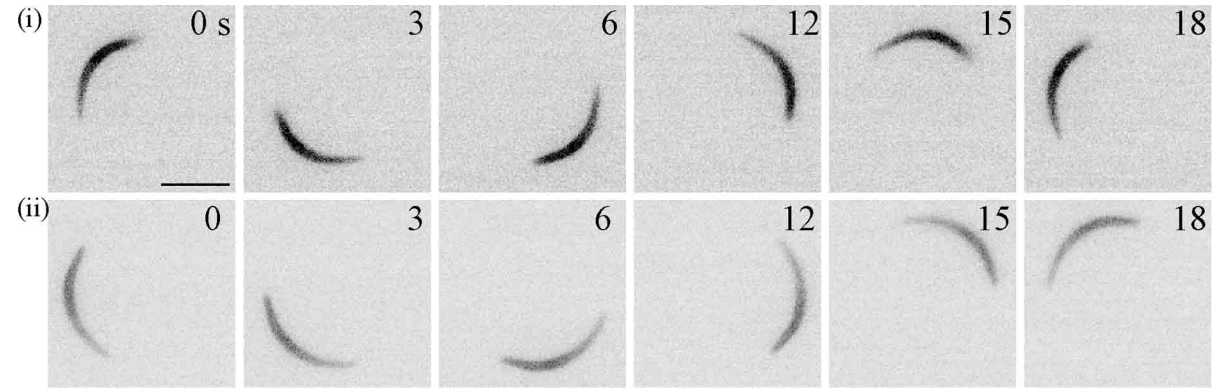

Fig 3.12: Localization of *Pf*-coronin-mCherry overexpressed under *uis3* promoter.

In contrast to *Pb*-coronin, which could not be solubilized, *Pf*-coronin was readily soluble (Olshina et al, 2015). Additionally, the biochemical characterization showed that *Pf*-coronin bundles actin filaments. Since *Pb*-coronin is the closest homologue of *Pf*-coronin, it could be speculated that *Pb*-coronin also bundles actin filaments. One way to test this hypothesis is to localize *Pf*-coronin-mCherry in *P. berghei*. The other way is to check if the replacement of *Pb*-coronin with *Pf*-coronin-mCherry rescues the phenotypes previously observed in *coronin(-)* parasites (Lepper, 2011). Consequently, I probed the localization of *Pf*-coronin-mCherry overexpressed under the control of *uis3* promoter (ref section 3.4). The microscopic observation

showed that *Pf*-coronin-mCherry was slightly enhanced at the rear but not at the periphery (Fig 3.12). Furthermore, I investigated the replacement of *Pb*-coronin with *Pf*-coronin-mCherry. The results of replacement were compared to endogenously tagged *Pb*-coronin-mCherry, WT-*Pb*ANKA and *coronin(-)* (ref section 3.4). As expected, no defects in oocysts numbers were observed (Fig 3.13A).

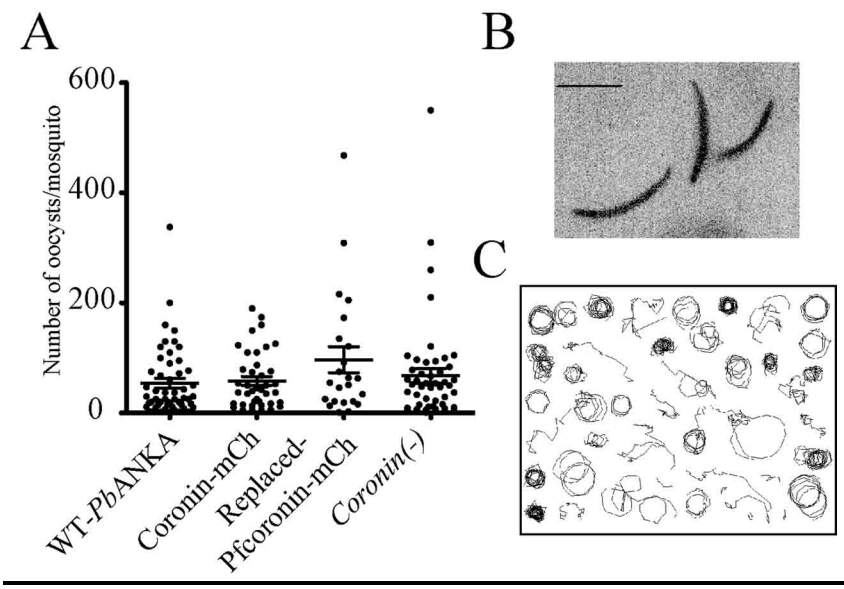

Fig 3.13: Oocysts and sporozoites of replaced Pfcoronin-mCherry: Graph showing number of oocysts per mosquito **[**A**]**. Localization of replaced *Pf*-coronin-mCherry **[**B**]**. Tracks of replaced *Pf*-coronin-mCherry sporozoites **[**C**]**

Determination of midgut and salivary gland sporozoites numbers and computation of their ratio displayed no significant difference for replacement parasite line in comparison to either WT-*Pb*ANKA or endogenous coronin-mCherry (Table 3.5). This suggests that *Pf*-coronin could complement the *Pb*-coronin during the salivary gland invasion.

Table 3.5: MGS and SGS of *Pf*-coronin-mCherry line:

	MGS (number of sporozoites)	SGS (number of sporozoites)	SGS/MGS
WT-Pb-*ANKA*	28000 (50)	13000 (75)	0.46
Endogenous Coronin-mCherry	41000 (50)	14000 (79)	0.35
Replaced_Pfcoronin-mCherry	41800 (121)	13600 (142)	0.33
Coronin(-)	19000 (202)	2900 (247)	0.15

However, the analysis of *in vitro* gliding motility showed that only 48% of *Pf*-coronin-mCherry parasites glide in counterclockwise circles compared to 80% and 76% of WT-*Pb*ANKA

and endogenous-coronin-mCherry respectively. This percentage is higher than *coronin(-)* sporozoites which showed only 4% gliding. Microscopic observation of *Pf*-coronin-mCherry replacement in the *P. berghei* sporozoites suggested that *Pf*-coronin localizes to the cytoplasm (Fig 3.13B). The speed of *Pf*-coronin-mCherry parasite line was although significantly less than that of WT and endogenous coronin-mCherry, it was still significantly higher than *coronin(-)* (Fig 3.14A). Furthermore, the inoculation of HepG2 cells with sporozoites of *Pf*-coronin-mCherry parasite line suggested that the sporozoites were able to infect the HepG2 cells *in* vitro. The sizes of the liver stage *Pf*-coronin-mCherry parasites were analogous to the sizes of endogenous coronin-mCherry and WT-*Pb*ANKA (Fig 3.14B).

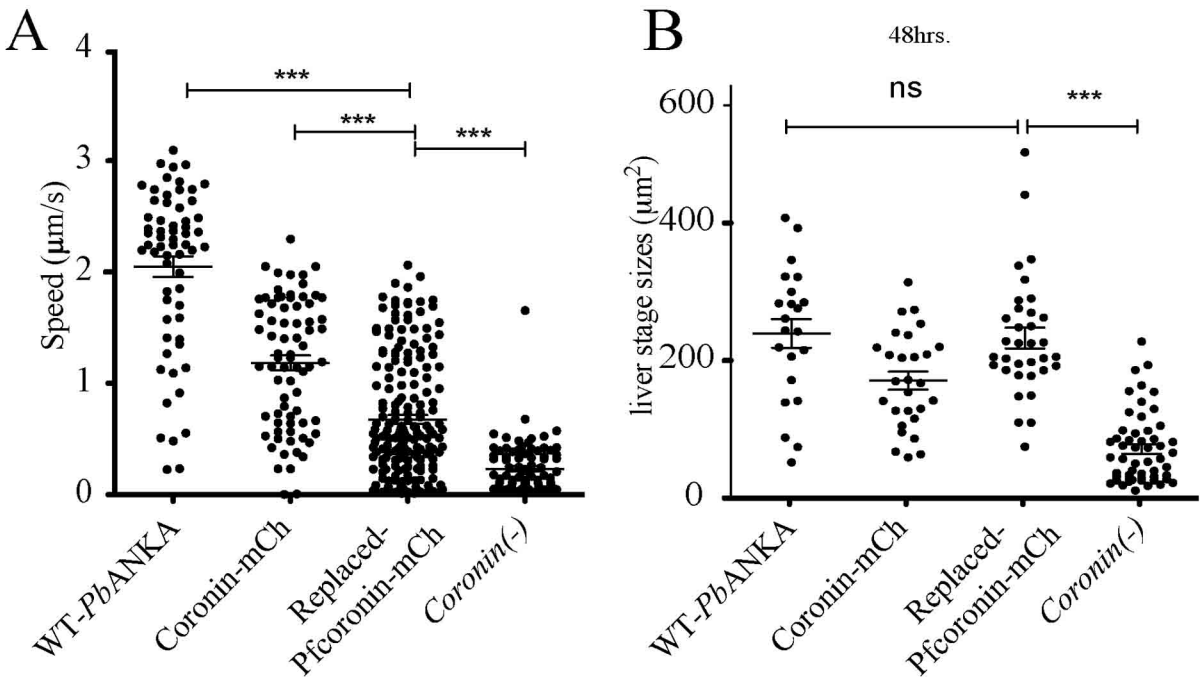

Fig 3.14: Speeds and liver stage sizes of replaced Pfcoronin-mCherry [A-B]. Comparison of speeds **[**A**]**. Comparison of sizes of liver stage parasites 48 hrs. post infection **[**B**]**.

Nevertheless, to probe if the intermediate *in vitro* gliding motility translates into mice infections *in vivo,* I conducted two experiments. (i) the intravenous injection of 10000 sporozoites, (ii) natural transmission of sporozoites with bites of 10 mosquitoes per mouse. The observed prepatency period was 3 days post infection in either case and the number of mice that succumbed to the experimental cerebral malaria (ECM) (5/7 in i.v. injection and 5/8 in bite back) was in line with the data obtained for endogenous coronin-mCherry and WT-*Pb*ANKA parasite

line. Altogether, this indicates that *Pf*-coronin is able to complement *Pb*-coronin in the life cycle stages of *P. berghei,* with the exception of differential localization and slight differences in gliding motility.

3.7 *In vivo* migration of *coronin(-)* sporozoites

Given that coronin deletion leads to defect in the *in vitro* actin-based motility and the development of liver stage parasites, it could be expected that coronin knock out parasites may not reach and invade the hepatocytes. Yet it was surprising to me that the *coronin(-)* sporozoites are able to infect the hepatocytes and establish the further blood stage infection *in vivo*. Therefore, it could be hypothesized that coronin knock out sporozoites may not exhibit any *in vivo* migratory defects.

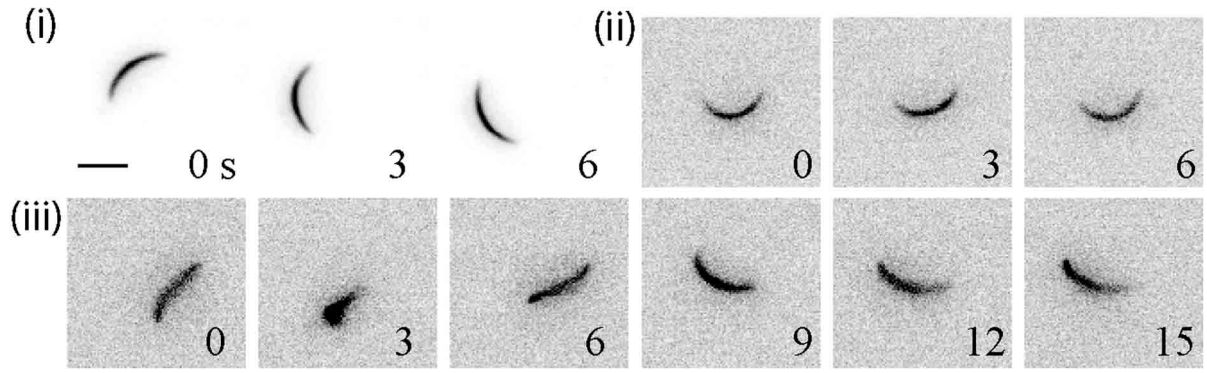

Fig 3.15: *In vitro* migration of *coronin(-)* fluo line: Stills from video microscopy of WT fluo line sporozoites (i), *coronin(-)* fluo line sporozoites *in vitro* gliding assay (ii-iii).

To probe this, it was necessary to image coronin knock out *Plasmodium* sporozoites *in vivo*. This further necessitates the deletion of coronin in the fluorescent background. To this end, I used already existing selection marker free parasite line that expresses mCherry under the sporozoite specific 5'UTR and GFP under the blood stage specific 5'UTR. Despite the expression of foreign proteins mCherry and GFP, this parasite line (referred to as WT fluo hereafter) behaves similar to the WT-*Pb*ANKA *in vivo* and *in vitro* (Klug D, unpublished). Thus, I knocked out coronin in WT fluo line, which is refereed to as *coronin(-)* fluo line. The video microscopic analysis of *in vitro* gliding motility for WT_fluo and *coronin(-)* fluo lines showed that indeed WT fluo glides like WT-PbANKA and *coronin(-)* fluo glides like *coronin(-)* (Fig 3.15).

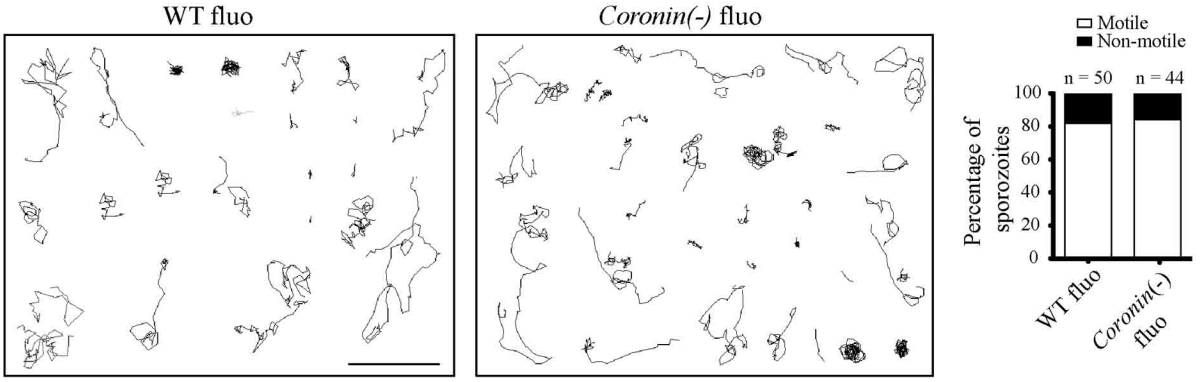

Fig 3.16: *In vivo* migration of *coronin(-)*_fluo line: *In vivo* migration tracks of WT fluo (left) and *coronin(-)* fluo line (middle); (scale bar = 100 µm). Graph showing percentage of *in vivo* motile and non-motile sporozoites of WT fluo parasite line (n = 50) and *coronin(-)* fluo line (n = 44); (right).

Furthermore, I imaged *in vivo* migration. The percentage of motile sporozoites of *coronin(-)_fluo* was in line with the percentage of motile sporozoites of WT-fluo (Fig 3.16). Tracking the migration pattern of this parasite line suggests that there is neither the defect in the migratory pattern of *coronin(-)* fluo line (Fig 3.16) nor a significant reduction in the migration speed when compared to the WT-fluo as a control (Graph 3-6).

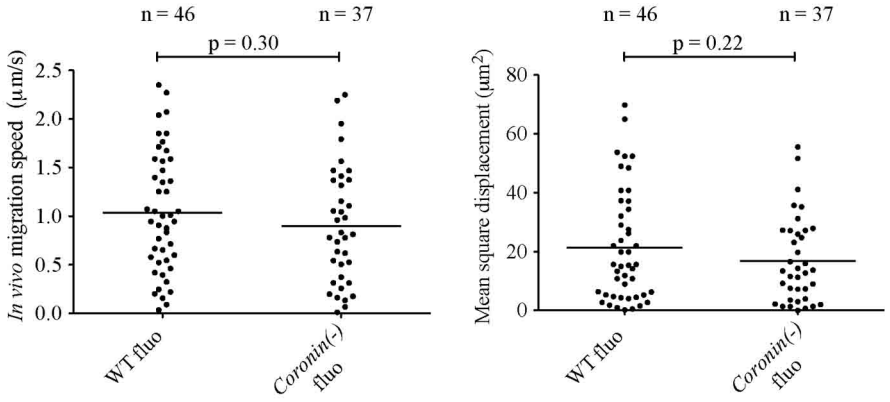

Graph 3-6: Graph showing speed and MSD of *coronin(-)* fluo line: *In vivo* migration speeds of WT_fluo (n = 46) and *coronin(-)* fluo line (n = 37) (left). *In vivo* mean square displacements of WT_fluo (n = 46) and *coronin(-)* fluo line (n = 37) (right).

3.8 Coronin serves as a molecular tool to dissect signaling for sporozoite motility.

Coronin is present on the periphery of the salivary gland sporozoites and upon activation by BSA immediately localizes to the rear of now motile sporozoites. Hence, this unique property of coronin could be exploited. Binding of the ligands to specific receptors relays activation

signals, which in turn leads to intracellular calcium release or activation of pathways like cAMP, phospholipase C etc. Using specific inhibitors and effectors of proteins in these pathways with coronin-mCherry as a tool for visualization of activation, it is possible to unfold the steps involved in calcium signaling.

3.8.1 Coronin elucidates crucial steps in calcium signaling.

Little is known about the nature of the extracellular activating ligand and the sequence of events leading to sporozoite activation upon ligand binding. Given the different localization patterns of coronin-mCherry in the activated sporozoites v/s non-activated sporozoites, I sought to use it as a visual tool to dissect signaling events. This is similar to the previously used calcium sensor (Carey et al, 2014); yet easier to detect. Activation of sporozoites with BSA elevates the levels of cytoplasmic calcium (Carey et al, 2014). I thus investigated if coronin relocalization appears prior to or after the increase in intracellular calcium following external ligand stimulation. To this end I stimulated sporozoites overexpressing coronin-mCherry with BSA and then chelated intracellular calcium ions with BAPTA-AM (1,2-bis(o-aminophenoxy)ethane-N,N,N',N'-tetraacetic acid)-Acetoxymethyle ester). I found that treatment with BAPTA-AM redistributed coronin-mCherry from the posterior to the cytoplasm (Fig 3.17).

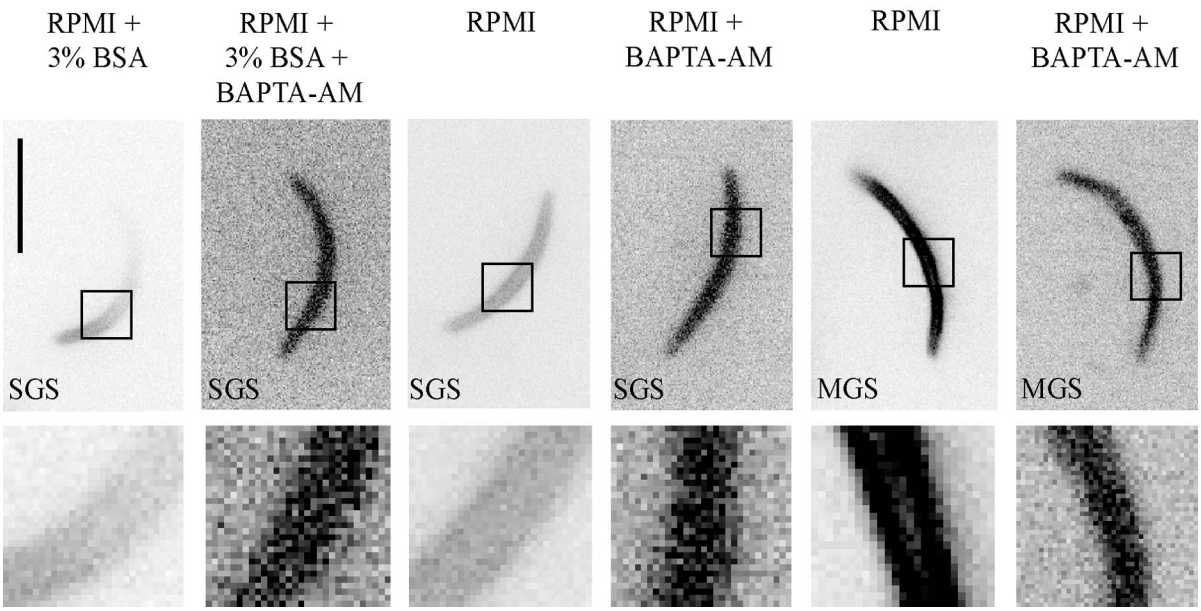

Fig 3.17: Effect of calcium chelation on coronin localization: Localization of overexpressed coronin-mCherry in sporozoites in salivary gland sporozoites (SGS) and midgut sporozoites (MGS) in the presence or absence of 50 μM BAPTA-AM and/or BSA.

This was surprising because according to my previous hypothesis if intracellular calcium causes actin dependent posterior localization of coronin then chelation of intracellular calcium would lead to actin independent peripheral localization of coronin. To get further insights, I treated non-activated salivary gland and midgut sporozoites with BAPTA-AM. This resulted in the cytoplasmic localization of coronin. Thus, it is possible that there exists a basal level of calcium that localizes coronin to the periphery in the non-motile sporozoites such as those transmitted by the mosquito. Upon stimulation by ligands in the skin an increase in calcium leads to microneme secretion and coronin relocalization. To test this, I treated these parasites with non-activating medium containing calcium agonists; either ionomycin or ethanol. It is previously known that an increase in intracellular calcium leads to the secretion of vesicles (Carruthers et al, 1999; Gantt et al, 2000). Both treatments resulted in actively moving parasites with a polarized coronin-mCherry localization (Table 3.6). This motility could not be sustained for more than 10 mins.

Table 3.6: Effect of calcium chelation on sporozoite motility.

Sporozoites	SGS	SGS	SGS	SGS	MGS	MGS
3% BSA	+	+	-	-	-	-
50 µM BAPTA - AM	-	+	-	+	-	+
Motile (Rear)	83	15	18	7	2	0
Motile (periphery)	0	5	0	0	0	0
Non-motile (Periphery)	14	19	51	34	85	36
Non-motile (Cytoplasm)	3	61	31	59	13	64

Nevertheless, the ligand-dependent calcium elevation appears to be upstream of coronin relocalization (Fig 3.18A). Others have shown that increased intracellular calcium also leads to massive exocytosis that mediates invasion in the liver (Gantt et al, 2000) and hence I speculate that different levels of calcium mediate different functions at different stages of the sporozoite life (Fig 3.18B).

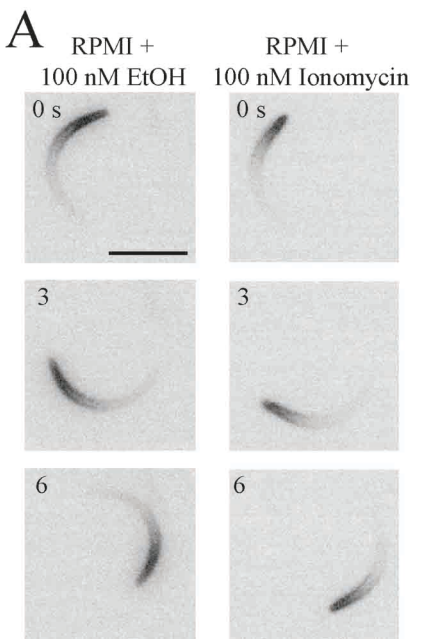

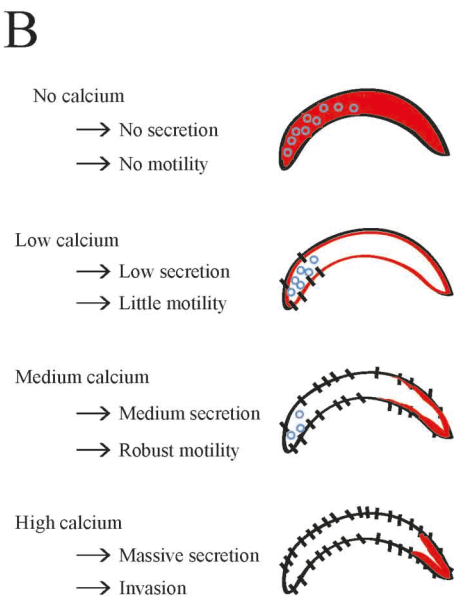

Fig 3.18: Effect of calcium increase on coronin and motility: Stills from a video microscopy showing the localization of overexpressed coronin-mCherry in SGS in RPMI + 100 nM ethanol (left) or 100 nM ionomycin (right) [A]. A hypothetical model displaying the relationship among release of intracellular calcium ion, localization of coronin (red), motility and invasion [B]

Later I probed a potential involvement of kinases and cAMP signaling in activation of gliding motility using inhibitors of cAMP-protein kinase A (PKA) pathway viz. H89 and SQ22536. These inhibitors inhibited sporozoite motility to some degree as was shown previously (Figs 3.19A and 3.19B, done by Miriam Reinig) (Kebaier & Vanderberg, 2010). Conversely, when I stimulated cAMP production in the absence of BSA with forskolin sporozoites were moving confirming previous results (Kebaier & Vanderberg, 2010). Remarkably, when sporozoites halted their movement during inhibition by PKA inhibitors, the coronin-mCherry signal stayed polarized on the rear (Figs 3.19C and 3.19D). This is in contrast to our previous observation as the inhibition of motility with actin modulating compounds altered the localization of coronin from rear to the periphery (section 3.2). Thus, it could be imagined that the inhibition of cAMP-PKA pathway does not actively alter actin filament dynamics, instead it only pauses the continuous processing of the actin filaments. To test this, I added 1000 nM cytochalasin D to sporozoites pre-incubated with BSA and H89. This resulted in the peripheral localization of coronin (Fig 3.19C).

Activator of cAMP pathway: Forskolin is an activator of adenyl cyclase, an enzyme that converts ATP to cAMP. Forskolin was previously tested to activate sporozoite motility (Kebaier & Vanderberg, 2010). However, cAMP is a second messenger of calcium signaling pathway and

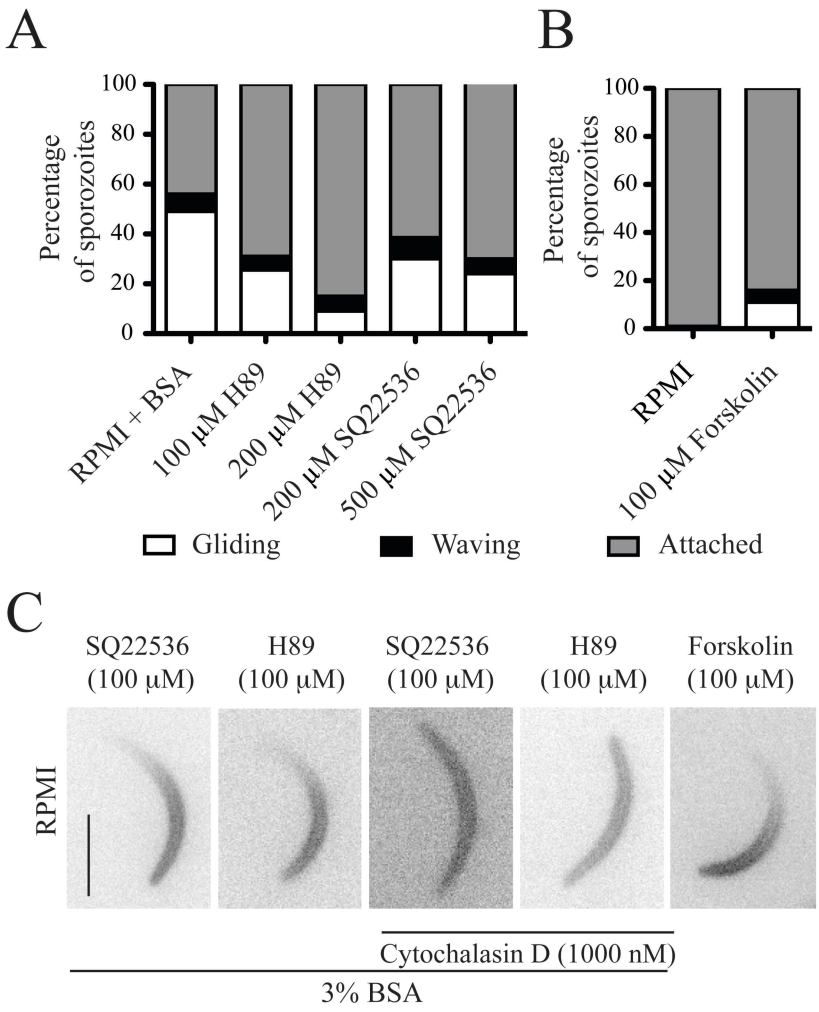

D

3% BSA	+	+	+	-
Inhibitor	SQ22536 (100 µM)	SQ22536 (500 µM)	H89 (100 µM)	Forskolin (100 µM)
Motile (Rear)	37	6	29	34
Motile (Non-rear)	0	0	0	0
Non-motile (Rear)	32	55	48	4
Non-motile (Non-rear)	31	38	23	62

Fig 3.19: cAMP-PKA pathway in sporozoite motility - Inhibitors of kinases stop sporozoite motility in a dose-dependent fashion (n > 150) (A). Forskolin stimulates sporozoite motility (n > 150) (Motility assay was done by Miriam Reinig) (B). Coronin-mCherry stays at the rear in activated sporozoites stopped with PKA inhibitors while it relocalizes to the periphery when additionally cytochalasin is applied. Forskolin leads to the localization of coronin-mCherry to the rear. Scale bar: 5 µm (C). Table showing percentages of motile and non-motile sporozoites under the indicated conditions and the associated localization patterns of coronin-mCherry. Between 105 and 120 sporozoites were examined per condition (D).

coronin localization is an event before cAMP activation. Thus, it is plausible that forskolin may not localize coronin to the rear of the motile sporozoites. Thus, I treated P. berghei sporozoites with 100 µM of forskolin. To our surprise, coronin localizes to the rear in both motile and non-motile sporozoites (Figs 3.19C and 3.19D). It could be because the active products of cAMP

pathway are causing intracellular calcium release. PKA activated by cAMP is known to cause calcium release from intracellular stores of calcium (Zanassi et al, 2001). This calcium release therefore results in coronin's localization to the rear of the sporozoite.

This, together with the previous observations on coronin mutants suggests that actin filaments are still at the rear of the parasite when kinases are inhibited. This, it is highly like that kinases regulate proteins involved in the dynamics of actin filaments including coronin and the inhibition of kinases partly freezes these dynamics. One possible way to test this is to bleach the mCherry fluorescence and measure the recovery of coronin-mCherry (Fig 3.20A). In the non-activated and non-motile sporozoites the half recovery was the fastest suggesting that there is freely diffusible coronin. Provided the coronin-mCherry overexpression resulted in an increased motility even in non-activated sporozoites, I measured the half recovery time for these motile sporozoites. Surprisingly, these non-activated motile sporozoites recovered significantly slower than the non-motile ones. The sporozoites activated with serum for motility also recovered as slow as the non-activated motile sporozoites. This different recovery times in motile sporozoites and non-motile sporozoites suggest that in motile sporzoites coronin is bound to actin filaments. It could also be interpreted that the on-off rate of coronin to actin filament in motile sporozoites is lesser than that in non-motile sporozoites. Interestingly though, the stabilization of actin filaments with 100 nM jasplakinolide did not result in significantly different recovery rate, whereas the inhibition of motility with 30 nM cytochalasin D significantly reduced the recovery time. Thus, it could be imagined that depolymerization of actin filaments with cytochalasin D causes actin nuclei and coronin bound to these nuclei diffuse slower than coronin alone. Next, I tested if the inhibition of PKA with 100 μM H89 has an effect on recovery. Indeed the recovery was significantly slower than both the activated and non-activated sporozoites. This suggests that the inhibition of PKA results in less dynamic actin filaments (Fig 3.20B). Furthermore, I tested if the recovery time depends on the localization or motility irrespective of presence of PKA inhibitor or actin modulator. For localization, I followed individual sporozoite for rear or non-rear localization and plotted their half recovery time in a graph. For motility, I classified each sporozoite as either motile of non-motile by setting a threshold of ½ circle in one min time and plotted their half recovery time separately. Interestingly, the half recovery time was independent of localization of coronin and motility of sporozoites (Fig 3.20B). This rules out the possibility that localization of coronin or motility of sporozoite may affect half recovery time.

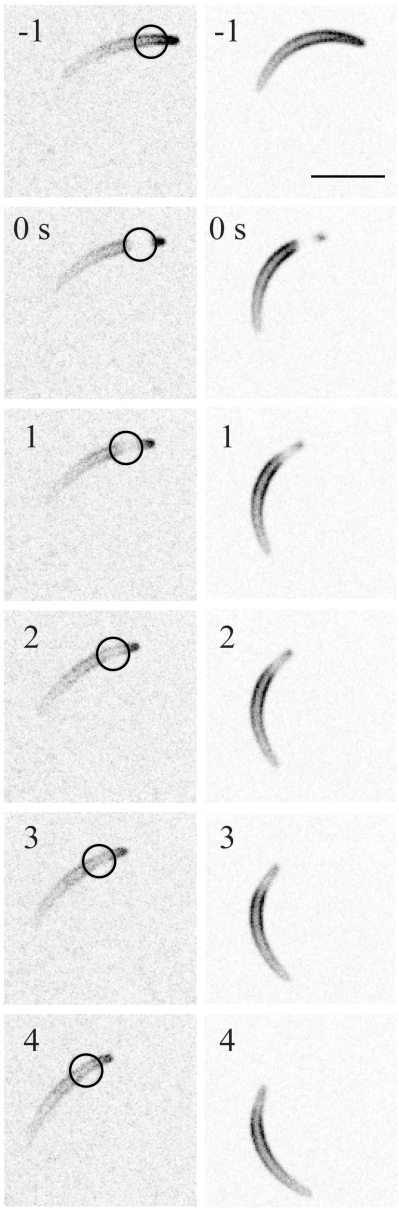

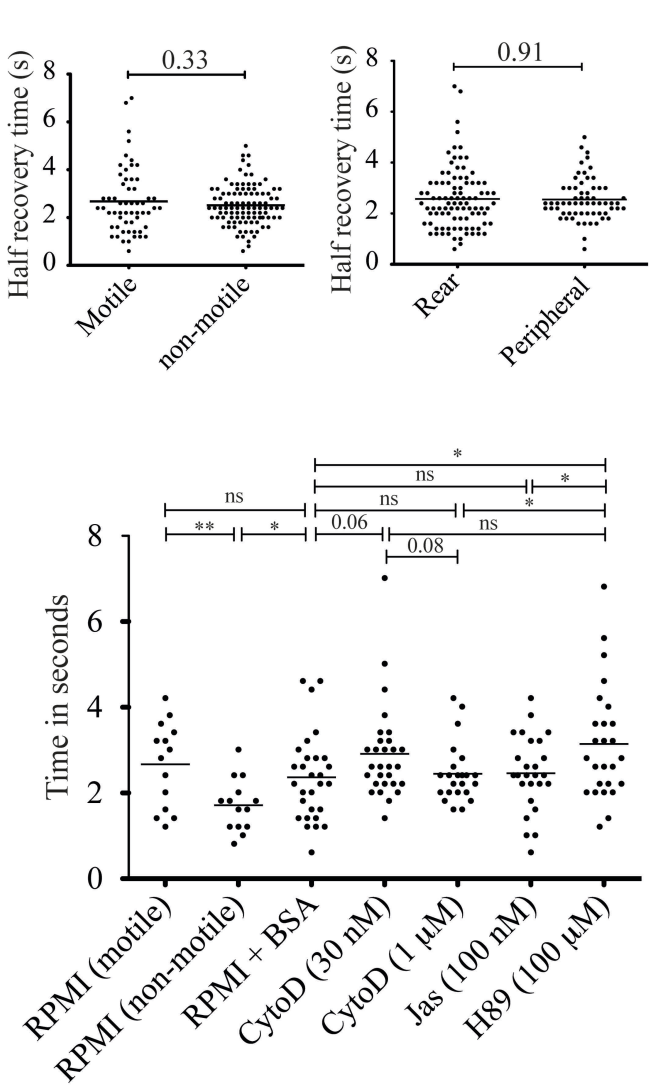

RPMI (motile)	RPMI (non-motile)	RPMI + BSA	Cyto D (30 nM)	Cyto D (1 µM)	Jas (100 nM)	H89 (100 µM)
2.7 ± 1.0	1.7 ± 0.6	2.4 ± 1.0	2.9 ± 1.1	2.4 ± 0.7	2.4 ± 0.9	3.1 ± 1.3

Fig 3.20: Fluorescence Recovery After Photobleaching (FRAP analysis) of coronin-mCherry - Examples of FRAP of sporozoites with coronin-mCherry localized to the rear. Scale bar: 5 µm. Circle indicates location of the bleaching spot (Imaging was done by Mirko Singer and Julia Sattler) (A). Coronin-mCherry recovers as fast in motile (>0.25 µm/s) as in non-motile (<0.25 µm/s) sporozoites if pooled across all conditions. Also there is no difference in recovery time depending on the localization of coronin-mCherry [top]. Quantitative analysis of FRAP data over a range of conditions. Average values (+/- S.D.) are indicated in the table. Bars show significant differences (* $p<0.05$; ** $p<0.01$), non-significances (ns) or p-values (Students t-test). Coronin-mCherry recovers significantly faster in non-motile sporozoites incubated in RPMI than in any other condition. With all other conditions there is no difference from each other with the exception of H89, where coronin-mCherry recovers significantly slower when compared to controls, 1 µM Cytochalasin D and 100 nM Jasplakinolide [bottom] (B).

3.9 Coronin overexpression shows no defect in the growth of *P. berghei*

3.9.1 Overexpression in the blood stages

Overexpression of coronin (CRN1) in *Saccharomyces cerevisiae* results in growth defect (Humphries et al, 2002). Since, coronin is not expressed in blood stages of *P. berghei*, I overexpressed coronin in the blood stages. For overexpression, I selected the 5'UTRs of two genes; actin and erythrocyte membrane associated antigen (EMAA). Overexpressed coronin was tagged with eGFP at its C-terminus for the localization. The strategy for generation of these parasite lines and genotyping PCR is shown (ref section 2.6). Since, the overexpression defect caused by coronin was attributed to the actin-binding sites of coronin, I also overexpressed coronin-8mut under the 5'UTR of actin, using a similar strategy as the negative control. To my surprise, over-expression of WT-coronin with either of the 5'UTRs did not result in any growth defect in the blood stages of the *P. berghei*. The morphology of the parasite in the red blood cells (RBCs) appeared normal when visualized under differential interference contrast microscopy (Figs 3.21A, 3.21B and 3.21D). As could be expected, the growth and morphology of parasites overexpressing the actin-binding ablated mutant form of coronin in blood stages was also normal. Further, I checked the localization pattern for WT coronin and coronin-8mut in the blood stages. This is because the difference in localization of WT-coronin and coronin-8mut is described (ref section 3.3). WT-coronin is more pronounced at the membrane periphery whereas coronin-8mut is localized in the cytoplasm, typically absent from nucleus (Fig 3.21). WT coronin localizes throughout the parasitophorous vacuole in the blood stages parasites while coronin-8mut is localized similarly but typically absent from the nucleus.

3.9.2 Overexpression in ookinetes

I cultured ookinetes of the parasite line 5'UTR$_{(EMAA)}$ - coronin-eGFP and 5'UTR$_{(actin)}$ – coronin-8mut-eGFP in vitro. Both cultures resulted in the formation of the ookinetes. When I looked at the localization of coronin in these ookinetes, WT-coronin was more pronounced in the periphery while coronin-8mut was distributed in the cytoplasm and more pronounced in the nucleus. This is contrary to what I have observed in sporozoites, where coronin-8mut was distributed in the cytoplasm and absent from the nucleus. The difference in the localization of same mutant form of coronin in two different stages of the parasite life cycle remains unexplained.

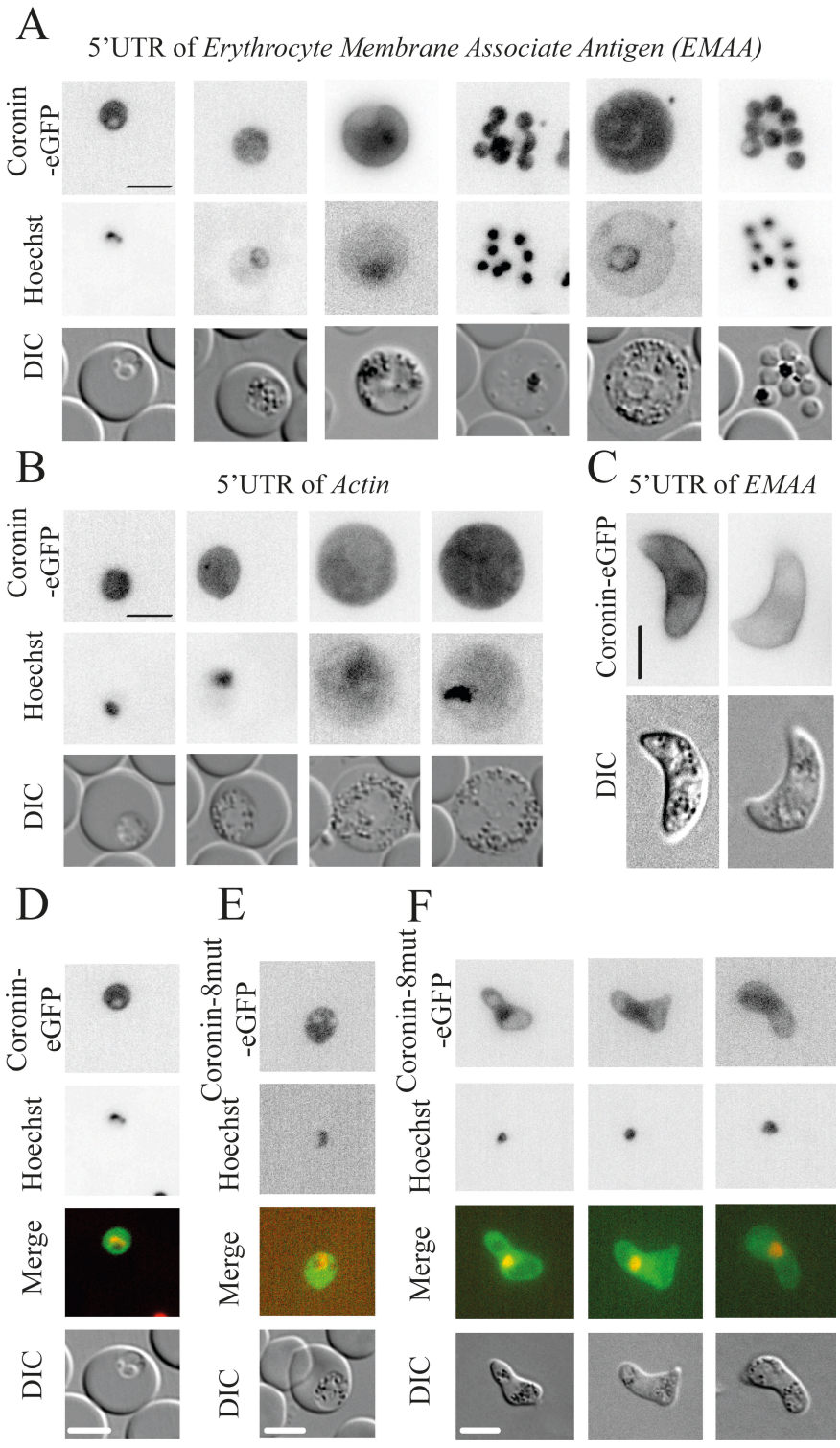

Fig 3.21: Overexpression of WT-coronin and coronin-8mut in blood and ookinete stages of *P. berghei* - Blood stages of *P. berghei* showing the coronin over-expressed from the 5' UTR of EMAA in ring, trophozoite, gametocyte and schizonts stages; coronin-eGFP (top), Hoechst (middle) and DIC (bottom) [A]. Blood stages of *P. berghei* showing the coronin-eGFP over-expressed from the 5' UTR of actin in ring, trophozoite and gametocyte stages; coronin-eGFP (top), Hoechst (middle) and DIC (bottom) [B]. Ookinetes showing the coronin-eGFP overexpressed from 5'UTR of EMAA; coronin-eGFP (top), DIC (bottom) [C]. Coronin-eGFP overexpressed from 5'UTR of actin showing coronin localizes to cytoplasm and nucleus in the blood stages [D]. Coronin-8mut-eGFP overexpressed from 5'UTR of actin showing coronin-8mut localizes to cytoplasm but not to the nucleus [E]. Coronin-8mut-eGFP overexpressed from 5'UTR of actin showing coronin localizing to both cytoplasm and nucleus but specifically pronounced in the nucleus [F].

4. Discussion

Motility is essential for *Plasmodium* parasites to continue their life cycle. Therefore, it is important to understand this motility, which is based on an actin-myosin motor. Actin is a protein known to exist both in monomeric (G-actin) and polymeric (F-actin) form. However, live F-actin dynamics have not yet been visualized in *Plasmodium* with conventional F-actin labeling techniques. Here, I sought to use coronin, a predicted F-actin-binding protein to detect the presence of actin filaments. Therefore, I generated a fluorescent fusion protein of coronin in *Plasmodium berghei* and observed its localization in motile and non-motile sporozoites. Given the low sequence identity of *Plasmodium* coronin with eukaryotic coronins, it was important to test the F-actin-binding properties of *Plasmodium* coronin. To this end, the treatment of motile sporozoites with actin modulating compounds altered the localization of coronin. Furthermore, site directed mutagenesis of the conserved potential actin-binding sites of *Pb*-coronin displayed three different localization patterns. This together with the replacement of endogenous coronin with these mutant forms shed some light on the stages that require coronin-mediated regulation of actin filaments.

Another aspect of this study was to understand the properties of extracellular ligands and calcium signaling that activate sporozoite motility. The use of a previously available parasite line overexpressing coronin-mCherry served as a tool to distinguish between activated and non-activated sporozoites (Lepper, 2011). Observing this localization in the presence of various inhibitors and effectors I could elucidate the key features of the calcium-signaling pathway.

Lastly, the overexpression of coronin in blood and ookinete stages was not deleterious to *Plasmodium* parasites. This is in contrast to the overexpression phenotype observed in yeast (Gandhi et al, 2010), however it was still possible to predict the presence and localization of actin filaments in these stages.

4.1 Expression of endogenous coronin

The C-terminal fluorescent fusion of *Pb*-coronin with mCherry suggested that coronin is weakly expressed in midgut sporozoites, salivary gland sporozoites and liver stages. Given the phenotypes observed with the *Pb-coronin(-)* parasites, which is typically the impaired invasion of salivary glands, aberrant gliding motility and the delayed development in the liver, it is not surprising to observe the expression of endogenous coronin in these three stages. Due to the low

expression of coronin in sporozoites, western blotting with an antibody against mCherry and against *Dd*-coronin could not detect the endogenous expression of coronin.

4.2 Localization of endogenous coronin

Coronin was localized throughout the periphery of midgut sporozoites in a medium with or without serum albumin (BSA). Thus, it could be speculated that in the non-motile sporozoite forms; the gliding motor cannot be activated by the addition of BSA. In contrast, the salivary gland sporozoites could be activated by the addition of serum albumin, which resulted in re-localization of coronin to the posterior of the now motile sporozoites. Since, coronin is an actin filament binding protein, it is likely that the short actin filaments are present (or accumulate) at the posterior end of the motile sporozoites. This postulation is also partly based on the spatial localization of *Plasmodium* actin as shown by an antibody generated specifically against apicomplexan actin. Since, the antibody specifically labels the ends of actin filaments, Angrisano *et al* predicted that actin filaments localize to both poles of *Plasmodium berghei* sporozoites in the presence of jasplakinolide (Angrisano et al, 2012b). However, the possibility that jasplakinolide causes the aggregation of actin could not be excluded (Lee et al, 1998). Recently, the silicon rhodamine dye known as Sir-actin was developed to detect the F-actin and is able to discriminate between aggregation of actin and actin filaments (Lukinavicius et al, 2014). However, the use of Sir-actin on activated *P. berghei* sporozoites did not result in any detectable fluorescence above background. This could be due to either the absence of actin filaments or the failure of Sir-actin to detect *Pb*-actin filaments. The first possibility could be ruled out, since there was no detectable increase in the fluorescence in the presence of jasplakinolide (Douglas R, unpublished).

Interestingly, the presence of actin modulating compounds does alter the localization of coronin in *P. berghei* sporozoites. This leads to a notion that *Plasmodium* coronin may also bind and through binding possibly to regulate actin filaments. In a closely related parasite *Toxoplasma gondii,* coronin also localizes to the posterior. But, its localization could not be altered in the presence of jasplakinolide or cytochalasin D (Salamun et al, 2014). Interestingly, the mouse coronin 1A localizes to the plasma membrane where it binds to PI(4,5)P2. Upon activation by growth factor phospholipase C hydrolyzes PI(4,5)P2 leading to a trans-location of coronin 1A from the membranes to the actin cytoskeleton (Tsujita et al, 2010). The localization of coronin from the periphery of *P. berghei* sporozoites to the rear upon activation by serum albumin could

be regarded as a similar translocation of coronin from the plasma membrane to the actin cytoskeleton. One way to test this hypothesis is to reduce PI(4,5)P2 from the membranes with ionomycin. Indeed *Pb*-coronin localized to the posterior of sporozoites. However, ionomycin also leads to increased calcium within the sporozoites and thus these results need to be taken with caution. The implications for this study are discussed in more detail in relation to phospholipase C binding sites of coronin and calcium signaling (sections 4.3 and 4.5)

With respect to the liver stages of *P. berghei*, I found that coronin is cytoplasmic in the parasitophorous vacuole. It was known that deletion of *Mm*-Coronin 1A, *Dd*-coronin and *Sc*-coronin induced defects in cytokinesis in the respective species (de Hostos et al, 1993; Goode et al, 1999; Moshous & de Villartay, 2014). Based on these findings together with the smaller liver stage sizes in the coronin knock out *P. berghei* parasites, it could be speculated that *Plasmodium* coronin may play a pivotal role in cytokinesis. However, yeast coronin has a domain similar to one of the well-known microtubule binding protein (MAP1B) (Goode et al, 1999). The absence of this MAP1-binding domain in *Plasmodium* coronin weakens the argument about the predicted function of coronin in cytokinesis during the *Plasmodium* liver stage growth. Furthermore, the deletion of coronin does not arrest the development of parasites in the liver. Therefore the role of coronin in liver stage development is still elusive. To this end, I also showed that *Plasmodium berghei* coronin is not expressed in the blood stages and also absent in ookinetes. This is in contrast to *Plasmodium falciparum* coronin, the closest homologue of *Pb*-coronin. *Pf*-coronin was detected in the blood stages and it could not be knocked out and is therefore considered essential. Thus, coronin seems to be divergent in closely related species of *Plasmodium*: In *P. berghei,* coronin is not essential in the blood stages whereas in *P. falciparum* it is essential (Olshina et al, 2015).

Furthermore, in order to probe the actin regulatory function of coronin in both sporozoites and liver stages, I decided to ablate actin-binding sites of coronin.

4.3 Localization of actin-binding sites ablated mutants of coronin

The multiple sequence alignment of *P. berghei* coronin with *S. cerevisiae* (yeast) coronin, *M. musculus* (mouse) coronin and *P. falciparum* coronin suggested that the actin-binding sites identified in both yeast and mouse coronins are also conserved in coronins from all sequenced *Plasmodium species.* Furthermore, to circumvent the problem of low expression of endogenous coronin, I continued to use the parasite line that overexpresses coronin under a sporozoite and

liver stage specific promoter of the *uis3* gene (Lepper, 2011). The site directed mutagenesis of the actin-binding sites of coronin tagged with mCherry and overexpressed as an extra copy showed three different localization patterns of coronin depending on the position and charge of the mutated residue. *Pb*-coronin is the only actin-binding protein tested in apicomplexans so far that localizes in three different ways depending on the state of the intrudced mutation. This suggests that each mutated residue may have a distinct role localizing coronin. The first mutational site R24, R28 corresponds to R30 of mammalian coronin1B, which is responsible for actin cable formation in S2 cells (Cai et al, 2007). The point mutation R30A only attenuates the actin cable formation whereas the R30D abrogates cables completely. Similarly, R24A, R28A showed no change in the localization of *Pb*-coronin whereas after reversal of charges at this site (R24E, R28E) coronin localized only to the periphery of the sporozoites. The other mutational sites K283, D285; E327, R330 and R349, K350 have only been tested for actin binding in yeast. When the 'charge to the alanine' strategy was applied to mutate yeast coronin at these sites, the yeast coronin failed to colocalize with the actin filaments at the cortical patches. Consistent with these findings, the charge neutralization or charge reversal mutations of *Pb*-coronin led to a localization to either the cytosol or the periphery. However, interestingly in mouse coronin, the residue corresponding to K350 of *Pb*-coronin was suggested to be one of the residues that bind the Gα subunit of G-protein coupled receptors (Jayachandran et al, 2014). Although, the Gα subunit has not been annotated in the *P. berghei* genome, its presence and expression cannot be easily overlooked. This is because the effector of the Gα stimulatory subunit, cholera toxin (CT) activates the motility of *P. berghei* sporozoites, while the effector of the Gα inhibitory subunit; Mas-7 inhibits this motility (Kebaier & Vanderberg, 2010). Consequently, the possibility that coronin relays a signal from Gα to other proteins cannot be ignored. Despite these interesting implications of K350, I decided to focus on the preliminary question as to why coronin is localizing close to the membrane. To answer this, I planned to use a mutant of coronin R349E, K350E fused to mCherry that specifically localizes to the membrane. The treatment of these sporozoites with cytochalasin D, ionomycin or both could not dissociate coronin from the membranes suggesting that the peripheral localization of *Pb*-coronin is independent of both F-actin and PI(4,5)P2. This is surprising to me as coronin was known to associate with PI(4,5)P2 both in mammals and in *P. falciparum* (Mueller et al, 2008; Olshina et al, 2015). The other candidate that might be interacting with coronin could be phospholipase C as is evident from T-

cells where it was shown that coronin orients phospholipase C in the membrane such that it can further hydrolyze PI(4,5)P2 (Mueller et al, 2008). Interestingly, mammalian coronin (P57) was first found as a contaminant while purifying phospholipase C (Suzuki et al, 1995). One way to probe the interaction of coronin with phospholipase C is to deliberately mutate one of them. However even in T-cells the binding interactions of coronin and phospholipase C are not mapped. Therefore the question whether *Pb*-coronin interacts with *Pb*-phospholipase C in the membrane is still difficult to address. The clue to this experiment may come from a structurally similar protein in eukaryotic cells that interacts both with Gα subunit and phospholipase C.

Alternatively, *Dd*-coronin and *Hs*-coronin 1C were shown to interact with the small GTPase Rac with a specific domain called the CRIB domain (Swaminathan et al, 2014; Tilley et al, 2015). Interestingly, the structure of *Pb*-coronin is similar to the CRIB domain. However the presence of Rac is still questionable in the small genome of *Plasmodium*. The quick way to address this question is to use a specific inhibitor of Rac and test its effect on the localization and *in vitro* motility of the sporozoites. It is also possible to mutate the CRIB domain and test the localization and phenotype of it in the life cycle stages of *P. berghei*. In a nutshell, the interacting partner of *Pb*-coronin in the membrane still remains unidentified.

4.4 Effects of actin-binding site mutations of coronin in the life cycle of *P. berghei*

Given that coronin localizes in three different ways based on the position of the residue mutated and the charge of the introduced mutation, different roles for coronin could be postulated in different stages of the life cycle. To test these, I replaced the endogenous coronin with four mutants; three mutants that localize differently and a 4th mutant having all actin-binding sites ablated. Further, I compared these transgenice parasites to WT-*Pb*ANKA and *coronin(-)*. Since, all the replacement mutants of coronin were mCherry tagged, I also included the endogenous coronin-mCherry parasite line as one of the controls. To begin with the life cycle analysis, I initially checked the number of oocysts formed in the midgut of mosquitoes infected with above transgenic parasites. There was no defect in the formation of oocysts. This is not surprising to me, as endogenous coronin is not expressed in gametocytes or ookinetes and the coronin knock out parasites also had no impact on the formation or development of the oocysts. Although actin is typically expressed from gametocytes to ookinete to oocysts stages, it appears that coronin-mediated regulation of actin is not a prerequisite for the formation of oocysts.

The next stage in the life cycle is the sporozoite stage, which develops within the oocysts. The non-significant reduction in the number of sporozoites formed in the oocysts of the coronin knock out and coronin mutants implies that coronin is not necessary for the development of sporozoites in the oocysts. The following phase in the *P. berghei* life cycle is the egress of sporozoites from the oocysts and invasion of the salivary glands. When the ratio of salivary gland sporozoites (SGS) to the midgut sporozoites (MGS) is calculated, the transgenice parasites displayed a significantly reduced ratio as compared to the WT-*Pb*ANKA and endogenous coronin-mCherry parasites. Similar reduction in the SGS/MGS ratio was also exhibited by *coronin(-)* parasites, which implies that indeed coronin in involved in the invasion of salivary glands.

Salivary gland sporozoites glide at high speed in circles and the deletion of coronin dramatically affects this motility. Therefore, should coronin be regulating actin-based motility, then the ablation of actin-binding sites should also affect *in vitro* gliding motility of sporozoites. The result agrees well with our prediction as the parasite lines harboring the K283A and the D25A mutant of coronin and the one harboring coronin in which all the actin-binding sites are ablated exhibited a defect in *in vitro* gliding similar to the coronin knock out. The parasite line harboring R24A, R28A mutant form of coronin showed no defect in *in vitro* gliding. This is consistent with the localization experiments with this mutant form of coronin as it localizes similar to the WT-*Pb*-coronin. To our surprise, I found that some sporozoites of the parasite line harboring R349E, K350E mutant form of coronin exhibited a small kink at the posterior while gliding, something I had not observed with any known mutant parasite lines so far. This together with the slow speed of this mutant parasite line implicates another specific function of coronin. To recollect from previous sections (section 4.3) K350 is the same residue that is shown to interact with Gα.

To progress in the life cycle, parasites have to invade and develop within liver cells. To test whether actin regulatory function is important for normal liver stage development, I performed a standard liver cell assay (section 3.4.4). The measurement of liver stage sizes suggested that the transgenic parasites harboring actin-binding sites ablated coronin grew normally within liver cells. Therefore, it is evident that although coronin plays a role in liver stage development, it is independent of actin. In addition, the possibility that *Pb*-coronin could regulate microtubules and therefore cytokinesis could be excluded (ref section 4.2). Hence, the

mechanism of how coronin assists in the development of *P. berghei* liver stages still remains elusive.

4.5 Purification of *Pb*-coronin

After the discovery of the differential localization patterns of coronin actin-binding site mutations and their phenotypic differences in salivary gland invasion and *in vitro* gliding motility by cell biological assays, it was important to determine the coronin-mediated regulation of actin biochemically. Consequently, it necessitated the purification of *Pb*-coronin. I employed various protein purification strategies. This includes the purification from the *E. coli* strains BL21, RIL, RIPL and XL1BL as well as purification by baculovirus mediated protein expression from insect cells SF21.

Expression of both *Pb*-coronin and *Pb*-coronin-8mut (the mutant form of coronin harboring all the actin-binding site mutations) was possible in insect cells alone. However, the expressed proteins could not be recovered from the insoluble fraction. This was surprising because it was possible to purify yeast coronin and mammalian coronin p57 from bacteria (Gandhi et al, 2010; Liu et al, 2006). In addition, it was also possible to purify the mouse coronin *Mm*-coronin 1A by baculovirus mediated protein expression from SF21 cells (Appleton et al, 2006). Interestingly, it has been shown that coronin has 7 WD40 repeats, which form a β-propeller structure. Therefore, it could be expected that any shorter construct of coronin that does not bear all WD40 repeats will not fold properly. Paradoxically though, the literature is replete with examples where scientists have purified GST fusions of shorter constructs of coronin and used them not only for *in vitro* actin binding assays but also for *in vivo* localization studies (Liu et al, 2006; Oku et al, 2003). Unfortunately, even the full length *Pb*-coronin remains insoluble in insect cells. Both *P. falciparum* and *T. gondii,* coronin could be purified from baculovirus mediated SF21 insect cells similar to the *Mm*-coronin 1A. However, expression of full length *Pf*-coronin undergoes degradation to form a shorter coronin fragment while still bearing all the predicted WD40 repeats and complete β-propeller (Olshina et al, 2015). It can be expected since *in silico* prediction of the coronin structure suggests that *Plasmodium* coronin exhibits a coiled coil region at its C-terminus. Similarly, *Tg*-coronin was purified and crystallized lacking the C-terminal coiled coil region (Salamun et al, 2014). It suggests that even in these closely related species coronin is very divergent. After several attempts at extracting and purifying coronin, I finally succeeded in extracting an insoluble form of coronin with guanidine hydrochloride. In

order to make coronin soluble and refold it, I used 27 different buffers and exchange conditions but with no success.

One way to bypass the *in vitro* biochemical assays with *P. berghei* coronin is to select coronin from a closely related species, whose role has been successfully tested *in vitro* and then probe if it could complement the function of *Pb*-coronin. Now, despite the low sequence identity across *P. berghei, P. falciparum* and *T. gondii*, the actin-binding sites are still conserved. Therefore, I investigated the localization of *Pf*-coronin and replaced the endogenous *Pb*-coronin with *Pf*-coronin-mCherry to probe its effects.

4.6 Localization and replacement with *Pf*-coronin-mCherry

To localize *Pf*-coronin in the sporozoite stage of *P. berghei,* I overexpressed the fusion of *Pf*-coronin-mCherry under a sporozoite specific promoter of the *uis3* gene, similar to the over-expression experiments of *Pb*-coronin and its actin-binding mutants. *Pf*-coronin was localized towards the rear end of the sporozoite but not as prominently as *Pb*-coronin. Also, *Pf*-coronin was not localized in the periphery, unlike *Pb*-coronin. Given the low sequence identity, these results might not be surprising. Curiously, replacement with *Pf*-coronin could complement the function of *Pb*-coronin almost completely when checked for the main *in vivo* effect of coronin ablation, ie the ratio of salivary glands to the midgut sporozoite numbers and sizes of the liver stages. Only the gliding motility assay suggests a slight defect in gliding of about 52% sporozoites, which could be expected, since the peripheral localization of *Pf*-coronin was not similar to *Pb*-coronin. However, the gliding defect did not result in any alteration during the hepatocyte infection both *in vivo* and *in vitro*. In fact, the normal development of preerythrocytic stages both *in vivo* and *in vitro* in the *Pf*-coronin replaced parasite line suggests that despite the low sequence identity, the actin-independent role in the preerythrocytic development is also fulfilled by *Pf*-coronin.

Pf-coronin has been shown to bundle actin filaments (Olshina et al, 2015). Given the conserved nature of similar actin-binding sites in *Pf*-coronin and *Pb*-coronin, it is likely that *Pb*-coronin bundles actin filaments. This coronin-mediated bundling of actin filaments together with the posterior localization of coronin indicates that the bundling of actin filaments occurs at the rear end of the sporozoite. The other possibility is that the bundles of actin filaments are formed at the front or along the periphery and F-actin bundles accumulate at the rear. It is plausible as the adhesion of motile sporozoites was also observed to be in the middle and rear of motile

sporozoites (Munter et al, 2009). As it has been demonstrated *in vitro*, the force exerted by an actin bundle of certain length is equal to the force exerted by an actin filament of same length (Footer et al, 2007). It could be imagined that the distribution of this force over a large surface area of an actin bundle causes the detachment of the cell. Indeed stalling forces have been visualized with traction force microscopy at the rear end (Munter et al, 2009). It could thus be that actin filament disassembly (in conjunction with cleavage of surface adhesins) at the rear is necessary for progressive gliding. In order to achieve this continuous cycles of attachment and detachment, it might be necessary to continuously dissociate and associate bundles of actin filaments. One way to do this might be to regulate the binding of coronin to actin by a posttranslational modification of coronin, e.g. phosphorylation. It was shown that phosphorylation of coronin 1B inhibits its binding to actin filaments (Cai et al, 2005; Oku et al, 2012; Xavier et al, 2012). It was also shown that coronin is phosphorylated in the Plasmodium proteome (Alam et al, 2015).

Lastly, the normal development of preerythrocytic stages both *in vivo* and *in vitro* in the *Pf*-coronin replaced parasite line suggests that irrespective of the low sequence identity, the actin-independent role in the preerythrocytic development is also fulfilled by *Pf*-coronin.

4.7 *In vivo* migration of *coronin(-)* sporozoites

Although the coronin knock out displays a defect in migration *in vitro* as well as a defect in salivary gland entry, it is surprising that it does not have any defect in migration in the skin *in vivo*. This excludes coronin as a target for intervention strategies against malaria infection. One can certainly argue that in *P. falciparum,* it may not be similar as coronin is expressed in blood stages. Nevertheless, my findings imply that the *in vivo* migration is different from *in vitro* motility. In line with this, deletion of the conserved sporozoite surface protein 3 (SSP3) in another rodent malaria parasite *P. yoelii*, also had a defect in the *in vitro* gliding motility without any impact on host cell traversal, *in vivo* and *in vitro* host cell infection (Harupa et al, 2014). Hence, it appears that the migration in 3 dimensions in a constrained environment (e.g. skin) is more robust from the migration in 2 dimensions (e.g. glass) without constraints. In other words, it is highly likely that the parasite has evolved its motility to adapt to different environmental constraints. However, the molecular genetic evidences supporting this notion are still limited and my study is one of the first to show through an effect of salivary gland entry but not skin traversal of a protein that modulates motility.

For example, one can simulate the *in vivo* conditions with various physico-chemical environmental cues *in vitro*. Recently, pillars of various diameters were used as physical cues to probe the preference of the sporozoites for pillars of certain diameter. This showed that sporozoites preferentially circled preferentially around pillars with a diameter similar to blood capillaries (Muthinja M, unpublished). In addition, it could be imagined that the migration patterns of sporozoites *in vivo* is due to the obstacles in its path. In fact, the placement of pillars close to each other (2-6 μm) was used to simulate *in vivo* conditions. Interestingly, the placement of pillars in close proximity was able to deviate the sporozoites from migrating in the usual circular gliding pattern (Hellmann et al, 2011).

4.8 Coronin in calcium signaling

The tri-peptides with a sequence RGD/E can serve as chemical cues. These are the features of extracellular matrix that interact with the integrin like motifs of the migrating cells, thereby activating them. Thus, generation of functionalized surfaces coated with RGD/E like tripeptides can simulate the presence of ligands *in vivo* (Perschmann et al, 2011). Together these evidences support the notion that the migration of sporozoites *in vivo* is truly different than their motility *in vitro*. This is also known from eukaryotic cells (Lammermann et al, 2008). However, these experiments obviously give more emphasis to surface contact as being essential for the migration of sporozoites while disregarding the role of serum albumin mediated signaling. Therefore this section of my thesis discusses the signaling involved in the activation and migration of malaria parasites.

Calcium is an important signaling molecule that regulates versatile processes like development, division, differentiation and migration in species ranging from bacteria to humans. Therefore, the mechanistic understanding of almost any fundamental process would remain incomplete without understanding its regulation by calcium. The migration of *Plasmodium* sporozoites is no exception to this. Previously, calcium signaling in *P. berghei* sporozoites was studied in the presence of small molecule inhibitors of cAMP-protein kinase pathway. This study quantified the percentage of motile sporozoites after treatment. However, the number of sporozoites tested for each inhibitor with varying concentrations was too low to be statistically reliable. Also, the cytosolic calcium concentrations were not measured during this study (Kebaier & Vanderberg, 2010). On the other hand, the use of a genetically coded FRET based calcium sensor TN-XXL suggested that the phosphotidylionositol-phospholipase C (PI-PLC) pathway is

essential for gliding motility. These two experimental evidences may not be contradictory as they could either separately or jointly regulate the motility of sporozoites. Given that the PI-PLC pathway is the effector of intracellular calcium release, which in turn is a prerequisite for the activation of adenyl cyclase, a protein that generates cAMP from ATP; it is tempting to study these pathways sequentially. To do so, I used a coronin-mCherry signal as a molecular marker for the activation of gliding motility (section 3.8). As expected, the chelation of intracellular calcium affected the localization of coronin and inhibited motility. Similarly, an increase in the calcium concentration by use of calcium agonists localized coronin to the rear of the sporozoites and activated their motility. These results illustrate that an increase in the intracellular calcium concentration and localization of coronin go hand in hand. When using inhibitors of the cAMP-PKA pathway, I observed that localization of coronin was still at the posterior end of non-motile sporozoites. This data suggested that coronin initially localizes in the cytoplasm and periphery. Upon activation of sporozoite motility, calcium is released from the intracellular stores and it localizes coronin to the actin cytoskeleton at the posterior pole. The interruption of motility by the cAMP-PKA pathway does not affect coronin localization or the activated gliding motor but it might interfere with the continuous processing of the gliding motor. It could be hypothesized that continuous processing of the gliding motor is a prerequisite for effective gliding. FRAP analysis suggested that the recovery of coronin-mCherry signal was slowed down in sporozoites treated with an inhibitor of cAMP-PKA pathway compared to no inhibitor control. However, the direct inhibition of gliding with actin modulating compounds like cytochalasin D and jasplakinolide increased the half recovery time only non-significantly. The statistical insignificance could be attributed to the low sporozoite numbers tested. Although, this data illustrates the importance of continuous processing of the gliding motor, how the signal is conveyed from calcium ions to the cAMP-PKA pathway is still a major question not only in *Plasmodium* but also in higher eukaryotes.

Recently, coronin was shown to activate adenyl cyclase, which in turn converts ATP to cAMP (Jayachandran et al, 2014). This along with my data suggests that coronin relays the calcium signal to the adenyl cyclase. To address this, one could inhibit the interaction between coronin and adenyl cyclase either by site directed mutagenesis of coronin or by using specific inhibitors of this interaction. This is because there is one coronin and three adenyl cyclases encoded in the genome of *Plasmodium* (http://plasmodb.org/) (Aurrecoechea et al, 2009) and

deletion of one adenyl cyclase, (ACα) has no effect on the gliding motility of *P. berghei* sporozoites. Interestingly though, ACα deletion has resulted in 50% reduction in the invasion of hepatocytes both *in vivo* and *in vitro* (Ono et al, 2008). It is really intriguing as the deletion of a protein that had no defect of the sporozoite gliding *in vitro* exhibits a defect in hepatocytes infection *in vivo* as well as *in vitro*. Therefore, it could be speculated that adenyl cyclase or cAMP-PKA pathway may have a role in signaling for either hepatocytic invasion of sporozoites or their development in hepatocytes. Similarly, an actin-independent role could also be speculated for coronin since *coronin(-)* form smaller sized liver stages. However, neither *coronin(-)* sporozoites were probed for hepatocyte invasion efficiency nor *adenyl cyclaseα(-)* sporozoites were tested for liver stage sizes. Nevertheless, the possibility that coronin signals the adenyl cyclase at multiple stages in the life cycle could not be excluded.

4.9 Overexpression of coronin in blood stages and ookinetes

It has been suggested in yeast that the over-expression of coronin leads to the formation of aberrant actin loop structures. This is deleterious to the growth of the yeast cells. Later, it was shown that a coronin overexpression defect depends on its coiled coil domain at the C-terminus that forms homo-oligomers (Humphries et al, 2002). Interestingly, the overexpression of coronin with ablated actin-binding sites had no deleterious defect (Gandhi et al, 2010). Although this overexpression defect has not yet been investigated in any other species, I sought to test it in the complex life cycle of *Plasmodium.* Evidence that coronin overexpression is not deleterious in the sporozoite stage comes from the experiments regarding the overexpression of coronin under sporozoite specific promoter of *uis3* gene (Lepper, 2011). Similarly, the overexpression of coronin in the blood and ookinete stages of *P. berghei* was also not deleterious. This suggests that the overexpression of coronin-mediated growth defect is not a universal phenomenon. Of importance is the aberrant loop structures of actin filaments formed by over-expression of coronin. Since, longer filaments of actin have not yet been visualized with *Plasmodium* actin, it is not surprising that the overexpression of coronin is not deleterious. Alternatively, it is possible that the coiled coil domain of *Plasmodium* coronin does not form homo-oligomers. This profound yet differential capacity of *Plasmodium* coronin could be made use of in visualizing actin filaments in *Plasmodium.* The overexpressed WT *Pb*-coronin localizes to the cytoplasm of the blood stage parasite typically excluded from the food vacuole while being highly pronounced around it. On the other hand, the *Pb*-coronin with the ablated actin-binding sites was typically

absent from both the food vacuole and nucleus. This recapitulates the localization of overexpressed coronin-8mut in sporozoites as it was also specifically absent in the nucleus (ref section 3.3). The functional significance of the exclusion of nuclear localization of coronin-8mut is unknown. Inspection of overexpressed coronin-eGFP in ookinetes displayed that coronin was extremely pronounced in the periphery as opposed to the cytosol but with no exclusion from the nucleus. In stark contrast, the over-expression of coronin with ablated actin-binding sites (coronin-8mut-eGFP) localized to the nucleus. Owing the overexpression of mutant coronin in blood stages and sporozoites, the localization of coronin-8mut-eGFP in ookienets is totally unexpected and therefore, it is difficult to speculate this difference.

5. Conclusion

Gliding motility is essential for the life cycle progression of the malaria parasites and its spread. Here I show that the actin-binding protein coronin regulates sporozoite motility and hepatocyte development in *Plasmodium berghei*. The deletion of coronin or the introduction of mutations into the actin-binding sites of coronin disrupts the otherwise highly directional motility of sporozoites. *Pf*-coronin is able to fully complement the in vivo functions of *Pb*-coronin suggesting strongly that coronin from *Pb*-coronin and *Pf*-coronin like those from higher eukaryotes, bundles actin filaments.

Coronin localizes to the periphery of non-moving sporozoites. Upon stimulation with serum albumin coronin relocalizes to the rear of the gliding parasites in an actin-dependent manner. This actin-dependent function of coronin is essential for directional motility, while in liver cells the function of coronin is actin-independent.

Activation of gliding motility requires an influx of calcium and is a prerequisite for the actin-dependent rear localization of coronin. Furthermore, cAMP-PKA (cyclic AMP-protein kinase A pathway) regulates actin dynamics in a way different than well-known actin modulating compounds: jasplakinolide or cytochalasin D. Together with recently published data my findings implicate two signaling pathways in sporozoites: calcium-dominated signaling during motility and cAMP-dominated signaling during invasion of liver cells.

6. Appendix

6.1 General protocol for characterization of newly engineered *P. berghei* parasite lines

1. Place an order for a mosquito cage and a mouse cage, 3 weeks and 1 week in advance to inject stabilates respectively.
2. Mice Day (-4): Inject 1 stabilate in 1 NMRI mouse (called parental mouse).
3. Mice Day (0): Prick a tail of the parental mouse and take a drop of blood on a slide.

- Smear this drop of blood and stain it with giemsa.
- Count the number of blood stage parasites per field of view under 100X objective for 10 fields with similar density of RBCs.
- Count the number of total RBCs in one field.
- Calculate the percentage of parasitized RBCs (parasitemia).
- Calculate the volume of blood that would contain 20 million infected erythrocytes and bleed that mouse.

4. Inject the calculated volume of blood of infected mouse into 3 naive NMRI mice.

With the ookinete culture from 1st mouse

5. Purify ookinetes using standard protocol. Check the expression and localization of the tagged protein and/or do ookinete motility assay for a gene knock out parasite line.

With the other 2 mice

6. Prick a tail of any one of the mice and take a drop of blood on a slide. Mix it with a drop of 1 µg/ml of Hoechst stain. Place a coverslip on top. Check expression and localization of the protein of interest in the blood stage (if any).
7. Take a drop of blood on a slide with a coverslip on top. Place the slide at 19^0 C for 10 min. Check exflagellation i.e. wiggling of RBCs, of these 2 mice on day3 and 4 (Good exflagellation is at least 4 events per field of view under 40X objective). Starve the mosquitos in a cage for 6 hr. at least.
8. Anesthetize the mice and place them on top of starved mosquitoes on the same day and next. (This is day0 of mosquito cage).

9. Day 1 of mosquito cage =>Take out 10-12 well-fed mosquitoes. Smear their mid-guts on a glass slide. Fix the slide with methanol. Stain the slide with giemsa. Look for ookinetes under 100X objective.
10. Day10 of mosquito cage =>
    - Aspirate 25 mosquitos from the cage. Dissect their mid-guts in one well of 24 well plate.
        - Permeabilization: Add 0.5% of NP40 and incubate at RT for 30 min.
        - Staining: Remove NP40 and add 0.1% of mercurochrome and incubate at RT for 60 min.
        - Washing: Remove the 0.1% mercurochrome solution and add phosphate buffered saline (PBS). Incubate at RT for 10 min.
        - Repeat washing step 3 times.
        - Oocysts are now stained.
        - Observe oocysts under 10X objective with green filter at zeiss microscope.
        - Count the number of oocysts in each infected mid-gut.
        - Also count the number of uninfected midguts.
    - Dissect the mid-guts of 5 mosquitos in a drop of PBS on a slide. Place a coverslip on top and observe for expression of tagged protein without any staining.
    - Seed HepG2 liver cells (see liver cell assay protocol for details).
11. Day13/14 of mosquito cage =>
    - Split liver cells and seed them in 24 well plate such that they are confluent on day 17/18.
12. Day16 of mosquito cage =>
    - Prepare a solution containing 3% BSA in RPMI buffer (3%BSA).
    - Dissect haemolymph (HL) sporozoites from 5-8 mosquitos with 3%BSA.
        - Add 3% BSA to get the total volume of 100 µl.
        - Take 6 µl of this in the neubauer's chamber.
        - Count the number of haemolymph sporozoites in the neubauer's chamber.
        - Determine the number of HL sporozoites per mosquito.
        - Add remaining solution containing HL sporozoites to 96 well plate.
        - Spin down the sporozoites at 1000 rpm for 3 min.
        - Image the HL sporozoites under 25X objective with time frame of 1 image per second for 3 min. of each movie. Image multiple movies by changing fields.

- Check the expression and /or localization of the tagged protein. (optional)

➢ Dissect mid-guts from same mosquitos in 100 µl of PBS. Crush them with a pestle and count them in Neubauer's chamber.

➢ Aspirate 40 female mosquitos and distribute them equally in 4 cups before leaving. Starve these mosquitoes overnight.

13. Day 17 of mosquito cage/ day 0 for bite back and i.v. mice=>

➢ Anesthetize four C57 BL/6 mice. Put them on the cups of over-night starved mosquitoes (1 mouse on each cup) for 10 min. Note down how many mosquitos feed on the mouse from each cup.

➢ Take out 25 mosquitos from the cage. Dissect mid-guts and salivary glands from these mosquitoes in 100 µL of PBS each.

➢ Crush the salivary glands in 100 ml of PBS and count sporozoites in Neubauer's chamber as mentioned for HL sporozoites. Determine the number of sporozoites per mosquito.

➢ Inject 10000 sporozoites intravenously in each of the four C57 BL/6 mice.

➢ Purify the remaining sporozoites with accudenz. (optional)

➢ Gliding assay: Spin the PBS solution containing purified sporozoites at 10000 rpm for 3 min. Remove the supernatant and resuspend the sporozoites in 100 ml of 3% BSA.

➢ Take these suspended sporozoites in a 96 well plate.

➢ Centrifuge at 1000 rpm for 3 min.

➢ Image their motility under 25X objective with a time frame of one image per 3 seconds for 5 min. Image multiple movies by changing fields.

➢ Check the expression and /or localization of the tagged protein (optional).

➢ Crush the isolated mid-guts. Dilute them 1:5 and count the number of mid-gut sporozoites.

➢ Determine the number per mosquito.

14. Day18 -25 of mosquito cage=>

➢ Dissect the leftover female mosquitos for counting of mid-gut sporozoites and salivary gland sporozoites as mentioned above.

➢ Use 50000 salivary gland sporozoites for liver cell assay.

➢ Repeat gliding assays on different days and 2-3 cages for each parasite line.

15. Day20 of mosquito cage / day 3 of bite back (bb) and intravenously (i.v.) injected mice

- Prick the tails of all the mice and take a drop of blood on a glass slide.
- Make smears.
- Let the smear air-dry.
- Fix the slides with 100% methanol.
- Stain the slides with giemsa.
- Make slides from today (day 3) till day 20 of bite back and i.v. mice. Note how many of these mice die before day12 and count the parasitemia of all of these mice till day 20.
    - Observe prepatent period (Time between the inoculation of the sporozoites and the first appearance of blood stage parasites).
    - Tabulate number of infected mice.
    - Plot the parasitemia curve.

Key characterization points

Ookinete (could be done any time separately)

Oocysts (between day 10 and 14 after feeding mosquito cage)

Midgut sporozoites (between day 14 and 17 after feeding mosquito cage)

Salivary gland sporozoites (between day 17 and 25 after feeding mosquito cage)

Liver and Blood stages –

Prepatency (till you see blood stages in bite back and i.v. mice)

ECM (till day 10 after bite back and i.v.)

Parasitemia (till day 20 after bite back and i.v.)

Bibliography

Alam MM, Solyakov L, Bottrill AR, Flueck C, Siddiqui FA, Singh S, Mistry S, Viskaduraki M, Lee K, Hopp CS, Chitnis CE, Doerig C, Moon RW, Green JL, Holder AA, Baker DA, Tobin AB (2015) Phosphoproteomics reveals malaria parasite Protein Kinase G as a signalling hub regulating egress and invasion. *Nature communications* **6:** 7285

Amino R, Thiberge S, Martin B, Celli S, Shorte S, Frischknecht F, Menard R (2006) Quantitative imaging of Plasmodium transmission from mosquito to mammal. *Nature medicine* **12:** 220-224

Angrisano F, Delves MJ, Sturm A, Mollard V, McFadden GI, Sinden RE, Baum J (2012a) A GFP-actin reporter line to explore microfilament dynamics across the malaria parasite lifecycle. *Molecular and biochemical parasitology* **182:** 93-96

Angrisano F, Riglar DT, Sturm A, Volz JC, Delves MJ, Zuccala ES, Turnbull L, Dekiwadia C, Olshina MA, Marapana DS, Wong W, Mollard V, Bradin CH, Tonkin CJ, Gunning PW, Ralph SA, Whitchurch CB, Sinden RE, Cowman AF, McFadden GI, Baum J (2012b) Spatial localisation of actin filaments across developmental stages of the malaria parasite. *PloS one* **7:** e32188

Appleton BA, Wu P, Wiesmann C (2006) The crystal structure of murine coronin-1: a regulator of actin cytoskeletal dynamics in lymphocytes. *Structure* **14:** 87-96

Aurrecoechea C, Brestelli J, Brunk BP, Dommer J, Fischer S, Gajria B, Gao X, Gingle A, Grant G, Harb OS, Heiges M, Innamorato F, Iodice J, Kissinger JC, Kraemer E, Li W, Miller JA, Nayak V, Pennington C, Pinney DF, Roos DS, Ross C, Stoeckert CJ, Jr., Treatman C, Wang H (2009) PlasmoDB: a functional genomic database for malaria parasites. *Nucleic acids research* **37:** D539-543

Baum J, Papenfuss AT, Baum B, Speed TP, Cowman AF (2006) Regulation of apicomplexan actin-based motility. *Nature reviews Microbiology* **4:** 621-628

Bergert M, Erzberger A, Desai RA, Aspalter IM, Oates AC, Charras G, Salbreux G, Paluch EK (2015) Force transmission during adhesion-independent migration. *Nature cell biology* **17:** 524-529

Bergman LW, Kaiser K, Fujioka H, Coppens I, Daly TM, Fox S, Matuschewski K, Nussenzweig V, Kappe SH (2003) Myosin A tail domain interacting protein (MTIP) localizes to the inner membrane complex of Plasmodium sporozoites. *Journal of cell science* **116:** 39-49

Bosch J, Turley S, Daly TM, Bogh SM, Villasmil ML, Roach C, Zhou N, Morrisey JM, Vaidya AB, Bergman LW, Hol WG (2006) Structure of the MTIP-MyoA complex, a key component of the malaria parasite invasion motor. *Proceedings of the National Academy of Sciences of the United States of America* **103:** 4852-4857

Brenner SL, Korn ED (1979) Substoichiometric concentrations of cytochalasin D inhibit actin polymerization. Additional evidence for an F-actin treadmill. *The Journal of biological chemistry* **254:** 9982-9985

Bretschneider T, Anderson K, Ecke M, Muller-Taubenberger A, Schroth-Diez B, Ishikawa-Ankerhold HC, Gerisch G (2009) The three-dimensional dynamics of actin waves, a model of cytoskeletal self-organization. *Biophysical journal* **96:** 2888-2900

Brown CM, Hebert B, Kolin DL, Zareno J, Whitmore L, Horwitz AR, Wiseman PW (2006) Probing the integrin-actin linkage using high-resolution protein velocity mapping. *Journal of cell science* **119:** 5204-5214

Bubb MR, Spector I, Beyer BB, Fosen KM (2000) Effects of jasplakinolide on the kinetics of actin polymerization. An explanation for certain in vivo observations. *The Journal of biological chemistry* **275:** 5163-5170

Cai L, Holoweckyj N, Schaller MD, Bear JE (2005) Phosphorylation of coronin 1B by protein kinase C regulates interaction with Arp2/3 and cell motility. *The Journal of biological chemistry* **280:** 31913-31923

Cai L, Makhov AM, Bear JE (2007) F-actin binding is essential for coronin 1B function in vivo. *Journal of cell science* **120:** 1779-1790

Calderwood DA, Shattil SJ, Ginsberg MH (2000) Integrins and actin filaments: reciprocal regulation of cell adhesion and signaling. *The Journal of biological chemistry* **275:** 22607-22610

Carey AF, Singer M, Bargieri D, Thiberge S, Frischknecht F, Menard R, Amino R (2014) Calcium dynamics of Plasmodium berghei sporozoite motility. *Cellular microbiology* **16:** 768-783

Carruthers VB, Giddings OK, Sibley LD (1999) Secretion of micronemal proteins is associated with toxoplasma invasion of host cells. *Cellular microbiology* **1:** 225-235

Cerna D, Wilson DK (2005) The structure of Sif2p, a WD repeat protein functioning in the SET3 corepressor complex. *Journal of molecular biology* **351:** 923-935

Chan KT, Roadcap DW, Holoweckyj N, Bear JE (2012) Coronin 1C harbours a second actin-binding site that confers co-operative binding to F-actin. *The Biochemical journal* **444:** 89-96

Chen Y, Ip FC, Shi L, Zhang Z, Tang H, Ng YP, Ye WC, Fu AK, Ip NY (2014) Coronin 6 regulates acetylcholine receptor clustering through modulating receptor anchorage to actin cytoskeleton. *The Journal of neuroscience : the official journal of the Society for Neuroscience* **34:** 2413-2421

Ciobanasu C, Faivre B, Le Clainche C (2014) Actomyosin-dependent formation of the mechanosensitive talin-vinculin complex reinforces actin anchoring. *Nature communications* **5:** 3095

Combe A, Moreira C, Ackerman S, Thiberge S, Templeton TJ, Menard R (2009) TREP, a novel protein necessary for gliding motility of the malaria sporozoite. *International journal for parasitology* **39:** 489-496

de Hostos EL, Bradtke B, Lottspeich F, Guggenheim R, Gerisch G (1991) Coronin, an actin binding protein of Dictyostelium discoideum localized to cell surface projections, has sequence similarities to G protein beta subunits. *The EMBO journal* **10:** 4097-4104

de Hostos EL, Rehfuess C, Bradtke B, Waddell DR, Albrecht R, Murphy J, Gerisch G (1993) Dictyostelium mutants lacking the cytoskeletal protein coronin are defective in cytokinesis and cell motility. *The Journal of cell biology* **120:** 163-173

Deibler M, Spatz JP, Kemkemer R (2011) Actin fusion proteins alter the dynamics of mechanically induced cytoskeleton rearrangement. *PloS one* **6:** e22941

Deligianni E, Morgan RN, Bertuccini L, Kooij TW, Laforge A, Nahar C, Poulakakis N, Schuler H, Louis C, Matuschewski K, Siden-Kiamos I (2011) Critical role for a stage-specific actin in male exflagellation of the malaria parasite. *Cellular microbiology* **13:** 1714-1730

Dent EW, Tang F, Kalil K (2003) Axon guidance by growth cones and branches: common cytoskeletal and signaling mechanisms. *The Neuroscientist : a review journal bringing neurobiology, neurology and psychiatry* **9:** 343-353

Douse CH, Green JL, Salgado PS, Simpson PJ, Thomas JC, Langsley G, Holder AA, Tate EW, Cota E (2012) Regulation of the Plasmodium motor complex: phosphorylation of myosin A tail-interacting protein (MTIP) loosens its grip on MyoA. *The Journal of biological chemistry* **287:** 36968-36977

Etienne-Manneville S (2008) Polarity proteins in migration and invasion. *Oncogene* **27:** 6970-6980

Figueroa JV, Precigout E, Carcy B, Gorenflot A (2004) Identification of a coronin-like protein in Babesia species. *Annals of the New York Academy of Sciences* **1026:** 125-138

Footer MJ, Kerssemakers JW, Theriot JA, Dogterom M (2007) Direct measurement of force generation by actin filament polymerization using an optical trap. *Proceedings of the National Academy of Sciences of the United States of America* **104:** 2181-2186

Friedl P, Gilmour D (2009) Collective cell migration in morphogenesis, regeneration and cancer. *Nature reviews Molecular cell biology* **10:** 445-457

Friedl P, Hegerfeldt Y, Tusch M (2004) Collective cell migration in morphogenesis and cancer. *The International journal of developmental biology* **48:** 441-449

Fujii T, Iwane AH, Yanagida T, Namba K (2010) Direct visualization of secondary structures of F-actin by electron cryomicroscopy. *Nature* **467:** 724-728

Galkin VE, Orlova A, Brieher W, Kueh HY, Mitchison TJ, Egelman EH (2008) Coronin-1A stabilizes F-actin by bridging adjacent actin protomers and stapling opposite strands of the actin filament. *Journal of molecular biology* **376:** 607-613

Gandhi M, Achard V, Blanchoin L, Goode BL (2009) Coronin switches roles in actin disassembly depending on the nucleotide state of actin. *Molecular cell* **34:** 364-374

Gandhi M, Jangi M, Goode BL (2010) Functional surfaces on the actin-binding protein coronin revealed by systematic mutagenesis. *The Journal of biological chemistry* **285:** 34899-34908

Gantt S, Persson C, Rose K, Birkett AJ, Abagyan R, Nussenzweig V (2000) Antibodies against thrombospondin-related anonymous protein do not inhibit Plasmodium sporozoite infectivity in vivo. *Infection and immunity* **68:** 3667-3673

Gatfield J, Albrecht I, Zanolari B, Steinmetz MO, Pieters J (2005) Association of the leukocyte plasma membrane with the actin cytoskeleton through coiled coil-mediated trimeric coronin 1 molecules. *Molecular biology of the cell* **16:** 2786-2798

Ge P, Durer ZA, Kudryashov D, Zhou ZH, Reisler E (2014) Cryo-EM reveals different coronin binding modes for ADP- and ADP-BeFx actin filaments. *Nature structural & molecular biology* **21:** 1075-1081

Gerisch G, Albrecht R, De Hostos E, Wallraff E, Heizer C, Kreitmeier M, Muller-Taubenberger A (1993) Actin-associated proteins in motility and chemotaxis of Dictyostelium cells. *Symposia of the Society for Experimental Biology* **47:** 297-315

Gerisch G, Albrecht R, Heizer C, Hodgkinson S, Maniak M (1995) Chemoattractant-controlled accumulation of coronin at the leading edge of Dictyostelium cells monitored using a green fluorescent protein-coronin fusion protein. *Current biology : CB* **5:** 1280-1285

Gilk SD, Gaskins E, Ward GE, Beckers CJ (2009) GAP45 phosphorylation controls assembly of the Toxoplasma myosin XIV complex. *Eukaryotic cell* **8:** 190-196

Goode BL, Wong JJ, Butty AC, Peter M, McCormack AL, Yates JR, Drubin DG, Barnes G (1999) Coronin promotes the rapid assembly and cross-linking of actin filaments and may link the actin and microtubule cytoskeletons in yeast. *The Journal of cell biology* **144:** 83-98

Gorbatyuk VY, Nosworthy NJ, Robson SA, Bains NP, Maciejewski MW, Dos Remedios CG, King GF (2006) Mapping the phosphoinositide-binding site on chick cofilin explains how PIP2 regulates the cofilin-actin interaction. *Molecular cell* **24:** 511-522

Green JL, Martin SR, Fielden J, Ksagoni A, Grainger M, Yim Lim BY, Molloy JE, Holder AA (2006) The MTIP-myosin A complex in blood stage malaria parasites. *Journal of molecular biology* **355:** 933-941

H S (2001) Cell Motility. *eLS*

Harupa A, Sack BK, Lakshmanan V, Arang N, Douglass AN, Oliver BG, Stuart AB, Sather DN, Lindner SE, Hybiske K, Torii M, Kappe SH (2014) SSP3 is a novel Plasmodium yoelii sporozoite surface protein with a role in gliding motility. *Infection and immunity* **82:** 4643-4653

Hegge S, Kudryashev M, Smith A, Frischknecht F (2009) Automated classification of Plasmodium sporozoite movement patterns reveals a shift towards productive motility during salivary gland infection. *Biotechnology journal* **4:** 903-913

Hegge S, Munter S, Steinbuchel M, Heiss K, Engel U, Matuschewski K, Frischknecht F (2010) Multistep adhesion of Plasmodium sporozoites. *FASEB journal : official publication of the Federation of American Societies for Experimental Biology* **24:** 2222-2234

Heinrich D, Youssef S, Schroth-Diez B, Engel U, Aydin D, Blummel J, Spatz JP, Gerisch G (2008) Actin-cytoskeleton dynamics in non-monotonic cell spreading. *Cell adhesion & migration* **2:** 58-68

Hellmann JK, Munter S, Kudryashev M, Schulz S, Heiss K, Muller AK, Matuschewski K, Spatz JP, Schwarz US, Frischknecht F (2011) Environmental constraints guide migration of malaria parasites during transmission. *PLoS pathogens* **7:** e1002080

Hellmann JK, Perschmann N, Spatz JP, Frischknecht F (2013) Tunable substrates unveil chemical complementation of a genetic cell migration defect. *Advanced healthcare materials* **2:** 1162-1169

Hisbergues M, Gaitatzes CG, Joset F, Bedu S, Smith TF (2001) A noncanonical WD-repeat protein from the cyanobacterium Synechocystis PCC6803: structural and functional study. *Protein science : a publication of the Protein Society* **10:** 293-300

Humphries CL, Balcer HI, D'Agostino JL, Winsor B, Drubin DG, Barnes G, Andrews BJ, Goode BL (2002) Direct regulation of Arp2/3 complex activity and function by the actin binding protein coronin. *The Journal of cell biology* **159:** 993-1004

Huttenlocher A, Horwitz AR (2011) Integrins in cell migration. *Cold Spring Harbor perspectives in biology* **3:** a005074

Ishikawa-Ankerhold HC, Gerisch G, Muller-Taubenberger A (2010) Genetic evidence for concerted control of actin dynamics in cytokinesis, endocytic traffic, and cell motility by coronin and Aip1. *Cytoskeleton* **67:** 442-455

Janmey PA, Lindberg U (2004) Cytoskeletal regulation: rich in lipids. *Nature reviews Molecular cell biology* **5:** 658-666

Janse CJ, Ramesar J, Waters AP (2006) High-efficiency transfection and drug selection of genetically transformed blood stages of the rodent malaria parasite Plasmodium berghei. *Nature protocols* **1:** 346-356

Jayachandran R, Liu X, Bosedasgupta S, Muller P, Zhang CL, Moshous D, Studer V, Schneider J, Genoud C, Fossoud C, Gambino F, Khelfaoui M, Muller C, Bartholdi D, Rossez H, Stiess M, Houbaert X, Jaussi R, Frey D, Kammerer RA, Deupi X, de Villartay JP, Luthi A, Humeau Y, Pieters J (2014) Coronin 1 regulates cognition and behavior through modulation of cAMP/protein kinase A signaling. *PLoS biology* **12:** e1001820

Jayachandran R, Sundaramurthy V, Combaluzier B, Mueller P, Korf H, Huygen K, Miyazaki T, Albrecht I, Massner J, Pieters J (2007) Survival of mycobacteria in macrophages is mediated by coronin 1-dependent activation of calcineurin. *Cell* **130:** 37-50

Kebaier C, Vanderberg JP (2010) Initiation of Plasmodium sporozoite motility by albumin is associated with induction of intracellular signalling. *International journal for parasitology* **40:** 25-33

Kennedy M, Fishbaugher ME, Vaughan AM, Patrapuvich R, Boonhok R, Yimamnuaychok N, Rezakhani N, Metzger P, Ponpuak M, Sattabongkot J, Kappe SH, Hume JC, Lindner SE (2012) A rapid and scalable density gradient purification method for Plasmodium sporozoites. *Malaria journal* **11:** 421

Kimura T, Taniguchi S, Toya K, Niki I (2010) Glucose-induced translocation of coronin 3 regulates the retrograde transport of the secretory membrane in the pancreatic beta-cells. *Biochemical and biophysical research communications* **395:** 318-323

Kost B, Mathur J, Chua NH (1999) Cytoskeleton in plant development. *Current opinion in plant biology* **2:** 462-470

Kovar DR, Harris ES, Mahaffy R, Higgs HN, Pollard TD (2006) Control of the assembly of ATP- and ADP-actin by formins and profilin. *Cell* **124:** 423-435

Kudryashev M, Lepper S, Baumeister W, Cyrklaff M, Frischknecht F (2010) Geometric constrains for detecting short actin filaments by cryogenic electron tomography. *PMC biophysics* **3:** 6

Lammermann T, Bader BL, Monkley SJ, Worbs T, Wedlich-Soldner R, Hirsch K, Keller M, Forster R, Critchley DR, Fassler R, Sixt M (2008) Rapid leukocyte migration by integrin-independent flowing and squeezing. *Nature* **453:** 51-55

Lee E, Shelden EA, Knecht DA (1998) Formation of F-actin aggregates in cells treated with actin stabilizing drugs. *Cell motility and the cytoskeleton* **39:** 122-133

Lee SF, Egelhoff TT, Mahasneh A, Cote GP (1996) Cloning and characterization of a Dictyostelium myosin I heavy chain kinase activated by Cdc42 and Rac. *The Journal of biological chemistry* **271:** 27044-27048

Lepper S (2011) Characterization of Plasmodium berghei actin and coronin. *PhD thesis*

Liu CZ, Chen Y, Sui SF (2006) The identification of a new actin-binding region in p57. *Cell research* **16:** 106-112

Liu SL, Needham KM, May JR, Nolen BJ (2011) Mechanism of a concentration-dependent switch between activation and inhibition of Arp2/3 complex by coronin. *The Journal of biological chemistry* **286:** 17039-17046

Logan-Klumpler FJ, De Silva N, Boehme U, Rogers MB, Velarde G, McQuillan JA, Carver T, Aslett M, Olsen C, Subramanian S, Phan I, Farris C, Mitra S, Ramasamy G, Wang H, Tivey A, Jackson A, Houston R, Parkhill J, Holden M, Harb OS, Brunk BP, Myler PJ, Roos D, Carrington M, Smith DF, Hertz-Fowler C, Berriman M (2012) GeneDB--an annotation database for pathogens. *Nucleic acids research* **40:** D98-108

Lukinavicius G, Reymond L, D'Este E, Masharina A, Gottfert F, Ta H, Guther A, Fournier M, Rizzo S, Waldmann H, Blaukopf C, Sommer C, Gerlich DW, Arndt HD, Hell SW, Johnsson K (2014) Fluorogenic probes for live-cell imaging of the cytoskeleton. *Nature methods* **11:** 731-733

Meissner M, Schluter D, Soldati D (2002) Role of Toxoplasma gondii myosin A in powering parasite gliding and host cell invasion. *Science* **298:** 837-840

Mishima M, Nishida E (1999) Coronin localizes to leading edges and is involved in cell spreading and lamellipodium extension in vertebrate cells. *Journal of cell science* **112 (Pt 17):** 2833-2842

Montell DJ, Yoon WH, Starz-Gaiano M (2012) Group choreography: mechanisms orchestrating the collective movement of border cells. *Nature reviews Molecular cell biology* **13:** 631-645

Morahan BJ, Wang L, Coppel RL (2009) No TRAP, no invasion. *Trends in parasitology* **25:** 77-84

Morgan RO, Fernandez MP (2008) Molecular phylogeny and evolution of the coronin gene family. *Sub-cellular biochemistry* **48:** 41-55

Moshous D, de Villartay JP (2014) The expanding spectrum of human coronin 1A deficiency. *Current allergy and asthma reports* **14:** 481

Mueller P, Massner J, Jayachandran R, Combaluzier B, Albrecht I, Gatfield J, Blum C, Ceredig R, Rodewald HR, Rolink AG, Pieters J (2008) Regulation of T cell survival through coronin-1-mediated generation of inositol-1,4,5-trisphosphate and calcium mobilization after T cell receptor triggering. *Nature immunology* **9:** 424-431

Munter S, Sabass B, Selhuber-Unkel C, Kudryashev M, Hegge S, Engel U, Spatz JP, Matuschewski K, Schwarz US, Frischknecht F (2009) Plasmodium sporozoite motility is modulated by the turnover of discrete adhesion sites. *Cell host & microbe* **6:** 551-562

Neer EJ, Schmidt CJ, Nambudripad R, Smith TF (1994) The ancient regulatory-protein family of WD-repeat proteins. *Nature* **371:** 297-300

Neer EJ, Smith TF (2000) A groovy new structure. *Proceedings of the National Academy of Sciences of the United States of America* **97:** 960-962

Oku T, Itoh S, Ishii R, Suzuki K, Nauseef WM, Toyoshima S, Tsuji T (2005) Homotypic dimerization of the actin-binding protein p57/coronin-1 mediated by a leucine zipper motif in the C-terminal region. *The Biochemical journal* **387:** 325-331

Oku T, Itoh S, Okano M, Suzuki A, Suzuki K, Nakajin S, Tsuji T, Nauseef WM, Toyoshima S (2003) Two regions responsible for the actin binding of p57, a mammalian coronin family actin-binding protein. *Biological & pharmaceutical bulletin* **26:** 409-416

Oku T, Nakano M, Kaneko Y, Ando Y, Kenmotsu H, Itoh S, Tsuiji M, Seyama Y, Toyoshima S, Tsuji T (2012) Constitutive turnover of phosphorylation at Thr-412 of human p57/coronin-1 regulates the interaction with actin. *The Journal of biological chemistry* **287:** 42910-42920

Olshina MA, Angrisano F, Marapana DS, Riglar DT, Bane K, Wong W, Catimel B, Yin MX, Holmes AB, Frischknecht F, Kovar DR, Baum J (2015) Plasmodium falciparum coronin organizes arrays of parallel actin filaments potentially guiding directional motility in invasive malaria parasites. *Malaria journal* **14:** 280

Ono T, Cabrita-Santos L, Leitao R, Bettiol E, Purcell LA, Diaz-Pulido O, Andrews LB, Tadakuma T, Bhanot P, Mota MM, Rodriguez A (2008) Adenylyl cyclase alpha and cAMP signaling mediate Plasmodium sporozoite apical regulated exocytosis and hepatocyte infection. *PLoS pathogens* **4:** e1000008

Orlicky S, Tang X, Willems A, Tyers M, Sicheri F (2003) Structural basis for phosphodependent substrate selection and orientation by the SCFCdc4 ubiquitin ligase. *Cell* **112:** 243-256

Pankova K, Rosel D, Novotny M, Brabek J (2010) The molecular mechanisms of transition between mesenchymal and amoeboid invasiveness in tumor cells. *Cellular and molecular life sciences : CMLS* **67:** 63-71

Perschmann N, Hellmann JK, Frischknecht F, Spatz JP (2011) Induction of malaria parasite migration by synthetically tunable microenvironments. *Nano letters* **11:** 4468-4474

Pieters J, Muller P, Jayachandran R (2013) On guard: coronin proteins in innate and adaptive immunity. *Nature reviews Immunology* **13:** 510-518

Pinder JC, Fowler RE, Dluzewski AR, Bannister LH, Lavin FM, Mitchell GH, Wilson RJ, Gratzer WB (1998) Actomyosin motor in the merozoite of the malaria parasite, Plasmodium falciparum: implications for red cell invasion. *Journal of cell science* **111 (Pt 13):** 1831-1839

Poupel O, Tardieux I (1999) Toxoplasma gondii motility and host cell invasiveness are drastically impaired by jasplakinolide, a cyclic peptide stabilizing F-actin. *Microbes and infection / Institut Pasteur* **1:** 653-662

Raftopoulou M, Hall A (2004) Cell migration: Rho GTPases lead the way. *Developmental biology* **265:** 23-32

Rappleye CA, Paredez AR, Smith CW, McDonald KL, Aroian RV (1999) The coronin-like protein POD-1 is required for anterior-posterior axis formation and cellular architecture in the nematode caenorhabditis elegans. *Genes & development* **13:** 2838-2851

Reisler E, Egelman EH (2007) Actin structure and function: what we still do not understand. *The Journal of biological chemistry* **282:** 36133-36137

Ridzuan MA, Moon RW, Knuepfer E, Black S, Holder AA, Green JL (2012) Subcellular location, phosphorylation and assembly into the motor complex of GAP45 during Plasmodium falciparum schizont development. *PloS one* **7:** e33845

Rothenberg ME, Rogers SL, Vale RD, Jan LY, Jan YN (2003) Drosophila pod-1 crosslinks both actin and microtubules and controls the targeting of axons. *Neuron* **39:** 779-791

Rouiller I, Xu XP, Amann KJ, Egile C, Nickell S, Nicastro D, Li R, Pollard TD, Volkmann N, Hanein D (2008) The structural basis of actin filament branching by the Arp2/3 complex. *The Journal of cell biology* **180:** 887-895

Rybakin V, Clemen CS (2005) Coronin proteins as multifunctional regulators of the cytoskeleton and membrane trafficking. *BioEssays : news and reviews in molecular, cellular and developmental biology* **27:** 625-632

Sahasrabuddhe AA, Nayak RC, Gupta CM (2009) Ancient Leishmania coronin (CRN12) is involved in microtubule remodeling during cytokinesis. *Journal of cell science* **122:** 1691-1699

Salamun J, Kallio JP, Daher W, Soldati-Favre D, Kursula I (2014) Structure of Toxoplasma gondii coronin, an actin-binding protein that relocalizes to the posterior pole of invasive parasites and contributes to invasion and egress. *FASEB journal : official publication of the Federation of American Societies for Experimental Biology* **28:** 4729-4747

Sattler JM, Ganter M, Hliscs M, Matuschewski K, Schuler H (2011) Actin regulation in the malaria parasite. *European journal of cell biology* **90:** 966-971

Schmitz S, Grainger M, Howell S, Calder LJ, Gaeb M, Pinder JC, Holder AA, Veigel C (2005) Malaria parasite actin filaments are very short. *Journal of molecular biology* **349:** 113-125

Schuler H, Matuschewski K (2006) Regulation of apicomplexan microfilament dynamics by a minimal set of actin-binding proteins. *Traffic* **7:** 1433-1439

Scott VR, Boehme R, Matthews TR (1988) New class of antifungal agents: jasplakinolide, a cyclodepsipeptide from the marine sponge, Jaspis species. *Antimicrobial agents and chemotherapy* **32:** 1154-1157

Shaw MK, Tilney LG (1999) Induction of an acrosomal process in Toxoplasma gondii: visualization of actin filaments in a protozoan parasite. *Proceedings of the National Academy of Sciences of the United States of America* **96:** 9095-9099

Shen B, Sibley LD (2014) Toxoplasma aldolase is required for metabolism but dispensable for host-cell invasion. *Proceedings of the National Academy of Sciences of the United States of America* **111:** 3567-3572

Siden-Kiamos I, Louis C, Matuschewski K (2012) Evidence for filamentous actin in ookinetes of a malarial parasite. *Molecular and biochemical parasitology* **181:** 186-189

Silvie O, Goetz K, Matuschewski K (2008) A sporozoite asparagine-rich protein controls initiation of Plasmodium liver stage development. *PLoS pathogens* **4:** e1000086

Singh BK, Sattler JM, Chatterjee M, Huttu J, Schuler H, Kursula I (2011) Crystal structures explain functional differences in the two actin depolymerization factors of the malaria parasite. *The Journal of biological chemistry* **286:** 28256-28264

Sixt M (2012) Cell migration: fibroblasts find a new way to get ahead. *The Journal of cell biology* **197:** 347-349

Smith TF (2008) Diversity of WD-repeat proteins. *Sub-cellular biochemistry* **48:** 20-30

Smith TF, Gaitatzes C, Saxena K, Neer EJ (1999) The WD repeat: a common architecture for diverse functions. *Trends in biochemical sciences* **24:** 181-185

Suetsugu S, Miki H, Takenawa T (1999) Identification of two human WAVE/SCAR homologues as general actin regulatory molecules which associate with the Arp2/3 complex. *Biochemical and biophysical research communications* **260:** 296-302

Suzuki K, Nishihata J, Arai Y, Honma N, Yamamoto K, Irimura T, Toyoshima S (1995) Molecular cloning of a novel actin-binding protein, p57, with a WD repeat and a leucine zipper motif. *FEBS letters* **364:** 283-288

Swaminathan K, Muller-Taubenberger A, Faix J, Rivero F, Noegel AA (2014) A Cdc42- and Rac-interactive binding (CRIB) domain mediates functions of coronin. *Proceedings of the National Academy of Sciences of the United States of America* **111:** E25-33

Tardieux I, Liu X, Poupel O, Parzy D, Dehoux P, Langsley G (1998) A Plasmodium falciparum novel gene encoding a coronin-like protein which associates with actin filaments. *FEBS letters* **441:** 251-256

Tilley FC, Williamson RC, Race PR, Rendall TC, Bass MD (2015) Integration of the Rac1- and actin-binding properties of Coronin-1C. *Small GTPases* **6:** 36-42

Tsujita K, Itoh T, Kondo A, Oyama M, Kozuka-Hata H, Irino Y, Hasegawa J, Takenawa T (2010) Proteome of acidic phospholipid-binding proteins: spatial and temporal regulation of Coronin 1A by phosphoinositides. *The Journal of biological chemistry* **285:** 6781-6789

Usatyuk PV, Burns M, Mohan V, Pendyala S, He D, Ebenezer DL, Harijith A, Fu P, Huang LS, Bear JE, Garcia JG, Natarajan V (2013) Coronin 1B regulates S1P-induced human lung endothelial cell chemotaxis: role of PLD2, protein kinase C and Rac1 signal transduction. *PloS one* **8:** e63007

Vanderberg JP (1974) Studies on the motility of Plasmodium sporozoites. *The Journal of protozoology* **21:** 527-537

Varnai P, Balla T (1998) Visualization of phosphoinositides that bind pleckstrin homology domains: calcium- and agonist-induced dynamic changes and relationship to myo-[3H]inositol-labeled phosphoinositide pools. *The Journal of cell biology* **143:** 501-510

Vicente-Manzanares M, Webb DJ, Horwitz AR (2005) Cell migration at a glance. *Journal of cell science* **118:** 4917-4919

Vinson CR, Hai T, Boyd SM (1993) Dimerization specificity of the leucine zipper-containing bZIP motif on DNA binding: prediction and rational design. *Genes & development* **7:** 1047-1058

Watanabe M, Suzuki T, Kim M, Abe Y, Yoshida Y, Sugano S, Yamamoto T (2011) Coronin7 forms a novel E3 ubiquitin ligase complex to promote the degradation of the anti-proliferative protein Tob. *FEBS letters* **585:** 65-70

Watson AJ, Katz A, Simon MI (1994) A fifth member of the mammalian G-protein beta-subunit family. Expression in brain and activation of the beta 2 isotype of phospholipase C. *The Journal of biological chemistry* **269:** 22150-22156

Williams HC, San Martin A, Adamo CM, Seidel-Rogol B, Pounkova L, Datla SR, Lassegue B, Bear JE, Griendling K (2012) Role of coronin 1B in PDGF-induced migration of vascular smooth muscle cells. *Circulation research* **111:** 56-65

Williamson RC, Cowell CA, Hammond CL, Bergen DJ, Roper JA, Feng Y, Rendall TC, Race PR, Bass MD (2014) Coronin-1C and RCC2 guide mesenchymal migration by trafficking Rac1 and controlling GEF exposure. *Journal of cell science* **127:** 4292-4307

Wolf K, Friedl P (2006) Molecular mechanisms of cancer cell invasion and plasticity. *The British journal of dermatology* **154 Suppl 1:** 11-15

Wolf K, Mazo I, Leung H, Engelke K, von Andrian UH, Deryugina EI, Strongin AY, Brocker EB, Friedl P (2003) Compensation mechanism in tumor cell migration: mesenchymal-amoeboid transition after blocking of pericellular proteolysis. *The Journal of cell biology* **160:** 267-277

Wong W, Webb AI, Olshina MA, Infusini G, Tan YH, Hanssen E, Catimel B, Suarez C, Condron M, Angrisano F, Nebi T, Kovar DR, Baum J (2014) A mechanism for actin filament severing by malaria parasite actin depolymerizing factor 1 via a low affinity binding interface. *The Journal of biological chemistry* **289:** 4043-4054

Xavier CP, Rastetter RH, Blomacher M, Stumpf M, Himmel M, Morgan RO, Fernandez MP, Wang C, Osman A, Miyata Y, Gjerset RA, Eichinger L, Hofmann A, Linder S, Noegel AA, Clemen CS (2012) Phosphorylation of CRN2 by CK2 regulates F-actin and Arp2/3 interaction and inhibits cell migration. *Scientific reports* **2:** 241

Yadav R, Larbi KY, Young RE, Nourshargh S (2003) Migration of leukocytes through the vessel wall and beyond. *Thrombosis and haemostasis* **90:** 598-606

Yasuda T, Yagita K, Nakamura T, Endo T (1988) Immunocytochemical localization of actin in Toxoplasma gondii. *Parasitology research* **75:** 107-113

Yin HL, Janmey PA (2003) Phosphoinositide regulation of the actin cytoskeleton. *Annual review of physiology* **65:** 761-789

Yonezawa N, Nishida E, Iida K, Yahara I, Sakai H (1990) Inhibition of the interactions of cofilin, destrin, and deoxyribonuclease I with actin by phosphoinositides. *The Journal of biological chemistry* **265:** 8382-8386

Zanassi P, Paolillo M, Feliciello A, Avvedimento EV, Gallo V, Schinelli S (2001) cAMP-dependent protein kinase induces cAMP-response element-binding protein phosphorylation via an intracellular calcium release/ERK-dependent pathway in striatal neurons. *The Journal of biological chemistry* **276:** 11487-11495

Zhang XF, Hyland C, Van Goor D, Forscher P (2012) Calcineurin-dependent cofilin activation and increased retrograde actin flow drive 5-HT-dependent neurite outgrowth in Aplysia bag cell neurons. *Molecular biology of the cell* **23:** 4833-4848